



REPUBLIC OF TURKEY
MARMARA UNIVERSITY
INSTITUTE OF HEALTH SCIENCES

**THREE-DIMENSIONAL STEREOFOTOGRAMMETRIC
EVALUATION OF FACIAL SOFT TISSUE ASYMMETRIES
BEFORE AND AFTER ORTHOGNATHIC SURGERY IN
SKELETAL CLASS III PATIENTS**

GEORGIOS LOGOTHETIS
MASTER THESIS

DEPARTMENT OF ORTHODONTICS

SUPERVISOR
Asst. Prof. Dr. KADIR BEYCAN

ISTANBUL, 2020

THESIS APPROVAL FORM

Institute : Marmara University Institute of Health Sciences

Programme : Master of Sciences (MSci.)



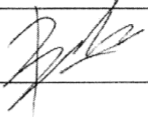
Department : Orthodontic Department

Owner of the Thesis : Georgios LOGOTHETIS

Exam Date & Time : 10.01.2020 - 11:00

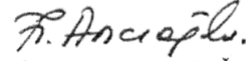
Title of the Thesis : Three-Dimensional Stereophotogrammetric Evaluation of Facial Soft Tissue Asymmetries Before and After Orthognathic Surgery in Skeletal Class III Patients.

This study has been approved as a MSci. Thesis in regard to content and quality.

	Title, Name-Surname (Affiliation)	Signature
Supervisor	Dr.Öğr.Üyesi Kadir BEYCAN (Marmara Üniv.)	
Member	Prof.Dr.AhuACAR (Marmara Üniv.)	
Member	Dr.Öğr.Üyesi BerzaYILMAZ (Bezmialem Üniv.)	

APPROVAL

This thesis has been deemed by the aforementioned jury in accordance with the relevant articles of "Marmara University Graduate Education and Examination Regulations" and has been approved by Administrative Board of Institute with decision dated 24.01.2020 and numbered 32



Prof. Dr. Feyza ARICIOĞLU
Director of Institute of Health Sciences

BEYAN

Bu tezin kendi çalışmam olduğunu, planlamasından yazımına kadar hiçbir aşamasında etik dışı davranışımın olmadığını, tezdeki bütün bilgileri akademik ve etik kurallar içinde elde ettiğimi, tez çalışmasıyla elde edilmeyen bütün bilgi ve yorumlara kaynak gösterdiğimi ve bu kaynakları kaynaklar listesine aldığımı, tez çalışması ve yazımı sırasında patent ve telif haklarını ihlal edici bir davranışımın olmadığını beyan ederim.

22.10.2019

Georgios LOGOTHETIS



STATEMENT:

I affirm that this thesis study belongs to me. There is no immoral attitude in all stages from the planning stage of thesis to the writing stage. I gained all the information in the terms of academic and ethical rules. I stated sources for the information gained not with this study. I showed the source in the list of sources, and again there is no copyright infringement in study and writing stage.

22.10.2019

Georgios LOGOTHETIS



I. ACKNOWLEDGEMENTS

First of all, I would like to thank my thesis supervisor Asst. Prof. Dr. Kadir Beycan. Without his contribution, this thesis would not be possible. His office door was always open when I ran into trouble, guiding my efforts through the right path.

I would also like to thank Prof. Dr. Fulya Özdemir and Prof. Dr. Ahu Acar. Despite being the head of the department, they never fail to help anyone working there. Their experience assisted me a lot throughout the duration of my Master program.

I would also like to express my deepest gratitude to all my dear professors Prof. Dr. Sibel Biren, Assoc. Prof. Dr. Çağla Asst. Prof. Dr. Nuray Yılmaz, Asst. Prof. Dr. Yasemin Bahar Acar, for their incredible efforts throughout my Masters and their sharing of their knowledge and expertise. It has been my honor. Without their passionate participation and input, this thesis could not have been successfully conducted.

Moreover, I would like to thank all my friends and colleagues in the department. I am grateful for all the new friendships that I made and all the unforgettable moments that we shared together. You were my family away from home and you will always be remembered.

Above all, I must express my very profound gratitude to my wonderful family, my parents and my sister, for providing me with unfailing support and continuous encouragement throughout my years of study and through the process of researching and writing this thesis. This accomplishment would not have been possible without them.

II. CONTENT

1. SUMMARY	1
2. ÖZET.....	2
3. INTRODUCTION AND AIMS.....	3
4. LITERATURE REVIEW.....	5
4.1 Class III Malocclusion	5
4.1.1 Prevalence of Class III malocclusion.....	5
4.1.2 Components of Class III malocclusion	5
4.1.3 Etiology of Class III malocclusion.....	6
4.1.4 Treatment of Class III malocclusion	7
4.2 Orthognathic Surgery	8
4.2.1 Definition of orthognathic surgery	8
4.2.2 Types of orthognathic surgery	8
4.2.2.1 Orthognathic surgery in the maxillary area.....	8
4.2.2.2 Orthognathic surgery in the mandibular area	9
4.2.3. Facial soft tissues and interventions during orthognathic surgery	10
4.2.4. The management of the nasal region	11
4.2.5. Side effects of orthognathic surgery	11
4.2.6. Stability of the outcome of orthognathic surgery.....	12
4.3 Facial Asymmetry	13
4.3.1 Historical review of facial asymmetry	13
4.3.2. Does facial symmetry equal to facial attractiveness?	14
4.3.3. Etiology of facial asymmetry	16

4.3.4. Asymmetry prevalence on Class III patients	18
4.4 Methods for Three-dimensional Surface Acquisition and Analysis of the Facial Soft Tissues.....	19
4.4.1 Radiographic methods	19
4.4.1.1 Computed tomography	19
4.4.1.2 Cone Beam Computed tomography	20
4.4.2. Non radiographic methods	21
4.4.2.1 Stereo-photogrammetry.....	22
4.4.2.2 Laser scanning.....	23
4.4.2.2.1 Laser scanners with fixed units	23
4.4.2.2.2 Portable or mobile laser scanners.....	25
4.4.2.3 Structured light technique	26
4.4.2.3.1 Systems with a single camera	27
4.4.2.3.2 Systems with two or more cameras.....	27
4.4.2.3.2.1 Moiré fringe patterns	27
4.4.2.3.2.2 OGIS Range Finder RFX-IV.....	28
4.4.2.3.2.3 CAM 3D systems	28
4.4.2.3.2.4 C3D systems.....	28
4.4.2.3.2.5 3dMD system	29
4.4.2.3.2.5.1 The technical parts.....	29
4.4.2.3.2.5.2 The procedure of image capturing.....	30
4.4.2.3.2.5.3 The working principles.....	32
4.4.2.3.2.5.4 The process of the 3D model.....	33
4.4.2.3.2.5.5 The natural head position	33
4.4.2.3.2.5.6 Scientific validation of the 3dMD face system	34

4.4.2.3.2.6 Video imaging	37
4.4.3 Analysis of 3D data.....	38
4.4.3.1 Analysis of asymmetry	38
5. MATERIALS AND METHODS	40
5.1 Patient Selection.....	40
5.2 Data Collection	41
5.3 Data Assessment	43
5.4 Statistical Analysis	53
6. RESULTS	54
6.1 Reliability Test.....	54
6.2 Demographics of The Study Group	56
6.3 Comparison of The Degree of Asymmetry between Time Intervals.....	56
6.4 Comparison of The Degree of Asymmetry between Time Intervals for Subgroups	64
6.4 Comparisons Regarding The Mid-sagittal plane	68
6.5 Volumetric and Surface Analyses.....	70
7. DISCUSSION	76
7.1. Discussion of the Aim	76
7.2. Discussion of Materials and Methods.....	77
7.3. Discussion of the Results	81
8. CONCLUSION.....	87
9. REFERENCES.....	88
10. CURRICULUM VITAE.....	111

III. ABBREVIATIONS

- 2D: Two-Dimensional
- 3D: Three-Dimensional
- BSSO: Bilateral Sagittal Split Osteotomy
- CBCT: Cone Beam Computed Tomography
- CT: Computed Tomography
- FA: Fluctuating Asymmetry
- ICP: Interactive Closest Point
- IVRO: Intraoral Vertical Ramus Osteotomy
- Md: Mandibular region
- Mx: Maxillary region
- MRI: Magnetic Resonance Imaging
- MSP: Mid-sagittal plane
- N: Nasion
- NHP: Natural Head Position
- NSAID: non-steroid anti-inflammatory drugs
- PA: Procrustes Analysis
- RGB: Red Green Blue
- RIF: Rigid Internal Fixation
- RMS: Root Mean Square
- SD: Statistical Deviation
- STL: a 3d geometry-only STereoLithography file format (3D Systems) native to widely used CAD/CAM software, additive manufacturing and 3D printing.
- Sur: Surface
- T: Total region
- TMJ: Temporomandibular Joint
- TSB: a highly-precise 3d geometry file format (Tricorder Surface Binary) containing high resolution image texture data and proprietary to 3dMD.
- Vol: Volume

- %: Percent
- °: Degree



IV. FIGURE LIST

Figure 1: 3dMDface System (Atlanta, GA, USA) - Multiple camera system with structured light patterns to obtain a 3D image.	30
Figure 2: Facial surface capturing with the use of the 3dMDface System (Atlanta, GA, USA), used in Marmara University, Faculty of Dentistry, Department of Orthodontics.....	42
Figure 3: 3D photographs after cropping in T0 (frontal and lateral view)	43
Figure 4: Facial surface in a tsb file format (left). Facial surface in a stl file format (right).	44
Figure 5: Superimposition of the original and mirrored 3D model, creating a clear midline path to create a facial mid-sagittal plane.....	45
Figure 6: Superimposition of original and mirror 3D image shows a clear facial midline path for the creation of the facial MSP by the software.	46
Figure 7: Color map of the location of facial asymmetry. Red and blue areas represent areas of bigger asymmetry values as the color's intensity increases.....	47
Figure 8: The calculation of the angulation difference among mid-sagittal planes between T0 and T1. The grey model represents the T0 and the orange represents the T1 facial surface.....	48
Figure 9: Segmentation of the facial surface to 3 (left) and 4 parts (right), respectively. 1: Upper face, 2: Midface, 3: Lower face, 4: Maxillary and 5: Mandibular part.....	50
Figure 10: The X-axis of the face (B) is parallel to the Frankfort horizontal plane (A). The segmentation planes are perpendicular to the Y-axis of the face and the MSP.....	50
Figure 11: Color maps showing the asymmetry levels in each facial area after segmentation.	51

Figure 12: Volumetric analysis of the hemifaces and their parts. The A line represents the 25mm distance between the Or point and the posterior segmentation wall.....	52
Figure 13: RMS values and SD before and after surgery. 6, 9, 23 numbers represent each a patient's number.....	57
Figure 14: Linear correlation between RMS values before surgery and RMS difference after surgery.	59
Figure 15: Linear correlation between RMS values before surgery and RMS difference after surgery for midface.....	60
Figure 16: Linear correlation between RMS values before surgery and RMS difference after surgery for lower face.....	61
Figure 17: Linear correlation between RMS values before surgery and RMS difference after surgery for the maxillary area.....	62
Figure 18: Linear correlation between RMS values before surgery and RMS difference after surgery for the mandibular area.....	63

V. TABLE LIST

Table 1: A categorization of the devices for 3D surface acquisition (Kau and Richmond, 2010).....	21
Table 2: Definitions of the Nasion, Subnasale, Helion, Gnathion, Orbitale, Porion points.....	49
Table 3: Single observer’s agreements between repeated measurements (0 = T0 time interval, 1 = T1 time interval, T = Total surface, U = Upper face, M= Midface, L = Lower face, Mx = Maxillary region, Md= Mandibular region, Vol = Volume, Sur = Surface, MSP= angle between mid-sagittal planes).....	54
Table 4: Comparison between RMS values before and after surgery.....	56
Table 5: Difference between each segmentation part between T0 and T1 time intervals.....	58
Table 6: Correlation between RMS values before surgery and RMS difference after surgery.....	59
Table 7: Correlation between RMS values before surgery and RMS difference after surgery for midface.	60
Table 8: Correlation between RMS values before surgery and RMS difference after surgery for lower face.	61
Table 9: Correlation between RMS values before surgery and RMS difference after surgery for the maxillary area.	62
Table 10: Correlation between RMS values before surgery and RMS difference after surgery for the mandibular area.	63
Table 11: Youden Index Association criteria and Area under the ROC curve (AUC) for RMS=1,0689.	64

Table 12: Criterion values and coordinates of the ROC curve.	65
Table 13: Descriptive statistics for Low and High RMS groups before surgery.	66
Table 14: Comparison between RMS values before and after surgery for the Low RMS group.	66
Table 15: Comparison between RMS values before and after surgery for the high RMS group.	66
Table 16: Comparison between RMS values before and after surgery for each facial part separately for LOW RMS group.	67
Table 17: Comparison between RMS values before and after surgery for each facial part separately for HIGH RMS group.	68
Table 18: Descriptive statistics for the angle between the MSPs before and after surgery.	68
Table 19: Correlation between the absolute difference in RMS values before and after surgery with the difference in the angulation of the mid-sagittal planes before and after surgery.	69
Table 20: Correlation between the absolute difference in RMS values for each facial part before and after surgery with the difference in the angulation of the mid-sagittal planes before and after surgery.	69
Table 21: Comparison of the absolute volumetric difference between hemifaces for T0 and T1 time intervals.	70
Table 22: Correlation between preop RMS and absolute volumetric difference value between hemifaces for each facial part.	71
Table 23: Correlation between postop RMS and absolute volumetric difference value between hemifaces for each facial part.	72

Table 24: Comparison of the absolute volumetric difference between hemifaces for T0 and T1 time intervals for the Low RMS group.	72
Table 25: Comparison of the absolute volumetric difference between hemifaces for T0 and T1 time intervals for the High RMS group.	73
Table 26: Correlation between the absolute volumetric difference between hemifaces before and after surgery with the difference in the angulation of the mid-sagittal planes before and after surgery.	74
Table 27: Correlation between volumetric and surface values for each facial part before surgery.	75
Table 28: Correlation between volumetric and surface values for each facial part after surgery.	75

“Three-dimensional Stereophotogrammetric Evaluation of Facial Soft Tissue Asymmetries Before and After Orthognathic Surgery in Skeletal Class III patients”

Name of the student: Georgios Logothetis

Supervisor: Asst. Prof. Dr. Kadir Beycan

Department: Department of Orthodontics, Faculty of Dentistry, Marmara University

1. SUMMARY

Aim: To investigate the asymmetry levels of the facial surface before and after the Class III orthognathic surgery procedure with the use of stereophotogrammetry.

Materials and Methods: The sample of this retrospective study consists of three-dimensional (3D) facial images of 40 skeletal Class III orthognathic surgical patients (19 males, 21 females), mean age 20,44 years (ranging from 17 to 27 years old). The 3D images acquisition took place at the T0 (before surgery) and T1 (6 months after surgery) time intervals. The 3D models were cropped, mirrored and the original and mirrored version were registered together. A mid-sagittal plane (MSP) was created and a Root Mean Square (RMS) value was automatically calculated by the system. The face was divided into parts (upper, mid, lower face subdivided to maxillary and mandibular region). Finally, volumetric and surface analyses were performed.

Results: A non-significant decrease in RMS values was observed between the two time intervals ($P>0,05$). A statistically significant correlation was found between the initial asymmetry levels and the amount of asymmetry correction after surgery ($r=0.653$, $P<0.01$). The sample was separated into two subgroups, of 20 patients each, of Low and High RMS values. A statistically significant increase in the asymmetry levels was found for the Low RMS group ($P<0.05$) and a significant decrease in asymmetry was found for the High RMS group for the whole facial surface ($P<0.01$) and for the lower and specifically the mandibular facial parts ($P<0.05$). A significant correlation between the change in RMS values and the changes in angulation of the MSP plane was observed ($r=-0.392$, $P<0.05$).

Conclusion: Patients showing increased initial symmetry levels end up more asymmetric after surgery and patients with higher values of initial asymmetry show bigger improvement in their symmetry levels.

Keywords: Asymmetry, Orthognathic surgery, Class III, Stereophotogrammetry, Three-dimensional imaging

“İskeletsel Sınıf III Hastalarda Ortognatik Cerrahi Öncesi ve Sonrası Meydana Gelen Yumuşak Doku Asimetrilerinin Üç Boyutlu Steryofotogrametrik İncelenmesi”

Öğrencinin ismi: Georgios Logothetis

Danışman: Dr. Öğr. Üyesi Kadir Beycan

Bölüm: Ortodonti Anabilim Dalı, Marmara Üniversitesi

2. ÖZET

Amaç: Bu çalışmanın amacı, Sınıf III ortognatik cerrahi öncesi ve sonrası, yüz bölgesindeki yumuşak doku asimetrilerinin steryofotogrametri ile incelenmesidir.

Gereç ve Yöntem: Retrospektif çalışma örneklemini; ortalama yaşları 20.44 olan (17-27 arasında değişen) 40 iskelet Sınıf III hastanın (19 erkek, 21 kadın), üç boyutlu (3B) yüz görüntüleri oluşturmaktadır. 3B yüz görüntüleri T0 (ameliyattan önce) ve T1 (ameliyattan 6 ay sonra) zaman aralıklarında alınmış ve Etkileşimli En Yakın Nokta (ICP) algoritması kullanılarak ayna görüntüsü alınmış versiyonları ile karşılaştırılmıştır. Sonrasında bir orta oksal düzlem (MSP) yaratılmış, yüz 5 parçaya (üst, orta, alt yüz, maksiller ve mandibuler) bölünmüş ve sistem tarafından otomatik olarak, yüzün ve yüz parçaların asimetri seviyelerini gösteren Kök Ortalama Kare (RMS) değeri elde edilmiştir.

Bulgular: Tüm yüz ve her parça için, iki zaman aralığı arasında RMS değerlerinde anlamlı olmayan bir düşüş gözlemlendi ($P>0,05$). İlk asimetri düzeyleri ile ameliyat sonrası asimetri düzeyleri arasında istatistiksel olarak anlamlı bir korelasyon bulundu ($r=0.653$, $P<0.01$). Bu bulguların daha fazla detaylandırılması amacıyla örneklem, her biri 20 hastadan oluşan Düşük ve Yüksek RMS değerlerine sahip iki alt gruba ayrıldı. Düşük RMS grubu için asimetri seviyelerinde istatistiksel olarak anlamlı bir artış bulundu ($P<0.05$).

Sonuç: Başlangıç asimetri değeri yüksek olan hastalar ameliyat sonrası artmış simetri değeri göstermektedir.

Anahtar Kelimeler: Asimetri, Ortognatik cerahi, Sınıf III, Steryofotogrametri, Üç boyutlu görüntülem

3. INTRODUCTION AND AIMS

A major concern in orthognathic surgeries is the aesthetic matters and the achievement of facial symmetry. Therefore, a proper surgery planning is mandatory, taking into consideration all the factors affecting the skeletal relationships and all the aesthetic parameters. To improve the prognostic value of the surgery planning and achieve results closer to the future outcomes of the surgery, a proper analysis of the response of the facial soft tissues to the movements of the bony tissues is mandatory (Aboul-Hosn Centenero and Hernández-Alfaro, 2012; Donatsky et al., 2009). Nowadays, most of the techniques we base our surgical treatment planning appear to have restrictions in imaging details and in-depth focus and usually involve radiologic diagnostics that expose the patients into radiation (Kim et al., 2013; Park et al., 2013; Yáñez-Vico et al., 2011).

Facial symmetry is a theoretical concept, since it is almost impossible to find a perfectly symmetric face in the general population. According to this, even faces that are considered symmetric present limited discrepancies regarding the size and position of the two sides of the facial surface (Farkas, 1994). It was found that it is usually the lower facial third presenting more frequent and higher levels of asymmetry when compared with the middle and upper facial thirds (Severt and Profitt, 1997).

The facial asymmetry can usually occur because of skeletal, dental, functional or soft tissue related reasons, but usually it is due to a combination of the mentioned reasons. For example, a maxillary displacement might result to an occlusal canting or to the shift of the dental midline, resulting in further asymmetric effects on the lips and occlusal plane (Cheong and Lo, 2011; Bergeron et al., 2008), or a mandibular midline deviation can result in asymmetries in the cheeks and the lower face contour areas (Ishizaki et al., 2010). Most importantly, a jaw asymmetry can be the reason of functional or even psychological problems, making its correction mandatory (Verze et al., 2012). According to these, the facial asymmetry, when corrected with a combination of orthodontic and surgical treatment, should aim on the correction of both the occlusal planes and the dental midlines, as well as to the alignment of the chin with the facial midline, to the leveling of the lips and the oral commissures and to a symmetric display of the dental and soft tissues during smiling (Ko et al., 2009).

Many methods have been introduced for the measurement and analysis of the soft tissue symmetry. Traditionally, facial symmetry was calculated from two-dimensional photographs or x-rays, which presented significant flaws, since a three-dimensional concept can't be properly interpreted in two-dimensions (Moraes et al., 2011). To surpass these limitations, three-dimensional techniques were introduced, with either the use of radiation or not. Lately, techniques using stereophotogrammetry have been extensively used for the measurement of the facial asymmetry, providing a reliable and convenient solution with no radiation exposure on the facial surface (Wermker et al., 2014). The major technique for calculating facial asymmetry so far, in two or three dimensions, has been the use of facial landmarks, to assess the same points in both sides of the facial surface, as well as for the assessment of the mid-sagittal plane of the face. In our study, a different approach is used, which offers a 3D and global evaluation of the whole facial surface and its levels of asymmetry, not focusing on user's manual assessment of landmark points, without the use of single points and linear measurements. This can be achieved with the use of a sophisticated computer algorithm which takes into consideration 10.000-16.000 points on the facial surface to calculate a global asymmetry score (Meyer et al., 2009).

Our study focuses on looking closely to the levels of symmetry on the facial soft tissues, before and following the orthognathic surgery procedure, individually, comparing the alterations in the values of asymmetry in those two time intervals. The purpose of this analysis is to have an insight on the effects of the bony tissue movements on the facial soft tissues, giving us valuable clues about the predictability of the soft tissue responses and the evaluation of the symmetry levels of the post-surgical facial surface. Therefore, this thesis aims to answer the following questions:

- 1) Is there a reliable, landmark-independent method for the calculation of facial asymmetry, taking into consideration the whole facial surface?
- 2) Is the orthognathic surgery procedure adequate for the improvement of facial symmetry?
- 3) Can the soft tissue response following the surgical procedure be calculated and correlated significantly with the movements of the skeletal tissues

4. LITERATURE REVIEW

4.1 Class III Malocclusion

4.1.1 Prevalence of Class III malocclusion

The predominance of Class III malocclusions shifts significantly among populaces and inside them, extending from 0% to 26% of the general population (Hardy et al., 2012). Not to exclude the pseudo-Class III malocclusions, observed mainly in patients with deciduous or mixed dentition. In adolescents between 8-12 years of old, it was found that a percentage of anterior crossbites around 60% to 70% were delegated pseudo-Class III malocclusions (Lin, 1985). Asians have the lead in the prevalence of Class III malocclusion, with percentages ranging from 9-19% (Chan 1974; Braun et al., 1999). Caucasians show a lower prevalence of 1-5% (Haynes 1970; Foster and Day 1974; Lee et al., 2011), Latin population had a rate of 5% (Silva and Kang, 2001), Indian population around 1,2%. According to NHANES III, the third National Examination Survey, Class III malocclusion shows 0.8% prevalence in white population, 1.6% in Mexican-American and a 2% rate in black population (Proffit et al, 1998).

Finally, according to Sayin and Turkkahraman (2004), Gelgor et al (2007), Uslu et al (2009), the rates of Class III malocclusion in Turkish population showed a variety of results (12%, 18.44% and 10.3%, respectively) (Tasios, 2015).

4.1.2 Components of Class III malocclusion

Class III Angle classification (Angle, 1899) first referred to a condition where the lower teeth were occluding more mesially than normal, for at least the length of one bicuspid. These days it is conceived as a skeletal discrepancy which can be the result of either mandibular prognathism, maxillary deficiency or both. Studies have shown that mandibular prognathism appears as etiology for 20% to 46% of the Class

III subjects, while maxillary retrusion as etiology ranges from 19,5% to 37%. Moreover, 7,5% to 60% of Class III cases are due to a combination of both mandibular excess and maxillary deficiency (Sanborn, 1955; Dietrich, 1970; Jacobson et al, 1974; Ellis and McNamara, 1984; Guyer et al, 1986; Williams and Andersen, 1986).

In general, Class III subjects are found to have a smaller, but not more retrusive maxilla than Class I subjects. On the other hand, Class III subjects have larger and more protrusive mandibles (Wolfe et al., 2011).

4.1.3 Etiology of Class III malocclusion

Class III is a polygenic disorder, resulting from an interaction between susceptibility genes and environmental factors. Polygenic inheritance means that the phenotypic trait can be connected to at least two susceptibility genes and the environmental effect on them. Hereditary examination of families with Class III phenotype underpins the speculation of polygenic legacy. In a study (Litton et al., 1970), the families of 51 probands with Class III malocclusion were examined and the finding showed that almost the 13% of their siblings displayed the trait. Furthermore, the families of patients treated with orthognathic surgery showed a high pervasiveness of Class III malocclusion.

Subsequently, the genetic and environmental factors induce the regulation of the mandibular growth through the condylar cartilage. Condylar cartilage is a significant growth site in the mandible and it structures also some portion of the temporomandibular joint (Coprav et al., 1988). It has been shown that experimentally generating a Class III malocclusion has been ascribed to an expanded pace of condylar development (Kiliaridis et al., 1999). Consequently, the hypothesis was formed, that the condylar cartilage can be affected by changes in the biophysical environment, making it possible that the Class III malocclusion may be hastened under these biomechanical conditions by the legacy of qualities that incline to Class III phenotypes.

Nowadays, many researches are focused on exploring the genetic factors responsible for the Class III malocclusion. Many genome-wide scans have found that these susceptibility genes are likely to be located in chromosomal loci 1p36, 12q23 and

12q13 (Xue et al., 2010). Each gene associated with this specific biological pathway may be an applicant gene that is connected with Class III malocclusion.

4.1.4 Treatment of Class III malocclusion

For the treatment of Class III malocclusion, we can base our treatment modalities to three approaches. The choice is dependent on many factors, like the skeletal relationship between maxilla and mandible, the severity of the skeletal discrepancy and the growth stage of the patient. These three approaches include:

1. Growth manipulation during early growth stages, by using orthopedic appliances like Face mask for maxillary advancement, modified maxillary protraction headgear (MMPH)
2. Orthodontic camouflage by dentoalveolar correction of the disharmony of the jaws
3. Orthodontic treatment combined with orthognathic surgery.

The growth manipulation procedure has the requirement of the patient being in growing stage. We use this treatment modality in patients with maxillary deficiency with a mandible size and position around the normal values. This approach, though, can be risky for patients with excessive mandibular growth or overdeveloped mandible. Furthermore, the possibility of a relapse during later years has been mentioned in many articles (Hagg et al., 2003; Baccetti et al., 2004).

In cases where the patient has passed the growth spurt, the treatment options are limited to a dental orthodontic camouflage or orthognathic surgery. By orthodontic camouflage, we refer to a treatment aiming to provide a stable, functional and aesthetic dental occlusion while correcting, as much as possible, the facial profile, without having the possibility to correct the skeletal discrepancy. Again in this treatment option, the skeletal and dental discrepancy shouldn't be excessive and a favorable period for it is the late pubertal stage (usually 16-17 years of old) or maybe a little earlier on female patients (Baccetti et al., 2007). The camouflage treatment usually includes the use of Class III elastics, extraction of selective teeth or distalization of teeth in the lower dental arch with the use of skeletal anchorage.

In some cases, though, that the jaw discrepancy becomes excessive, making a camouflage treatment impossible or risky with severe side-effects. Then, the ideal treatment option is a combination of orthodontic treatment with orthognathic surgery. Same counts for cases with skeletal asymmetries or deformities. The choice of a surgical treatment has the advantages of a more overall approach, with the correction of skeletal and dental discrepancies.

4.2 Orthognathic Surgery

4.2.1 Definition of orthognathic surgery

Orthognathic surgery is the surgical correction of dentofacial deformities with a combination of orthodontic and maxillofacial treatment. The word “orthognathic” derives from the Greek words “ortho” and “gnathos”, meaning “straighten” and “jaw” respectively. The orthognathic correction can be isolated to one jaw or concurrently on both jaws. This manipulation of the elements of the facial skeleton aims to restore the proper anatomic and functional relationships on the dentofacial area, changing the relations not only of the facial bony structures, but the soft tissues as well.

4.2.2 Types of orthognathic surgery

4.2.2.1 Orthognathic surgery in the maxillary area

The most common type of surgery in the maxillary area is the Le Fort I type of osteotomy. This surgical procedure gives the surgeon freedom to relocate the maxilla in any direction of the three dimensions. It is also very usual for the maxillary surgery to be performed together with mandibular setback surgery, leading to optimal and stabile results.

The surgery follows certain steps and procedures when performed. Initially, there is the dismemberment of the soft tissues, where maxilla and nasal aperture are exposed. Around 35mm superior to the occlusal plane of the maxilla, an osteotomy of the posterior zygomatic maxillary buttress is performed. The osteotomy proceeds to the

thicker bony tissues of the buttress and to the narrow bone of lateral maxillary wall and continues by cutting the thicker bone of the piriform rim. Then, the cutting line continues to the junction of the maxilla and the pterygoid plate, followed by the separation of the cartilaginous septum of the nasal floor and the split of the bony septum and lateral nasal wall. This makes it possible for the maxilla to be freed from the pterygoid plates with the use of osteotome malleting. At this point, finger pressure applied at the anterior part of the maxilla is enough to perform a downfracture. After the maxilla is mobile, its final position is defined with the use of the surgical splint, designed by the orthodontist when the surgical treatment plan was made, and the two jaws are stabilized together with the use of wires or elastics. At this time, it is important that the bone and cartilage at the osteotomy's cutting line are adjusted in order to have an ideal contact area between the two parts and good aesthetic results. Finally, the transosseous fixation is performed with the use of bone plates, followed in many cases by bone grafting in the areas that it is needed for stabilization and lastly the wound is closed with a variety of sutures like V-Y mucosal (single or double), alar base cinch etc. (Proffit et al., 2003). This was a brief and basic description of the maxillary surgery procedure. For more detailed information, the reader can be redirected to orthognathic surgery textbooks, which can provide all the existing techniques and methods for this topic. (Proffit et al., 2003; Reyneke, 2010; Posnick, 2013).

4.2.2.2 Orthognathic surgery in the mandibular area

The main debate on orthognathic surgery in the mandibular area is the type of osteotomy that will be used for the mandibular setback. Intraoral vertical ramus osteotomy (IVRO) is still an option used in some cases, but the dominant osteotomy type nowadays is the bilateral sagittal split osteotomy (BSSO) (Monson, 2013). The BSSO was modified in the past in many ways (Hunsuck, 1968; Epker, 1977), leading to its current form which provides the listed advantages below (Proffit et al., 2007):

- Freedom of movements for the surgeon during repositioning. The surgeon can relocate the mandible forward or backwards or rotate the tooth-bearing segment down anteriorly according to the facial height's needs.
- It is highly compatible with the rigid internal fixation (RIF) techniques.

- An optimal and extensive bone-to-bone contact can be achieved after the fixation at the area of the osteotomy, which minimizes healing complications.
- It doesn't interfere in a big scale with the temporomandibular joint (TMJ) or the position of the masticatory muscles.

When it comes to the mandibular setback procedures, like in Le Fort 1 osteotomy, certain steps are being followed. First, the soft tissue incision is performed, followed by the elevation of the periosteum. This procedure gives the surgeon adequate access to the area in order to perform the osteotomy. The usual osteotomy pattern consists of cuts through the cortical bone, starting from above the lingula, on the medial side of the ramus, continuing down to the anterior part of the ramus onto the superior part of the mandibular body and followed by a curving inferiorly through the lateral cortical plate, including the inferior border. The osteotomy extends horizontally one half or two thirds of the anteroposterior dimension of the ramus posteriorly and as far as the second molar region anteriorly. Following the split of the ramus, the reposition of the mandible to its optimal position takes place, according to the surgical treatment plan. At this position, the mandible is sustained and fixed, mostly, nowadays, with the use of RIF due to the high effectiveness of this method (Proffit et al. 2003; Revneke, 2010; Posnick, 2013).

4.2.3. Facial soft tissues and interventions during orthognathic surgery

The procedure of orthognathic surgery is mostly focused on the bony tissues and the relocation of jaws, but the outcome of this procedure on the soft tissues shouldn't be underestimated, affecting the facial aesthetics and the stability of the result. At the time of the BSSO, there is always a possibility of the masseter muscles and the lower fibers of the temporalis muscle being stripped. Moreover, the medial part of the pterygoid muscle, the pterygomasseteric sling and the stylomandibular ligament are being stripped for optimal stability of the segments. The nasal region is also a primary concern during maxillary surgery. The final aesthetic outcome can be affected by interferences on the nasal septum, like the removal of the anterior nasal spine and the contouring of the piriform rim. Moreover, during the wound closure, the cinch and the V-Y lip closure suture are recommended, if the surgeon considers so

(Reyneke, 2010). Finally, a plenty of adjunctive procedures for aesthetic alteration of the nose, the chin, the neck and the lower face, the malar region or even the ears are available, in order to influence the final result on the soft tissues (Posnick, 2013).

4.2.4. The management of the nasal region

One of the areas that are greatly affected by the maxillary orthognathic surgery is the nasolabial region. The soft tissues of this area can be the subject to significant changes like elevation of the nasal tip (in cases of maxillary impaction or advancement), increased width of the alar base (after maxillary impaction), reduced length of the upper lip (after maxillary impaction), increased fullness of upper lip (after maxillary advancement) and increased upper lip length (after maxillary down grafting) (Reyneke, 2010). From all these, it becomes clear that the final soft tissue profile of the patient is not only determined by the hard tissue relocations, but also from the techniques used during the surgery to avoid undesirable side-effects. Examples of these techniques are the recontouring of the ANS area technique and a variety of techniques for suturing (alar base cinch suture, muscle resuturing etc.) and closures (VY lip closures, single or double etc.) (Proffit et al., 2003; Reyneke, 2010; Posnick, 2013). These techniques allow the surgeon, who will be the one to choose the most fitting one for each situation, to have a variety of options and modifications in order to guide him to an optimal final outcome. Therefore, the use of these techniques can't be systemized, as it depends on the surgeon's personal preference and experience.

4.2.5. Side effects of orthognathic surgery

An important side effect following the orthognathic surgery procedure is the postoperative swelling. The swelling, although it is severe and can affect the patient's perception about the surgery procedure (Neal and Kiyak 1991), is temporary and eventually withdraws. The swelling, as well as the muscle spasm (trismus), usually reach their peak from 48 to 72 hours after surgery (Al-Khateeb and Nusair, 2008) and have a great decrease during the first postoperative week (about 30%). After a 3 weeks to 1 month time interval, the remaining swelling is noted to range from 34% to 50%

and after a 3 month period this value drops to 5% - 20% (Yamamoto et al., 2016; van der Vlis et al., 2014; Kau et al., 2007). Some studies even note that a smaller amount of swelling can persist even 6-12 months after surgery (Day and Robert, 2006; van der Vlis et al., 2014).

Other side effects of orthognathic surgery can be pain, inflammation and a limited ability of mouth opening because of trismus (Phillips et al., 2008). Post-surgery pain peaks usually during the early post-surgery period and medications, commonly corticosteroids, are prescribed to relief from the pain (Schaberg et al., 1984; Weber and Griffin, 1994). Other options for medications are non-steroidal, anti-inflammatory drugs (NSAID) (Benetello et al., 2007), corticosteroids and NSAID combined (Bangbose et al., 2005) or enzyme preparations like serratiopetidase (Al-Khateeb and Nusair, 2008; Shetty and Mohan 2013). There were also non-pharmacological ways referred to relief from the side-effects of orthognathic surgery, such as manual lumph drainage (Szolnoky et al., 2007), soft laser (Braams et al., 1994; Røynesdal et al., 1993; Gasperini et al., 2014) and cryotherapy (Laureano Filho et al., 2005). The cryotherapy, or cold therapy, was used through the early ages and it is highly known for its beneficial influence on reducing post-surgical swelling, inflammation and pain, as well to the reduction of hematomas and bleeding. (McMaster and Liddle, 1980; Swanson et al., 1991; Rana et al., 2011; Moro et al., 2011; Abramson et al., 1996; Fruhstorfer, 1990; Schaubel, 1946). Moreover, it was shown that the low temperatures have a reductive effect on the activity of inflammatory enzymes (Abramson et al., 1996). There is a big variety of cooling methods, like gel packs, cold compresses or ice packs. On the other hand, side effects of cold therapy are also reported, like tissue injuries, disturbances of lymph drainage and microcirculation or chilblains.

4.2.6. Stability of the outcome of orthognathic surgery

One of the biggest concerns when it comes to orthognathic surgery, is the stability of its outcome, the presence or lack of relapse and the long-term preservation of the result of the surgery. Therefore, relapse can be observed in two types according to the time interval they occur, the immediate and the late relapse. Immediate relapse is usually encountered immediately after surgery and its cause is usually an error in

operation table, like a misplanning in surgical treatment plan, a wrong positioning of the temporomandibular joint or maybe inaccuracies in osteosynthesis. On the other side of the coin, a late relapse can appear after a noticeable time period has passed from the surgical procedure. A late relapse can be in the form of a partial or complete relapse towards the situation of the facial structures before the orthognathic surgery. Late relapse appears to have many reasons, like growth spurts, hard tissue remodeling due to the function of the masticatory system, an unstable occlusion after surgery or inability of the muscles of the face to adapt to the new relationships between jaws. Moreover, if a persistent habit exists at the function or at the orofacial muscle system, it can also be a cause of relapse (de Haan et al., 2013). It is reported that also sagittal corrections show more long-term stability than the vertical corrections of the jaws (Gallego-Romero et al., 2012).

4.3 Facial Asymmetry

4.3.1 Historical review of facial asymmetry

Since the beginning of mankind's recorded history, facial symmetry has been connected to concepts about facial attractiveness. Individual and collective concerns about facial attractiveness go back at least 4000 years ago, since the ancient Egyptian civilization. It is believed that Polycleitus, the ancient Greek sculptor, based on principles of the Egyptians, formed the first "neoclassical canons", coming from the word "kanones", meaning "rules" in Greek. These canons were defining the ideal proportions of the face, demanding the ideal face to follow the rules of symmetry with its division into two equal horizontal halves or three equal thirds, with the middle third being occupied by the nose. They also projected the ideal face to have equal distances between the same anatomical facial structures of each side. These canons are still in wide use in arts, like painting, sculpturing etc., but also still used as guidelines for plastic surgeons. Besides its ability to provide working guides for surgeons and artists, the neoclassical canons are not a reliable method of analyzing the human face in reality.

This brought us with two new approaches on analyzing the human face, the anthropometric and the cephalometric system. The anthropometric system was mostly based on hard tissue measurements, usually originating from skulls and there was a very few measurements that also included soft tissues. Most of the anthropometric researches were aiming to prove differences in the skulls of different human races, the ancestry of our skulls and the link between humans and apes, or even the superiority of the white humans against the black human population. From the other hand, the cephalometric system is mostly based on x-rays. It started from a simple dental analysis and proceeded to be a complex system for measuring the facial skeleton and even the facial soft tissues. The cephalometric system is widely used by orthodontists, surgeons and dentists nowadays, mostly for diagnostic and treatment planning purposes (Bashour, 2006).

4.3.2. Does facial symmetry equal to facial attractiveness?

There are 3 types of asymmetry in the human face, used to measure and describe the way the face is considered asymmetric. The term fluctuating asymmetry (FA) is referring to small and random traits in the general population, that make a face deviate in a small scale from the absolute symmetric face. The purely symmetrical face, for which the FA value is 0, is a very difficult characteristic to find in humans, so the FA value will almost never be an absolute 0. Another type of asymmetry is the directional asymmetry, which analyzes traits that show a significant size difference in either side of the face. The last type, the anti-symmetry, can be distinguished by bimodal distributions, due to adaptive functions at the face. Facial asymmetry can also be separated to static, where the face is analyzed in rest position, and dynamic, where the asymmetry can be apparent with facial expression.

It is found that in cases of a high degree of asymmetry, for example in cases of asymmetries due to chromosomal abnormalities, this asymmetry is linked with a lower attractiveness rate (Thornhill and Moller, 1997). The question of attractiveness is mostly debated when smaller degrees of fluctuating asymmetries are being observed, which can be connected to the asymmetries found in the general population. Many studies explored the presence of this connection by defining 12 and 14 landmark facial

points to assess the facial symmetry, showing a positive relation between symmetry and attractiveness (Hume and Montgomerie, 2001; Jones et al., 2001). More recently, other studies, by defining even more than 14 landmarks, assessed asymmetry and found more limited relationship between symmetry and attractiveness (Farrera et al., 2015), or even no significant correlation between them (Simmons et al., 2004). A study on 3D face scans found the attractiveness not to be influenced by the levels of symmetry (Kaipainen et al., 2015). Another study showed that faces presented fluctuating and directional types of asymmetry and concluded that the fluctuating type was related to attractiveness, while the directional type was not. A considerable problem with this type of studies is the 2D photos used to assess asymmetry. 2D photos can easily mislead the authors to believe in the presence of a higher degree of asymmetry, which can actually be caused by any head rotation, or head inclination to one side during the photo acquisition. For this reason, research with the use of 2D photographic images has not being an absolutely reliable method to assess facial symmetry and its link to attractiveness.

Photo manipulation, on the other side, has been proved to be a useful tool in our goal to discover the relationship between symmetry and attractiveness. Initially, the articles using photo manipulation were simply creating a symmetric face from a hemiface and the mirror reverse of it, which led to slightly unusual faces that the observers couldn't find attractive (Langlois et al., 1994). A solution to this came by Grammer and Thornhill (1994) by blending faces with each other in order to create more symmetric facial surfaces. These symmetrical faces were found to be more attractive than average. Other studies combined mirroring with blending of the faces and some of them found a connection between attractiveness and symmetry (Rhodes et al., 1998), although some came with opposite results (Swaddle and Cuthill, 1995). Lately, another method of photo manipulation appeared, by averaging the asymmetries of left and right side of the face while the initial texture map of the face stays the same. This way, the symmetrical images were created with big precision and led to a positive correlation between attractiveness and symmetry (Perrett et al., 1999; Little and Jones, 2006).

When it comes to the method of choice for evaluation of symmetry and attractiveness, two ways of questioning have been mainly used. The first way is to just present

symmetrical and asymmetrical faces to the observer and ask for their rating of attractiveness. This way supports the idea that when the attractiveness difference between symmetry and asymmetry is clear, there should be also fluency on distinguishing the more attractive face. The studies using these methods found a positive connection between symmetry and attractiveness (Grammer and Thornhill, 1994; Langlois et al., 1994; Perrett et al., 1999, Rhodes et al., 1998). The second way, named “2afc task of symmetry”, was to present the symmetrical and non-symmetrical face next to each other to the observer and ask for his preference in attractiveness. An add-on to this method was to also include score rating in order to find the difference in attractiveness with precision (Quist et al., 2012). These studies also showed a general preference for symmetrical faces. Finally, another study (Lewis, 2017) raised the question of how the ability of an individual to detect asymmetry in a face can influence the attractiveness rating, questioning the 2afc method for creating bias by drawing the observer’s attention towards a trait that in different situations would be ignored. They concluded that there is a significant ability of the observers to detect asymmetry.

4.3.3. Etiology of facial asymmetry

As well as the etiology of Class III malocclusion, facial asymmetry is also found to derive from a combination of genetic and environmental factors at the fetal, the infant and the adolescent time stages (Lundström, 1995; Pirttiniemi, 1994; Haraguchi et al, 2002).

It was reported that, except from mandibular prognathism, around 50% of skeletal abnormalities at the facial region can be attributed to inheritance, while the rest 50% may be attributed to environmental factors (Proffit, 2000). This makes it possible that inheritance can be blamed entirely for a severe dentofacial deformity (Mulick, 1965). When it comes to etiological classifications, asymmetry of the face can be distributed to 3 categories: the congenital asymmetry which arises prenatally, the developmental asymmetry which occurs during growth deriving from unknown etiologies and the acquired asymmetry, which can be the result of an injury or a disease (Hegtvedt, 1993; Cohen, 1995; Reyneke et al, 1997).

The congenital asymmetry is not common, but it can have severe effects on the form

and function of the face. For example, intrauterine pressure at the head of the fetus or birth canal pressure during parturition might end up in the molding of the facial bones and the skull, creating an obvious skeletal asymmetry on the face. Fortunately, in these cases, if the birth growth continues without abnormalities, the deformation ends up stabilizing or even better improving (Darras et al, 2015).

The developmental type of asymmetry is usually not connected to syndromes and its nature is idiopathic. It is not rare that a metabolically normal growing individual is affected by this type of asymmetry, which although it is not present during birth and infancy, it gradually develops, usually becoming noticeable in teenage years (Shah and Yoshi, 1978; Cheong and Lo, 2011). An unilateral vertical growth increase on the mandible can also cause maxillary compensatory changes that can show up clinically in the form of an occlusal cant in the maxilla. The more the unilateral growth of the mandible, the more the maxillary changes will be, due to its compensatory nature (Obwegeser and Makek, 1986).

The acquired type of asymmetry usually appears during childhood and can occur due to condyle fracture from a trauma. A history of trauma was observed in 14% of the individuals showing asymmetry (Severt and Proffit, 1997). These fractures can interrupt the normal growing pattern on one side of the mandible and cause an asymmetry due to the continuation of the normal development of the opposite side, which can cause the chin to deviate towards the fracture's side. The more early the incident of the fracture, the better the prognosis for the asymmetry will be (Proffit, 2000).

Another reason accused for causing facial asymmetry can be an abnormal muscular activity, as it can affect the formation of the bone at the areas where the muscles attach to the bony structures. Furthermore, muscles can affect the deposition of the bones and be responsible for their displacement (Gorlin et al, 1990; Proffit et al, 2000). This dysfunction of the muscles can be the result of some damage caused to their motor nerves. Therefore, the dysfunction or the atrophy of the muscles can cause underdevelopment on some relative facial parts, resulting in a deficiency in soft but also hard tissues (Washburn, 1946; Gardner et al, 1980; Byrd, 1984; Proffit et al, 2000).

4.3.4. Asymmetry prevalence on Class III patients

Asymmetry is a common finding in Class III patients. It was found that 23% of the orthodontic patients presented asymmetry which is clinically noticeable (Willems et al, 2001) and the same observation was made for the 21-38.6% of the patients who showed dentofacial deformities (Samman et al, 1992; Severt and Proffit, 1997; Chew, 2006). This percentage increases when we specify a group of patients with Class III malocclusion and prognathism of the mandible as it reaches the rate of 40-80% (Severt and Proffit, 1997; Willems et al, 2001; Haraguchi et al, 2002; Yoon et al, 2004; Chew, 2006). Facial asymmetry can also refer to occlusal cant, discrepancy of the zygomatic arch, deviation of the nasal tip or orbital dystopia (Severt and Proffit, 1997), which makes it even more vital to be examined in patients with Class III malocclusion.

It was found that the facial deviation was most commonly observed in the lower vertical third of the face, compared to the upper and middle thirds. Severt and Proffit (1997), in an examination of 1460 patients showing dentofacial deformity due to asymmetry of the face, reported that a percentage of 34% from the subjects showed clinical detectable types of asymmetry. Furthermore, patients with a Class II malocclusion presented lower rates of asymmetry, while patients with Class II skeletal relationship showed asymmetry percentages of 40%. The 74% of incidents of asymmetry were located in the lower third of the face, 36% in the midface and just 5% in the upper third of the face. This can be explained by the presence of the mandible, which is the only mobile part of the facial skeleton and its growth keeps on for longer time interval when compared to maxilla (Haraguchi et al, 2002; Kwon et al, 2006).

In the Japanese population, a study of 220 patients with Class III skeletal malocclusion showed 80% prevalence of asymmetry in the bony tissues and 56% prevalence in the soft tissues (Haraguchi et al., 2002).

Studies of fluctuating asymmetries have reported that it is a more common incident that the right half-face appears wider when compared to the opposite side (Shah and Yoshi, 1978; Burke, 1979; Koff et al., 1981; Farkas et al., 1981; Koff et al., 1985; Ferrario et al., 1993). This finding, though, was opposed by other studies, that found

equal dimensions on left and right hemifaces (Peck et al, 1991; Ferrario et al, 1995) or even the left half of the face to appear wider (Vig and Hewitt, 1975; Chebib and Chamma, 1981).

4.4 Methods for Three-dimensional Surface Acquisition and Analysis of the Facial Soft Tissues

4.4.1 Radiographic methods

The most usual radiographic methods for 3D soft tissue imaging used to analyze the results of orthognathic surgery are the Computed Tomography (CT) as well as the Cone Beam Computed Tomography (CBCT). Both of these methods have the advantage of being able to incorporate both the hard tissues and the overlying soft tissues in a single image. The main disadvantage, though, of these methods is the exposure of the patient to ionizing radiation during the time of the image acquisition.

4.4.1.1 Computed tomography

The computed tomography (CT) is a valuable tool for the medical sciences since 1967 when it was first introduced in the medical field by the name of Medical CT. It was Hounsfield, though, who developed the 3D version of CT (Xia et al., 2001; Kau et al., 2005; Swennen et al., 2005). CT scans have the ability to generate computerized three-dimensional images with the combination of radiographic methods with computerized volumetric reconstruction. By including information about both the soft and hard tissues, CT makes the superimposition of data of two different timings possible, with the use of landmarks on the hard and soft tissues as an anchor unit (Swennen et al., 2005). Moreover, it is possible for the user to enhance the 3D image with the use of many providing options such as opacity, brightness or specific area isolation, leading to the visibility levels that can provide the most information (Quintero et al., 1999; Swennen et al., 2005). Furthermore, the proper positioning of the head is not an issue for the CT scans, as the image is positioned later to the desired position with the use of the computer software (Swennen et al. 2005). In the field of orthodontics, CT scans haven't been used widely. This is mostly due to

their operation cost, the dedicated facility that they require and their cost-time efficiency, due to the “stack” of slices they require to compose the final image. But the main concern about CT is the patient’s radiation exposure which can’t be justified just for diagnostic purposes (Kau, 2010).

4.4.1.2 Cone Beam Computed Tomography

Cone Beam Computed Tomography (CBCT) became available for use later, during the 1990s period (Kau et al. 2005). The main advantage of the CBCT compared to the CT is the much less radiation the patient is exposed to, due to a single scanning rotation that is required around the head of the patient to get the final image (Mah et al., 2003; Kau et al. 2005; Swennen et al., 2005). This alone is enough to bring the CBCT in the spotlight in orthodontics, in diagnostic terms or in terms of research. The specified use of Craniofacial CBCT for the face, made it possible to develop features that could outrun the conventional CT in terms of craniofacial use. The CBCT uses an X-ray tube of low radiation and the produced beam is more focused and with a pretty lessened radiation scatter when compared to the conventional CT (Mah and Hatcher, 2003). This way, the volumetric scanning requires much less capacity from the X-ray tube and the utilization of the X-ray is importantly increased (Sukovic, 2003). It has been reported that the entire radiation of the exposure to a CBCT is equal to the one of a full series of periapical radiographs of the mouth and it is estimated to be around 20% lower than the radiation of a conventional CT (Mah et al., 2003). By the years, CBCT system’s size and cost decreased and became accessible to a bigger group of specialists. Also the addon of a custom-made exposure chamber reduced even more the radiation exposure. These days, when comparing the quality of the CT and CBCT images, not so much diversity can be noticed as CBCT is able to provide a view of the full head, the skull or selective regions (Kau et al., 2005).

When it comes to the limitations, CBCT is still lacking in the exact mapping of the muscles and the muscle’s attachments. To image these structures without any radiation, a magnetic resonance imaging (MRI) can be used with success. Also, in a CBCT scan, the soft tissue are not displayed in the true texture and color of the skin.

(Khambay et al. 2002) For that reason, 3D devices such as stereophotogrammetry or laser scanning have still be preferred for the soft tissue imaging.

4.4.2. Non radiographic methods

This section will be dedicated to present a synopsis of the different devices that can be used for the 3D image acquisition of the face and their pros and cons will be analyzed. These devices can be categorized as shown in Table 1.

Table 1: A categorization of the devices for 3D surface acquisition (Kau and Richmond, 2010)

Photogrammetry	Traditional stereo-photogrammetry
Lasers	Fixed units Medical Graphics and Imaging Group, UCL Cyberware Laboratory 3030/SP Others Portable and mobile Minolta Systems (Model 700, 900, 910, 9i) Polhemus hand-held (Fastscan)
Structured light	Single camera Multiple camera Moiré patterns OGIS Range Finder RFX-IV CAM, three-dimensional Shape system C3D-dimensional stereo-photogrammetry (Glasgow) – computer aided 3dMDface system Others
Video-imaging	Motion-Analysis
Radiation sources	Three-dimensional cephalometry Computed tomography scans Cone beam computed tomography
Others	Magnetic resonance imaging Ultrasound

4.4.2.1 Stereo-photogrammetry

Photogrammetry refers to the act of measuring photographs. For the last 80 years, photogrammetry has been widely used in dentistry and generally in medicine to recreate from photographic proliferations the 2D or 3D measurements (Berghagen, 1951; Richmond, 1984). This method was standardized after modification in order to measure specific anthropometric dimensions to an accuracy level close to the direct methods. For stereo-photogrammetry, at least two cameras are used in a stereo-pair configuration to be able to capture 3D coordinates from the morphology of the face. This way multiple photos are combined together and a 3D image is created (Kau, 2010). In the early photogrammetric days, a 3D mapping of the facial structures was costly and laborious so cartographers' techniques were used in order to combine contour mappings and varying subintervals (Burke, 1984). These methods had been also used for the surgical correction of abnormal faces by volumetric and biostereometric analyses (Bjorn et al., 1953; Berkowitz and Cuzzi, 1977). In 1967, a new method was introduced, that made it possible to project the face with a radial grid (Beard and Burke, 1967). This provided the user with plentiful points that combine correspondence and facial measurements. For this, a pair of stereometric cameras were combined with a special type of flash unit which was mounted in between the two lens systems. The pair of semi-metric cameras were mounted to a frame 50cm apart with a 15 degrees convergence angle and a flash unit in between to project a grid to the face (Ras et al., 1995). This grid aids the two photographs' registration and creates a depth perception. The described systems were run through validity and reliability tests and were used on cleft lip and palate patients and for facial asymmetry analyses.

4.4.2.2 Laser scanning

Laser scanning is a method used wisely in engineering nowadays in order to obtain three-dimensional data from items (Blais, 2004). The advantage of the laser scanning is the ability to detect even the tiniest of microscopic defects in aerospace and automotive industries.

The laser technology was implemented with optical principles which can be recognized as a stereoscopic method that facilitates the distance calculation from the object with a use of a directional light source combined with the use of a detector. A laser light source then illuminates the face and the reflected light is being captured by digital cameras. Afterwards, the laser beams is leaded towards the scanning object by being “deflected” through a mirror and with the use of triangulation geometry, laser beam’s final deflection angle is obtained. When the laser beam reaches the physical object, it is scattered and this procedure is captured by a detector. Geometric principles are being used to calculate the distances between the detector, the object and the source and the data are translated to coordinates (x-,y-,z-).

According to the mechanism of beam production, the laser devices used for 3D scanning can be categorized into two groups: slit and single point scanners. The slit scanner is a preferred solution when it comes to facial scanning, due to its mechanical and optical simplicity, as well as the lesser time it takes for scanning an object than the single point scanner (Blais, 2004). Another division of laser scanners is fixed scanners and portable-mobile scanners.

4.4.2.2.1 Laser scanners with fixed units

The first attempt for facial scanning was done by Moss and his co-workers in 1989, introducing the Medical Graphics Imaging (MGI) system. For this system, the laser beam used was low-power, helium-neon, which was projected to the facial surface and was observed through a television camera in an oblique angle. It had a wavelength of 632,8 nm and its power not was exceeding the 1 mW. For every 2,8 rotation degrees, a scan of the subject was performed and when the scanning was reaching more central portions, this was changing to every 1,4 degrees. This leded to

a sum of around 20.000 coordinate points with a quoted precision of 0,5 mm. The skin was exposed to the laser beam for a period smaller than 10 mins (Moss, 1989). The system had an independent validation within 0,9 mm and a reproducibility of the facial morphology of 1 mm for an average adult face. (Aung et al., 1995; Ismail et al., 2002). This method had a major disadvantage of the long time needed for a scan to be completed, being around 20 seconds.

Another model of a surface laser scanner became available for the public by Cyberware Laboratories. The scanner was called Cyberware Laboratory 3030/SP and was able to project a low-intensity laser beam onto the object in order for a highlighted profile to be created. Afterwards, a high quality video sensor was used to capture this profile from two view-points. In order for the whole object's shape to be captured, the system was digitized thousands of the highlighted profiles within seconds. Simultaneously, a secondary video sensor was collecting color information. This scanner had the capability of capturing 262.144 points and each of them could be defined by space coordinates and RGB color values.

When the validity of this device in the measurement of anthropometric landmarks was tested, issues like motion artifacts, inaccuracy in the process of digitization, biologic variation and poor identification of landmarks came up (Bush and Antonyshyn, 1996). The ideal positions were met when the position of the head was in the midpoint of the gantry used for scanning and when the Frankfurt horizontal plane appeared to be around 10 degrees higher than the horizontal plane. In these conditions, the full range of measured landmarks were optimally visualized and the localization variance of the landmarks was lesser than 0,6 mm on the three axes of space.

This scanner was later used for superimposition of 3D images onto CT images (Girod et al., 1995) and for the creation of facial contours, units and subunits (Okada, 2001). This was achieved by defining shadows, highlights and borderlines between areas as described by a technique from Barnett and Whitaker (Barnett and Whitaker, 1986).

A different research group made a use of this system like a Playstation ® motion platform, measuring data of the area, as well as volumetric data from patients with facial swelling (Ji et al., 2002). These data were transferred then to a design program aided by computer in Microsoft Windows environment. This software used the face of the patient as a symmetry axis and a specific reference point for symmetry was

acquired from both hemifaces. The facial area of the patient was calculated with the use of triangulation mechanism (Ras et al., 1995), but, unfortunately, the method of this calculation was not clear. This scanner was also used by Guest and his co-workers to evaluate the methods for superimposing soft tissue changes following orthognathic surgery (Guest et al., 2001).

4.4.2.2.2 Portable or mobile laser scanners

The first attempt to a portable laser scanner was the VI-digitizers by Minolta (Minolta Co, Ltd, Osaka, Japan) in 1997. Their moto was that those products were about to “revolutionize the way surface imaging was carried out” (Minolta, 2001). The 3D image acquisition with those noncontact systems was rapid, making its use possible in applications in the medical fields like maxillofacial surgery and orthodontics.

Minolta VI-700 was the first scanner of these series of digitizers. It could detect the object scanned by the triangulation of the distances of the laser beam and the scanned surface, width, depth and length and its reliability to reconstruct a 3D object was evaluated independently (Kusnoto and Evans, 2002). Tests for its reproducibility and accuracy were performed on dental study models, geometrically calibrated cylinders and plaster facial models at different distances between the scanner and the object. It was reported a 0,5 mm accuracy vertically in calibrated cylinder test and 0,3 mm horizontally, a molar width accuracy of 0,2 mm and a palatal depth accuracy of 0,7 mm at the dental study model test. The accuracy of the facial model was 1,9 mm. According to these results, this scanner has a big research potential due to its accuracy and its easy usage. (Da Silveira et al., 2003). This scanner had also been used to integrate 3D facial shapes with shapes of the dentition (Nagao et al., 2001) and on idiopathic scoliosis research (Hill et al., 2002).

Four years afterwards, an advanced version of this scanner was released by the same company, the VI-900. The manufacturing accuracy of its camera was reported to be 0.1mm. The laser emitted was class I, which makes it safe for the eyes (US Food and Drug Administration) and its wavelength was 690nm at 30 mW. The distance between object and scanner could range between 600-2500 mm and its scan time was 0.3 seconds in fast scan mode. The scanner used a one-half-frame transfer, charge-coupled

device and the data points it could acquire were around 307.000. The system's output data was 640x480 pixels for 3D data and the color data were RGB (Kau, 2010).

In the 2004 - 2005 period, Minolta released the newer models of the series, Minolta VI-910 and 9i, respectively. Although the operation principles were similar to the previous models, they came with extra features for faster scanning, better image resolutions and higher photorealistic quality.

A new scanner introduced is the Fastscan scanner (Polhemus Inc, Colchester, VT, USA), which has a lighter weight, is hand-held and can produce a laser beam with the wavelength of 670 nm. It is carried across the scanned object by the user in a spray-painting resembling way. It comes with a pair of optical cameras, symmetrical to laser generator's two sides in order to collect the laser beam's distortions. A device for electromagnetic tracking measures the location in the space. This device creates no need to use any rigid fixation or tripods. The scanning takes about 10 to 15 seconds to be finished. This device was used to study the swelling on the facial area following the surgical extraction of wisdom teeth (Kau, 2010). It has been reported an error in scanning of 4% in the volumetric data of swelling and issues about patient's head position (Harrison et al., 2004).

4.4.2.3 Structured light technique

The structured light technique is one more large division of systems for 3D data acquisition. Its philosophy follows the triangulation principles. The common procedure is that a "structured" light beam will be shined onto the target surface in order to scan the physical object. By the time the light beam illuminates onto the surface of the object, it is scattered. Those distorted and reflected patterns are then captured under a certain angle by a scheme of cameras in a fixed formation. This procedure uses the translation of the data to calculate final 3D coordinates.

4.4.2.3.1 Systems with a single camera

The first attempt to a single-camera system was in 2001, when Tuncay and his co-workers released a series of 25 dissimilar, high-density patterns of structured light that were evaluated with the use of a mannequin model which consisted of one skull, dressed in latex (Tuncay, 2001). The 3D imaging system consisted of one black and white charge-coupled camera and one monochrome display projector from liquid crystal, plugged into a Macintosh computer. The projectors and the cameras were located at an angle of 30 degrees from each other and the described mannequin model was being rotated for 180 degrees with 10 degrees increments. Although this method came with satisfying results, the systems accuracy dropped drastically when used on a human face (Nguyen, 1999; Tuncay, 2001).

Another system with a single camera was constructed by Enciso and his coworkers, including one digital camera, one slide projector and a pattern for calibration (Enciso et al., 2003). A digitizer was used for validation, they plotted the landmarks and calculated the linear distances between the distances produced by the image and the distances in reality. This system's error was found to be 0,48 mm to 1,55 mm.

4.4.2.3.2 Systems with two or more cameras

4.4.2.3.2.1 Moiré fringe patterns

One of the first attempts to use the structured light method to utilize “moiré” fringe patterns was described by Takasaki (Takasaki, 1970). By moiré topography imaging, we are referring to a technique for contour-mapping. What happens is that a “grating” is positioned near the object and through this grating, its shadow on the object is being observed. This results in moiré fringes that create a system of contour line from the object, under specific conditions.

A similar system was reported later, but with the use of a three-directional camera (Motoyoshi et al., 1992). These cameras were located “straight on” the patient with an angle of 45 degrees. A grating system was used to illuminate the facial surface, which

was captured from three shutters that were being controlled at the same moment. Unfortunately, the surface texture produced was not photorealistic and the surface reproduction of sharp features gave questionable results (Hajeer et al., 2003).

4.4.2.3.2.2 OGIS Range Finder RFX-IV

Another system used for 3D imaging of facial surfaces was the OGIS Range Finder RFX-IV, that consisted of a range finder by liquid crystal (OGIS Range Finder RFX-IV; OGIS Research Institute Co Ltd, Osaka, Japan). It was basically a light-based system and its resolution was around 0.4 mm. With this system, it was possible to measure more than 30.000 points in one second, originating from the whole facial surface. The facial landmarks were identified by the use of the software developed for this purpose, which was using 3D curvatures in addition to linear distances, as well as the discriminant analysis for the RGB information. C language was used for the software and the data were being extracted with a graphical interface build from X11.3 methods. This system only reached the stage of beta version (Kau, 2010).

4.4.2.3.2.3 CAM 3D systems

This system was another version of a structured light system (Nkenke et al., 2003). The structured light produced by the CAM 3D system (CamSorik GmbH, Braunschweig, Germany) followed a sequence of phase-shifted fringe patterns that were projected onto the object. Two charge-coupled device cameras was used to record the data, that are subsequently evaluated with a four-shift algorithm in order to get the final 3D data about the shape of the surface of the object.

4.4.2.3.2.4 C3D systems

The C3D system had been extensively researched from a group of maxillofacial surgeons and orthodontists (Ayoub et al., 2003; Ayoub et al., 1998; Ayoub and Stirrups 1993; Ayoub et al., 1997; Ayoub et al., 1996; Bourne et al., 2001; Hajeer et al., 2002; Hood et al., 2003). This systems uses a couple of stereo-pair

cameras, positioned on each part of the face of the patient. Under the control of a computer, a pattern of random texture or an untextured natural illumination is projected towards the facial surface. This way, corresponding points are found and the images can be lined up. This procedure of identification of corresponding points is named image matching, carried out from an automatic correlation from a computer. This technique produces parallel measurements group from every point in each stereo-paired images. The parallel measurements are subsequently translated into distances from the surfaces that were imaged with a process build on triangulation. This is called space re-section, which was a big step towards capturing the depth from a stereo-image. Before use, it is mandatory for the camera to be calibrated, which is called space intersection. This 3D system was tested on surgical orthodontic patients, infants and study models with success (Kau and Richmond, 2010).

4.4.2.3.2.5 3dMD system

The 3dMD system (Atlanta, GA, USA) is the combination of structured light technique and stereo-photogrammetry. It has a high quality capturing power, producing photorealistic pictures with the use of multiple cameras. Three cameras are used in every side of the face, two infrared and one color camera. The system projects a light pattern of random texture onto the subject and various digital cameras in different angles, located in an ideal formation are capturing the image simultaneously.

4.4.2.3.2.5.1 The technical parts

3dMD face System is a unit that has the ability to capture simultaneously more than a couple of images of the face and to create, after the data are being processed by a computer, a 3D representation of these images. This 3D image can be used and manipulated for many analyses and measurements. This sophisticated system can consists of a couple of modular camera units (MCUs) of machine vision cameras, a lightweight plate for calibration, a tripod and a tripod head, three external flash units, a computer workstation, monitor, keyboard and mouse, cables and connectors, a power supply and a power cord, as well as the software used for image acquisition and editing

(3dMDacquisition Software and optionally the 3dMDpatient Analysis Software, 3dMDImage Viewer and the 3dMDvultus Software). The MCU has the dimensions of 60 mm x 222 mm x 338 mm and its weight is not more than 3kg. There are two pods that consist the imaging part of the system. Each of them consists of three digital cameras (one machine vision color camera for texture and a pair of machine vision stereo cameras for geometry, a speckle projection lens and the flash panel).

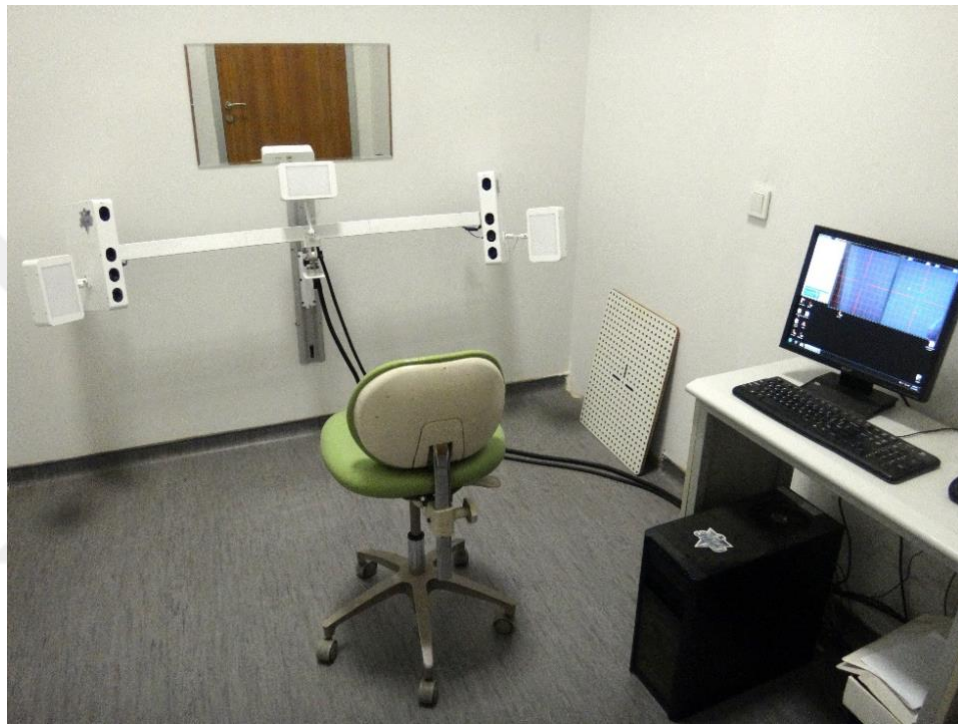


Figure 1: 3dMDface System (Atlanta, GA, USA) - Multiple camera system with structured light patterns to obtain a 3D image.

4.4.2.3.2.5.2 The procedure of image capturing

As instructed by the manufacturers, in order to capture an image of the object, it is positioned in distance around 95 cm from the modular units. The head, then, should be well fitted into the two viewpoint windows from the two cameras, shown in the computer monitor. The facial surfaces should be clearly visible in every camera view in order to achieve best coverage. The face should also be in the center of the window in the horizontal and vertical aspect. In order to have a better capturing of the area under the chin, the manufacturers suggest the head to be slightly extended. Any

accessories like eyewear or jewels should be removed prior to image capturing in order to have a better view of the area of the eyes and ears. Same counts for collars, clothing or necklace that covers the neckline area (Heike et al., 2010). It can also be helpful for the subject the use of a stocking cap for the better capturing of the head's shape. This should be performed with caution, in order for the skin to not be tensed, which can have an effect on the surface of the face (Heike et al., 2009).

The natural head posture is preferred during the acquisition of the image, due to its clinical reproducibility (Chiu and Clark, 1991; Lundstorm et al., 1995; Deli et al., 2013). Optimally during the image capturing, the subjects should make an effort to keep a neutral and relaxed expression of their face (Oh et al., 2008; Bush and Antonyshyn, 1996; Ferrario 2003; Hammond et al., 2004; Sforza et al., 2004).

Additionally, the operator should be the one who will also observe the mouth and the eyes of the subjects to be sure that there is no evident signs of tension on the face or expressions of emotion (Hajeer et al., 2004; Ozsoy et al., 2009; Sawyer et al. 2009). The mouth should be closed and the lips should be pressed together gently, otherwise it can lead to an increase to the vertical facial height and a differentiation in the position of the mandible. The closed mouth helps also in the positioning of the mandible to a resting posture in most of the cases. It is suggested that a visual target like a mirror could be of use to help the subject to target their gaze to an ideal direction and maintain a favorable expression and posture (Kau et al. 2006).

When on highest resolution, the image can be captured in 1,5 milliseconds, making this system proper for patients who lack cooperation like infants or babies with clefts (Lee, 2004; Honrado et al., 2006). The accuracy of the system is reported to be less than 0,5 mm according to the manufacturers and the clinical accuracy around 1.5% from the whole variance observed (Aldridge et al., 2005). It is possible for the operator to process the information directly and observe the system using the triangulating principles to resolve the imaged geometry from a different viewpoint of each of the four cameras. The areas of the geometry of the subject that the system has resolved in a precise triangulation can be observed on the monitor with a green pattern display. Subsequently, the software of 3dMD picks the most fitting data automatically from each viewpoint among the cameras. When the operator can not see those green indicators on an area, the capturing should be renewed, since the position of the subject

might have not been proper. Finally, the texture and the color of the soft tissues are layered on the wire frame.

4.4.2.3.2.5.3 The working principles

The technology used in 3dMD can be described as “active stereophotogrammetry” with the projection onto the subject of a random light pattern (Weinberg et al., 2006; Lane and Harrell, 2008; Tzou et al., 2014). This process can be exploited in order for a high-accuracy and high-quality image to be captured. A pair or more of synchronized cameras can be used for the recording of the images from various viewpoints and angles. Beforehand, a calibration is being performed with a use of objects with well-known geometry and dimensions. This calibration supplies the system with mathematical data in order to acquire a favorable stereoscopic reconstruction for the facial surface. The facial texture is also possible to be recorded by the system through a combination of 3D data with a detailed recreation of the characteristics of the whole facial surface. There is a group of numerous lights and cameras, positioned around the subject. These cameras are able to capture the subject’s images from different angles simultaneously. The positions of these cameras, as well as their focal lengths are already known, which makes it possible for all the picture to be combined into one final 3D image with the use of the computer software (Ayoub et al., 1996; Halazonetis, 2001; Cakirer et al., 2002; Hajeer et al., 2002; Ayoub et al., 2003; Hajeer et al., 2004; Swennen et al., 2005). The system is also creating 3D coordinates for every two dimensional point that is visible in the two cameras. That process is named triangulation. Another advantage, that this system has, is the use of its own projected light pattern, which makes it not dependent on extra light source or sensitive to ambient light (Lane and Harrell, 2008).

4.4.2.3.2.5.4 The process of the 3D model

After the capturing and the processing of the 3D image, the 3D model of the facial surface becomes available to the monitor of the operator for examination from all possible angles and manipulation. That 3D surface model can be measured in many ways, such as linear, volumetric, angular or surface measurements. Furthermore, the superimposition of two models, acquired in different timings is possible and from the soft tissue variations between them, color-based histograms can be formed. The registration of the two models can be either by specific points or surface, but there should be caution to not select points or regions that were the subject of an intervention during the therapeutical procedure (Lee, 2004; Honrado et al., 2006). Lastly, there is an option provided by the system to export the 3D data in the desired format by the user (e.g. stl file) in order for it to be used or imported to a different software.

4.4.2.3.2.5.5 The natural head position

The term natural head position (NHP) was first established in 1862 by Broca (Broca, 1862), described as the position of “when a man is standing and his visual axis is horizontal”. This definition was modified in 1958 by Moorrees and Kean (Moorrees and Kean, 1958), described as “a standardized and reproducible orientation of the head in space when one is focusing on a distant point at eye level”. There are multiple studies confirming that NHP of the patient shows stability sagittally. It was found that there can be a possible deviation from 1,3 - 2 degrees by Bjerin (1957) and Moorrees and Kean (1958), and 1,5 to 2 degrees from Lundstrom et al. (1995) by the evaluation of deviations arising from lateral cephalograms in combination with photographs and a 1,9 degrees deviation by Cooke and Wei (1988) with a use of a mirror to help the orientation. This study was repeated after 15 years, reporting a deviation of 2,2 degrees when compared to the initial measurements (Peng and Cooke, 1999). The majority of studies until now reported that NHP is a reproducible method, except the study of Vig et al.(1980) which showed that patients who have a total nasal obstruction can present

higher deviations. In another study, Achilleos et al. (2000) showed that orthognathic surgery can cause deviations to NHP due to the physiologic adaptation of the patient to the surgery. Nonetheless, after one year since the surgery is performed, the NHP returns to the original position.

Although NHP has been proven reliable in the sagittal plane, it was not proved reproducible in the axial and coronal plane. It was until 2013 that Weber et al. tested if the NHP can be reproducible in all of the three planes of space. They used five different time points, ranging until one week after the initial measurement. They concluded that the differences between these five time points were not significant statistically in any plane of space. The only statistically significant variation was found when the mean angular deviations of all three planes were compared. The final conclusion was that NHP has a sufficient reproducibility in all planes and showed the lesser deviations in the coronal plane and the biggest deviations in the sagittal plane.

4.4.2.3.2.5.6 Scientific validation of the 3dMD face system

The 3dMD system was tested for its accuracy and precision by Luebbers et al. (2010) with the use of a phantom, under optimal conditions. A simulation of unpredictable clinical conditions was created with the change of different parameters such as distance, angle or system registration. There was no handling issues encountered by the system and the mean global error was around 0,2 mm. These parameters were not influenced by any head or camera position. Additionally, the new procedure for referencing did not affect also the accuracy and the precision of the system, that were reported to be adequate in a big scale for the clinical requirements and still advantageous over other techniques, such as 2D photographs or direct anthropometry. The sum of the errors occurred were insignificant and they concluded on the suitability of the system for documentation and evaluation of the surface of the face, appearing very promising for research in surgical procedures.

In a study, six different systems for 3D imaging were evaluated for accuracy and precision for the implementation of various scanning principles (Eder et al. 2013). The systems were tested on areas of complex anatomical levels. To test that, they used five skulls from sheep of various ages, and used 3 areas of different complexity. Area 1

was a high complexity area, area 2 presented moderate complexity, followed by area 3 of low complexity and smooth surfaces. They used 20 landmarks on each skull, resulting in measurements for 56 distances. The means of these measurements were compared. They used 3 methods for measurements: measurements from computer tomography, from coordinate machine and manual measurements. They used a variety of six 3D optical surface devices for imaging: 2 laser scanners, the FastSCAN™ (Polhemus Inc., Colchester, USA) and the Vivid 910® (Minolta Co., Ltd., Osaka, Japan), 3 fringe light projectors, the Comet® Vario Zoom 250 (Steinbichler Optotechnik GmbH, Traunstein, Germany), the PRIMOS® body and the TopoCAM® scanner (both GFMe- stechnik GmbH, Teltow, Germany). The 5 systems mentioned use the active triangulation principle. The last scanner is the DSP 400® (3dMD, Atlanta, USA), which is ideal for medical applications and uses the concept of passive triangulation of photogrammetry. The 6 systems were used to take five images of the sheep's skull in a standard and reproducible position to optimize data acquisition. The most accuracy was shown by the Vivid 910®, the DSP 400® and the Comet® Vario Zoom scanners, in all areas of all different complexity. Specifically, the highest accuracy in average in area 2 was measured by the DSP 400®, with the Comet Vario® Zoom coming second. The lowest accuracy was observed on FastSCAN™ in comparison to the rest of the scanners in every area examined ($P > 0.05$). Generally, the higher the surface complexity in an area, the lowest the 3D accuracy was observed. Moreover, a regression analysis was used for the evaluation of the scanner's accuracy of measurements according to the length of every distance measured manually. The DSP 400®, the Comet Vario® and the Vivid 910® showed the best agreement in respect to the whole length. Higher distances in average when compared to the manual measurements were observed by the FastSCAN™ system. Besides the FastSCAN™ and the DSP 400®, every other scanner reported a bigger difference in measurements when it came to short distances, and smaller differences when long-distance lengths were measured.

Another study, the 3dMD face system (Atlanta, GA, USA) was evaluated for the quality of its inter-rater accuracy in facial measurements on 3D facial images of adult individuals (Nord et al. (2015)). Although the precision of the 3dMDface system is known to be below 1 mm, they expected that the reliability of some landmarks may

not be ideal (Weinberg et al., 2006; Luebbers et al., 2010). The 3dMDface system was used to capture the photographs of the 8 subjects of this study. A room ideal for clinical photography was used without the use of natural light from any source, by the use of 2x4 sets of compact fluorescent lights. Two authors of the study marked 27 anatomical landmarks without interacting with each other with the use of the 3dMD Patient software. The two operators had not any previous experience with the system, similar systems or anthropology generally, but they only received a small introduction on the hardware and on the use of the software. The two operators, who were blinded from each other during the process, repeated the procedure of landmark placing six times, giving them 1296 variables for every operator. There was no significant difference statistically for the intra-examiner and the inter-examiner variability. The analysis showed that there were almost identical marks for every landmark placed by the two operators, as well as for the same operator on different days. They came to the conclusion that the 3dMD face system is capable of providing high level 3D virtual models for technical precision and that the system shows a high reliability when it comes to landmark identification. Besides this, they suggested the use of palpation of the real facial surface in order to easily identify some classical landmarks with the help of the underlying bone morphology, indicating a lesser reliability of these landmarks in the 3D models.

In a different study, the 3dMD DSP400® stereo-optical 3D scanner (Atlanta, GA, USA) was tested for its validity and reliability in vitro and in vivo from its ability to assess the swelling of the face and the changes in the volume of the face. 24 volunteers with and without any artificial swelling in the cheek area were scanned in vivo, two times in the morning and two times in the afternoon. Additionally, they scanned the head of a mannequin, in vitro, with or without the presence of various kinds of artificial swelling, which was applied externally. The differences in volume or due to artificial swelling in the cheek area were measured with the use of the 3dMD Vultus® software. Intraclass correlations of 0,89 and 0,99 were found for the in vivo and the in vitro measurements' reliability, respectively. They reported also the repeatability coefficients to be 1,3 ml and 5,9 ml for in vitro and in vivo, respectively. In vivo measurements showed a 1,2 ml decrease in volume and the in vivo a 0,2 ml decrease as well. In conclusion, the reliability and validity of the 3dMD system was proved for

a minimum of 5,9 ml on the volumetric facial differences, as well as for its ability to assess the facial swelling.

A study by Metzger et al. (2013), did a comparison between the data of the soft-tissues acquired from 3dMD (Atlanta, GA, USA) and from CBCT from the segmentation of soft-tissues, in order to examine the accuracy and the interchangeability of these two methods for the treatment planning of aesthetic issues in orthodontics.

They acquired an amount of 70 facial images from 3dMD and CBCT scans from the same faces within a time interval of some minutes. Afterwards, they registered and superimposed these scans with the use of the 3dMD Vultus software. With the use of these two imaging modalities, they obtained and analyzed the equivalence of 28 measurements from the soft-tissues. They found the differences to be statistically significant for mouth width, vermilion height, mouth symmetry, eye symmetry, total facial width and soft-tissue lip thickness measurements. Except of these areas, the differences between the two imaging methods were accepted as clinically unremarkable, from an orthodontic viewpoint.

Another study was made by Aldridge et al. (2005), reporting the 3D images captured with 3dMD system (Atlanta, GA, USA) of high repeatability, precision and comparability with different systems. They reported a very low error of digitization and observer error. They also noticed the lower precision of the system on some landmarks due to specific axes and due to the lower compliance on retaining the exact facial expression of the children in the group. They observed a small increase in their errors of the findings.

4.4.2.3.2.6 Video imaging

Another philosophy in 3D data acquisition is the 3D motion technique. This refers to the recording of a number of frames that are being captured every second with the use of a video camera, added to the original light-based systems. Possibly the earliest study on the 3Dmotion technique was conducted by Caruso et al. (1989), who proved the possibility of using 3D landmarks during a video capture in order to track jaw and lip movements during function. The first validation of a motion system was validated by Trotman et al. (1996) and this method was also used to measure facial

animations, movements of the soft tissues (Gross et al., 1996) or expressions of the face (Trotman and Faraway, 2004). The Motion-Analysis system (Motion Analysis Corporation, Santa Rosa, CA, USA), consisting of three video capturing cameras of 60 Hz, was used for the recordings. For the landmark marking on the face, reflective markers were used and the subjects were requested to follow various preassigned facial motions. From the analysis of the maximum motion amplitudes, it was shown that the 3D data can reach up to a 43% increase when compared to 2D (Gross et al., 1996). The results have also implied the landmarks during animations to be reliable for the full range of the motion in a moderate-to-excellent level. This system was also used for interlandmark and vector variations (Nooreyazdan et al., 2004; Trotman and Faraway, 2004) as well as for facial shape and gender analyses (Weeden et al., 2001). Later on, sound and virtual animation were added to the capabilities of the technique (Deng et al., 2006). Lastly, Eian and Poppele (2002) made another variation of the technique, by the use in their system of only one video camera, run by complex algorithms.

4.4.3 Analysis of 3D data

4.4.3.1 Analysis of asymmetry

A three-dimensional object can be considered bilaterally symmetric if a plane exists so that the reflection of the object is invariant to it. Hence, it is of major importance a plane like this to be calculated. For the calculation of the facial symmetry, a mid-sagittal plane (MSP) is being used for this purpose. Most of the algorithms used for symmetry extraction are intended for 2 dimensional applications (Liu et al., 2003; Reisfeld et al., 1990), but there are a lot of techniques, lately, designed for 3 dimensional application (Benz et al., 2002; Kazhdan et al., 2003; Minovic et al., 1992; O'Mara et al., 1996; Tuzikov et al., 2002). The two traditional methods for analyzing the hard-tissue symmetry are the panoramic and posterior- anterior radiographs. Also photographs and anthropometric methods had been in use for the evaluation of the asymmetry in the soft-tissues. It is clear that, the analysis of a three-dimensional concept like facial asymmetry on a two-dimensional level can cause losses of data.

The facial symmetry is most commonly assessed in 2D and 3D with landmark-dependent methods. Landmarks are marked in the same facial structures in each hemiface and through their distances, a degree of asymmetry is calculated. However, these methods have been widely questioned because of unreliability in the identification process. The landmarks are often not exactly marked in the middle of the facial surface, resulting in inaccurate MSP. Moreover, these methods are not capable of the asymmetry detection in areas where there are few landmarks and far between (Hartmann et al., 2007; Stauber et al., 2008). Due to these reasons, many researchers became interested in the development of surface-based and landmark-independent methods for the calculation of the facial asymmetry, that are based on thousands of points from the facial surface, allowing them to perform an analysis of the full face. This made methods like the facial maps with colored deviation or the analysis of the differences in the facial surface widely used recently. These methods can provide a clearer idea on the amount and localization of the facial symmetry, creating a basis for the improvement of the diagnostic and therapeutic tools available (Thornhill and Gangestad, 1999). The Interactive Closest Point algorithm (ICP) and the Procrustes analysis (PA) are two common methods to compute the mid-sagittal plane for 3D data. The ICP method is used for the alignment of 3D models based purely on the geometry of the two facial surfaces. The PA method is a morphometric approach for the determination of a MSP with the use of visually intact areas, not affected by the asymmetry as the reference.

5. MATERIALS AND METHODS

5.1 Patient Selection

For this retrospective study, 3D stereophotogrammetric images of patients with Class III skeletal relationship were captured. All these patients underwent a double-jaw orthognathic surgery with maxillary Le Fort I, mandibular BSSO osteotomy type operations and were treated in the Department of Orthodontics, Faculty of Dentistry, Marmara University.

The patients were chosen from the archive data of Marmara University, Faculty of Dentistry, Department of Orthodontics. This study's inclusion criteria included all Class III patients who underwent bimaxillary orthognathic surgery and had complete treatment and diagnostic records. The exclusion criteria were the presence of anomalies, including also patients with cleft of lip and palate, craniofacial syndromes, patients with a different skeletal relationship than Class III, patients with Class III skeletal pattern that underwent single jaw surgery and patients with incomplete or of poor quality records. Following these criteria, 40 patients (19 males, 21 females) were selected from the archive data of Marmara University, Dental School, Department of Orthodontics, Istanbul, Turkey. All patients underwent the bimaxillary surgery procedure between April 2012 and November 2018 by various surgeons in different healthcare facilities. The maxillary advancement was accomplished with a Le Fort I type of maxillary osteotomy, stabilized by RIF. The range of the osteotomy line extends from the lateral aspects of the piriform aperture until the maxillary conjunction with the pterygoid plates. For the mandibular set-back or rotation, a BSSO was performed, followed by RIF for stabilization.

According to the routine protocol in Department of Orthodontics of Marmara University, all patients involved signed consent forms to be included in the study. The study was approved by the Ethical Committee of the Institute of Health Sciences of Marmara University (29.11.2018-226).

5.2 Data collection

The 3dMD System (Atlanta, GA, USA) was used for the acquisition of the 3D photogrammetric images in a specially designed photo room in Department of Orthodontics, Faculty of Dentistry, Marmara University (Figure 2). The capturing time for a 3D image by the system is 1,5 milliseconds. As an overall protocol, the head of the subject was guided to a position to fit the point of view of the two camera windows showed on the monitor, by the adjustment of the distance between the subject and the modular unit. Moreover, the head positioned was centered vertically and horizontally in the window. The subjects were encouraged to slightly extend their head in order to improve the scanning quality of the areas underneath the chin. The acquisition of the 3D images was performed with a natural head posture of the subject, in a relaxed state, on an adjustable chair for the vertical height. To help with the standardization of the method, the subject was instructed to fully swallow, keep the lips closed in a relaxed position and occlude gently prior to scanning.

All the accessories, like eyewear, jewelry etc. or clothing in the neck and ear area, that could affect the capturing quality of the system were taken off by the subjects before capturing. A stocking cap was used sporadically to ensure the high capturing quality at the forehead area. Lengthy facial hair, also, were not preferred. The capturing procedure was performed repeatedly until an image of optimal quality was acquired. The 3D data was saved automatically by the system in an Tricorder Surface Binary (tsb) format and transformed later on to a Stereolithography (stl) format for our analyses.

The three-dimensional images were captured during 2 time intervals for every patient; before surgery (T0), usually ranging from a day until a couple of weeks before the operation, and 6 months after the operation (T1). The images were taken by various operators, hence following the same principles. The timing of the image acquisition was coordinated with the patient's regular control appointment, usually on the presurgical preparation appointments.

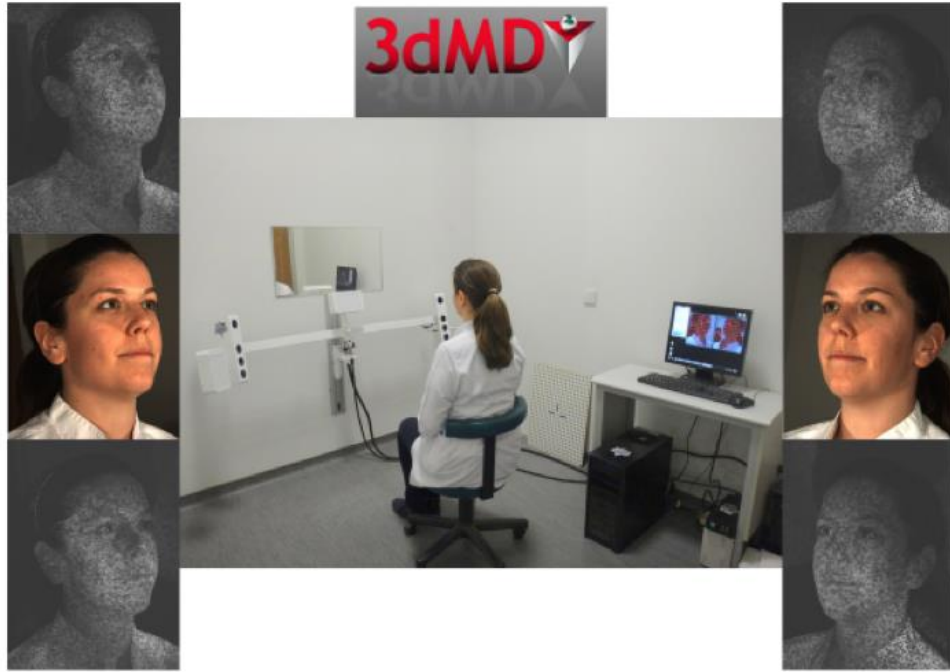


Figure 2: Facial surface capturing with the use of the 3dMDface System (Atlanta, GA, USA), used in Marmara University, Faculty of Dentistry, Department of Orthodontics.

5.3 Data Assessment

Following the selection of the 3D image with the finest quality, the 3dMDpatient software (3dMDpatient v4.1; Atlanta, GA, USA) was used for the initial crop of the 3D model (Figure 3). Automatic tools were provided by the software for the removing of “defects” like holes or spikes generated in the point cloud by the scanner. An area of the face of cylindrical shape, ranging from ear to ear (excluding the ears), was selected and the area of neck and shoulders was cropped out.

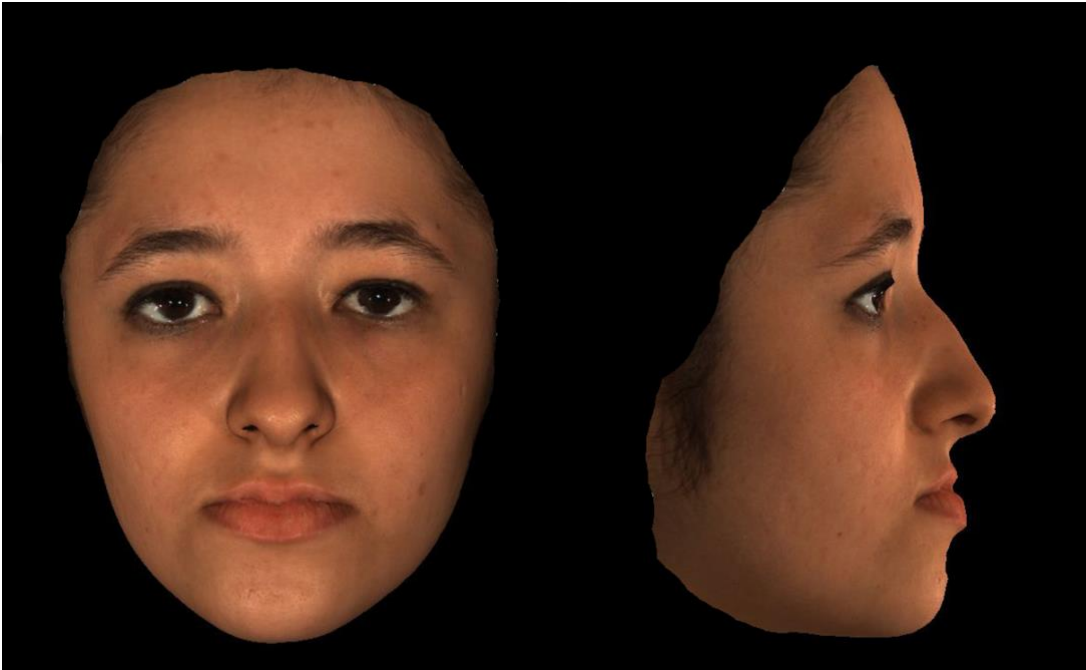


Figure 3: 3D photographs after cropping in T0 (frontal and lateral view)

With the use of the 3dMDpatient software, the two 3D models for the two time intervals (T0, pre-op: T1, post-op) were superimposed on each other. Firstly, a global registration was performed for the sum of 3D mesh points of each model in order to get a proximate superimposition. Subsequently, forehead and nasal dorsum areas were selected in each model and, based on this areas, a final superimposition was performed with the use of the Interactive Closest Point (ICP) algorithm, to minimize the average distance between the two surfaces. The forehead and nasal dorsum areas are proven to be stable in the three dimensions even if there is a change of posture from the patient and are considered the areas less affected by the process of the double-jaw surgery

(van der Meer et al., 2014). The RMS error of the registration progress of selected areas did not exceed the value of 0,5 mm. The tsb files were afterwards transformed to stl file format for the main analysis (Figure 4).

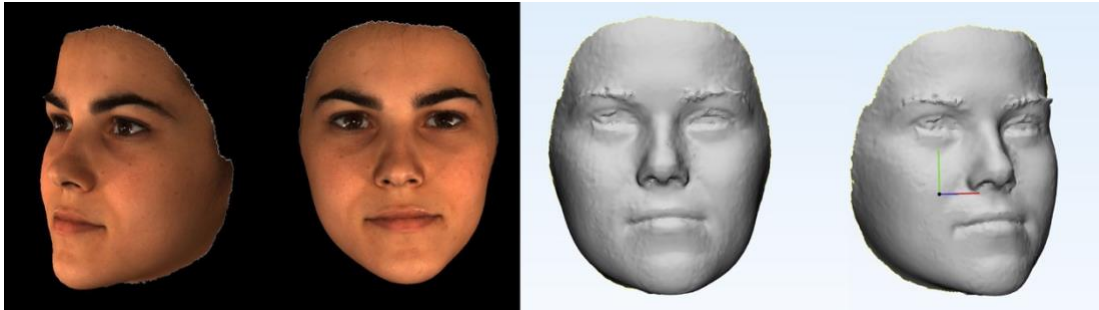


Figure 4: Facial surface in a tsb file format (left). Facial surface in a stl file format (right).

The STL files were subsequently transferred to a network workstation computer so that the analyses could be performed with the use of MIMICS and 3-matic softwares by Materialise (Materialise Europe, World Headquarters, Leuven, Belgium). Materialise Interactive Medical Image Control System (MIMICS) is an interactive tool for the preview and editing of CT, MRI images, STL files and 3D rendering of objects and 3-matic is a software particularly focused on viewing and editing of 3D images, providing also data from complex analyses. Therefore, these two software programs can be used for diagnostic, treatment planning and research purposes.

For each patient, the two already superimposed images for the two time intervals, were opened with the 3-matic software. The first step was to define the midsagittal plane (MSP) of each 3D image. For this reason, a mirror image of the pre-op 3D model was created in the software. This mirror image was afterwards finely registered with the original 3D image with the use of the automatic global registration procedure, for the sum of points of the two surfaces (Benz et al., 2002). The error of this method of registration reported a maximum error value of 0,1 mm. After this registration procedure, a clear midline path is visible between the original and the mirrored 3D model (Figure 5). This midline is the most accurate representation of the mid-sagittal plane (Hartmann et al., 2007). In order to create this plane, 3 points from the junction points of this midline path were selected after zooming into the area to a magnification scale of 1/100 μm to achieve maximum accuracy. From these 3 points, the software

was able to create a MSP according to the midline path between the two models (Figure 6).

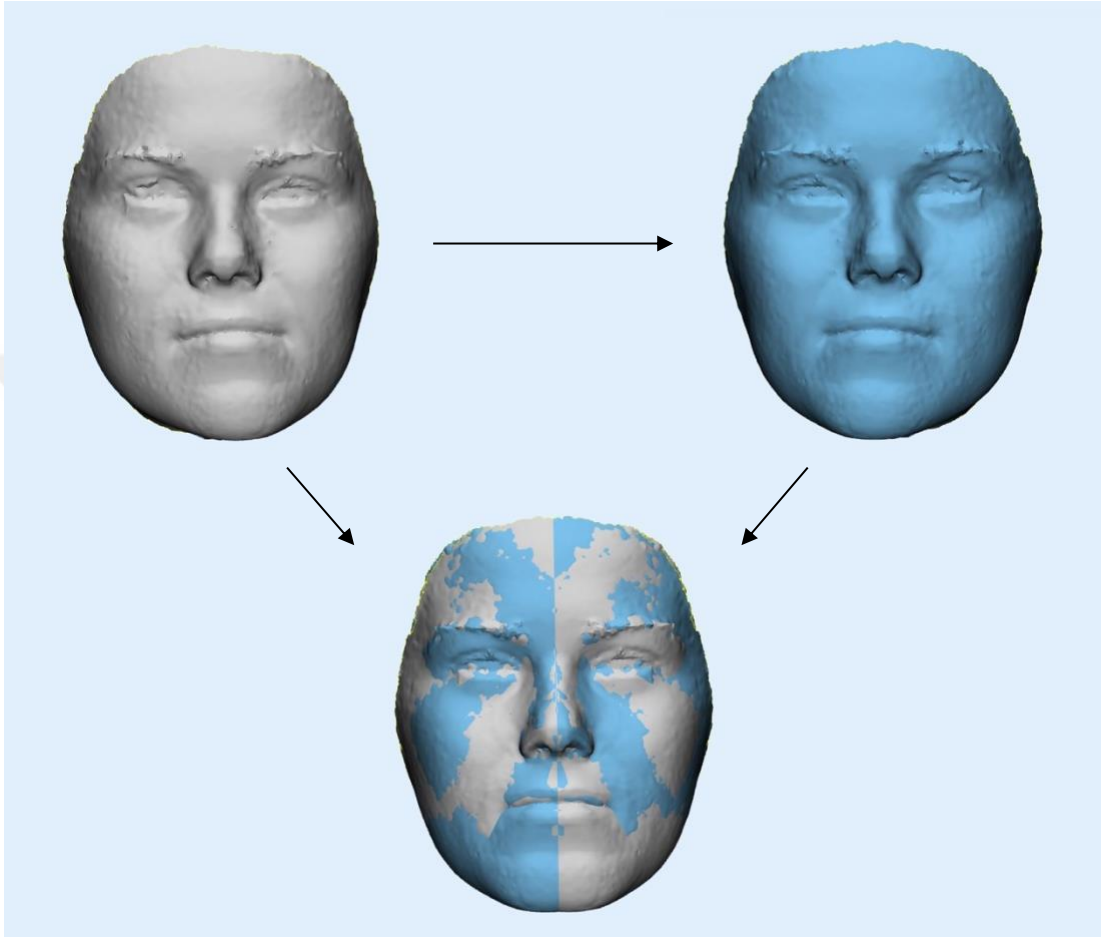


Figure 5: Superimposition of the original and mirrored 3D model, creating a clear midline path to create a facial mid-sagittal plane.

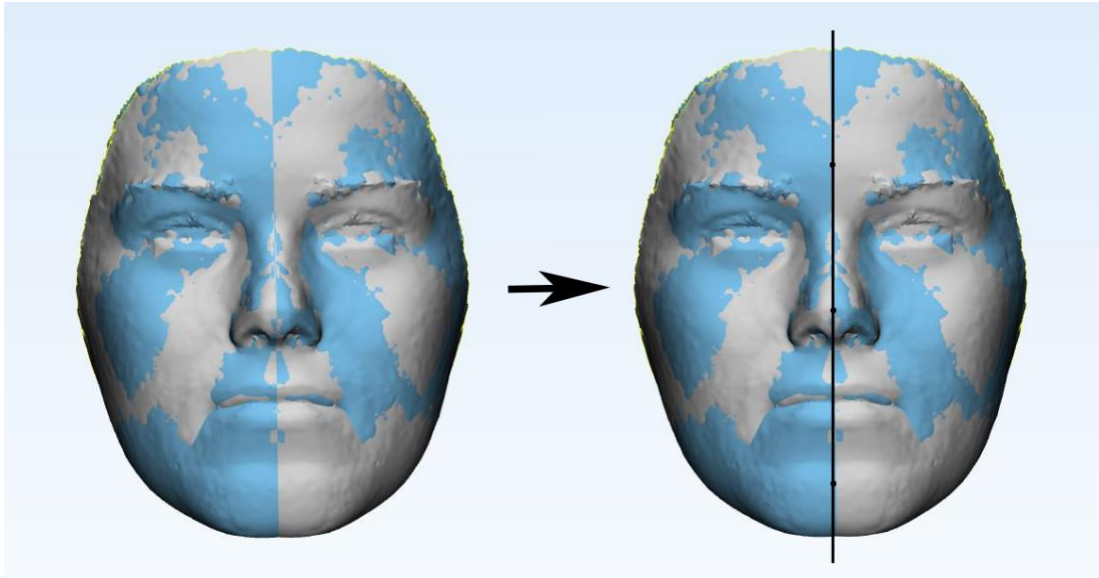


Figure 6: Superimposition of original and mirror 3D image shows a clear facial midline path for the creation of the facial MSP by the software.

In this formation of the mirrored and original model, the total facial asymmetry can be calculated with the comparison of the root mean square (RMS) value of the average distances between all points of the mirrored and original 3D image, calculated in mm. If (x_1, x_2, \dots, x_n) is a group of measured distances, the RMS value is a quadratic mean, deriving from the following equation:

$$RMS = \sqrt{\frac{x_1^2 + x_2^2 + \dots + x_n^2}{n}}$$

This value is automatically generated by the software by the comparison of the two 3D images, followed also by generation of a color-map of the differences between the two images, presented on the facial surface (Figure 7). This allows us to double-check the validity of the results, by eliminating the possibility that highly asymmetrical areas are located in unwanted points, like in “defects” from scanning, surrounding cutting edges or hair-covered areas. RMS value is a proven value for the calculation of facial asymmetry (Ozsoy, 2006) and as previously mentioned, it’s a positive value, with a minimum of 0 mm, in cases of absolute symmetry. The higher the RMS value, the higher the degree of asymmetry will be.

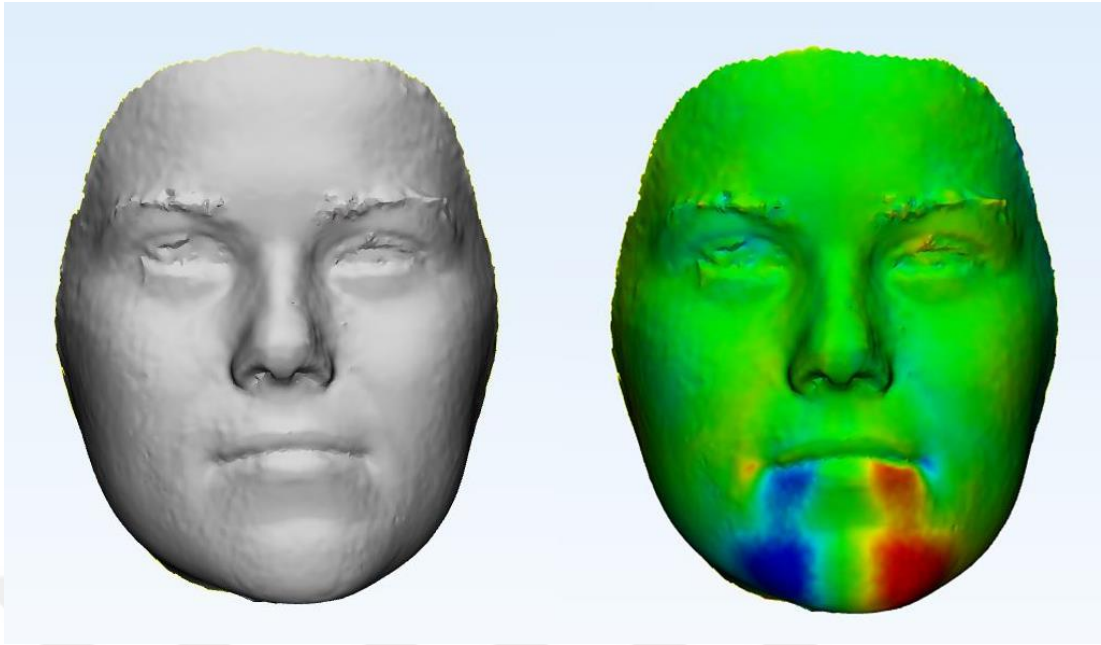


Figure 7: Color map of the location of facial asymmetry. Red and blue areas represent areas of bigger asymmetry values as the color's intensity increases.

The same procedure was repeated afterwards for the post-op model, giving us again a MSP and a RMS value, comparable with the pre-op value acquired. At this point, the angle between pre-op and post-op MSPs was calculated, to generate the absolute difference between them (Figure 8).

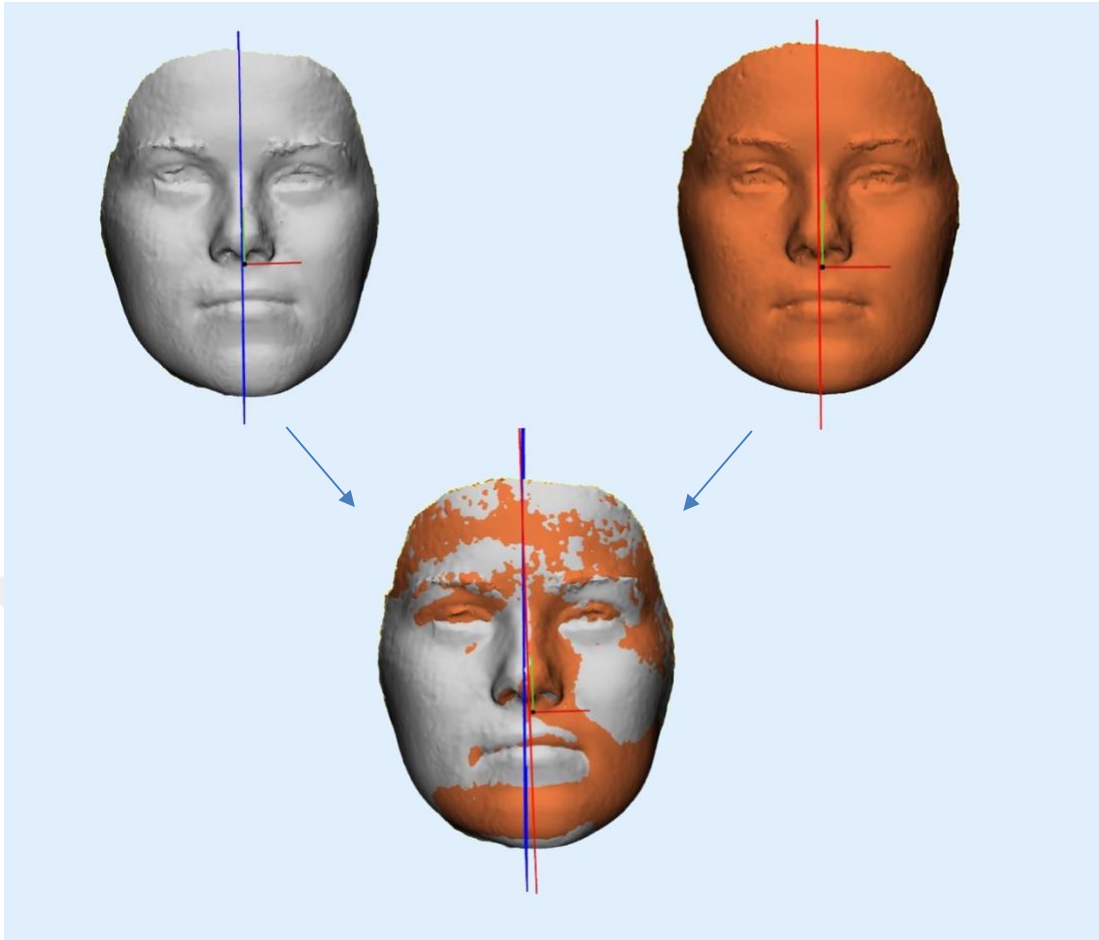


Figure 8: The calculation of the angulation difference among mid-sagittal planes between T0 and T1. The grey model represents the T0 and the orange represents the T1 facial surface.

Furthermore, the 3D face was divided into upper face (until the height of the Nasion point), midface (nasion to subnasale) and lower face (subnasale to gnathion). The lower face was subsequently subdivided to maxillary (subnasale to helion) and mandibular part (helion to gnathion) (Table 2).

Table 2: Definitions of the Nasion, Subnasale, Helion, Gnathion, Orbitale, Porion points.

Nasion (Na)	The most anterior point of the frontonasal suture in the median plane.
Subnasale (Sn)	The point where the lower border of the nose meets the outer contour of the upper lip.
Helion (He)	The point located at each labial commissure.
Gnathion (Gn)	The most anteroinferior point on the symphysis of the chin.
Orbitale (Or)	The lowest point in the inferior margin of the orbit.
Porion (Po)	The most superior point of the external auditory meatus.

This segmentation was performed with the marking of the nasion, subnasale and helion point on the 3D surface. With the use of these points to assess the height of the segmentation, planes were created with the use of the 3-matic software. These planes were created to be perpendicular to the MSP and to the Y-axis of the facial surface, passing from the point assessing their vertical height (nasion, subnasale, helion respectively). The X-axis of the facial surface was created to be parallel with the Frankfort horizontal plane that connects the Orbitale (Or) and the soft tissue equivalent to Porion (Po) points (Figure 10). As a result, the 3 planes created were parallel to each other and, according to them, the segmentation of the 3D face was performed by the software, providing us with the 5 segments mentioned (Figure 9,10,11).

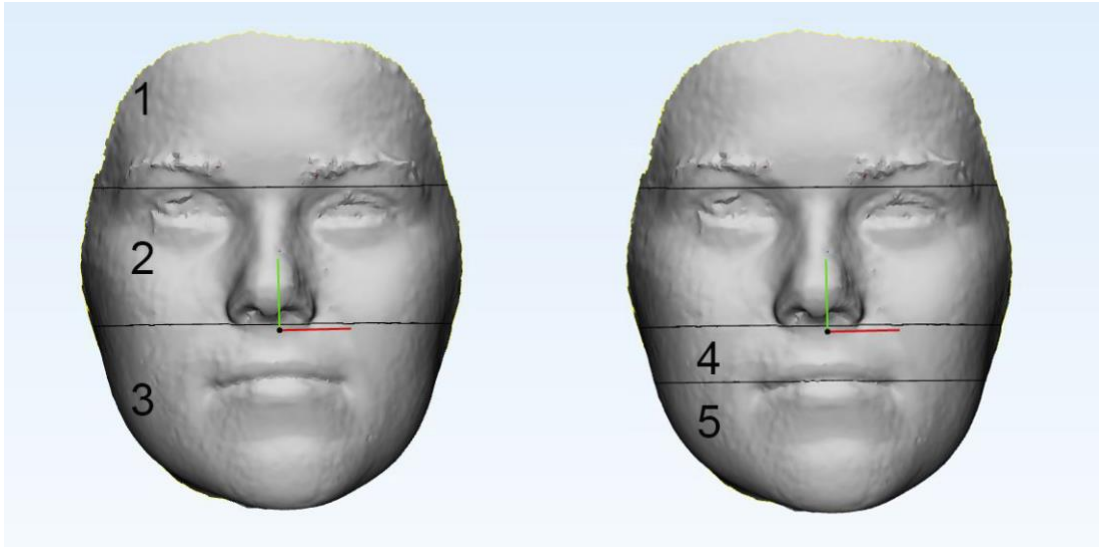


Figure 9: Segmentation of the facial surface to 3 (left) and 4 parts (right), respectively. 1: Upper face, 2: Midface, 3: Lower face, 4: Maxillary and 5: Mandibular part

For each segment and its mirrored image, an individual RMS value was calculated to provide us with a more specific idea about the localization of asymmetry in the facial surface. These individual RMS values were afterwards compared between pre-op and post-op models and for the equivalent parts of the face.

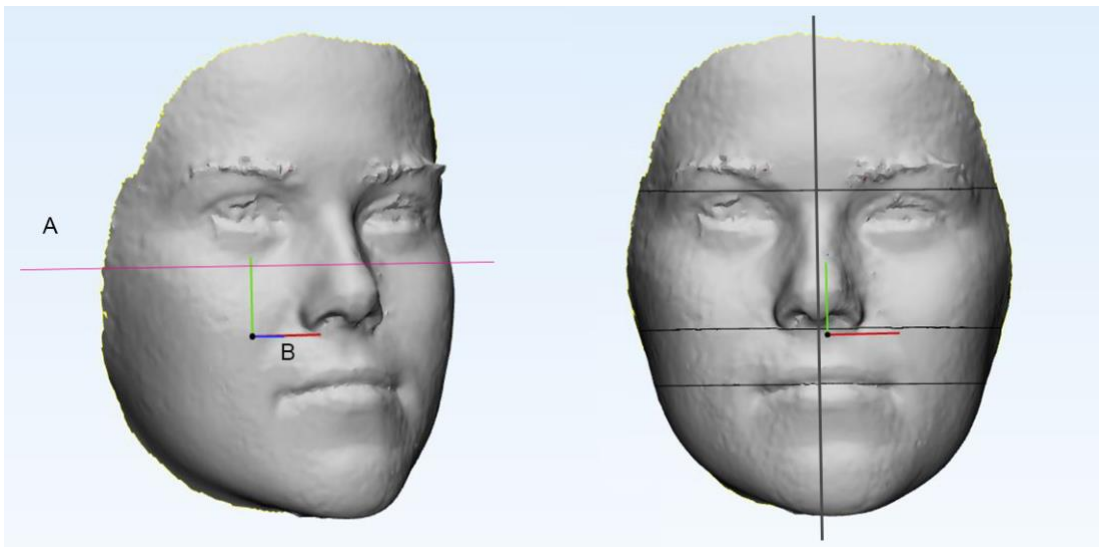


Figure 10: The X-axis of the face (B) is parallel to the Frankfort horizontal plane (A). The segmentation planes are perpendicular to the Y-axis of the face and the MSP.

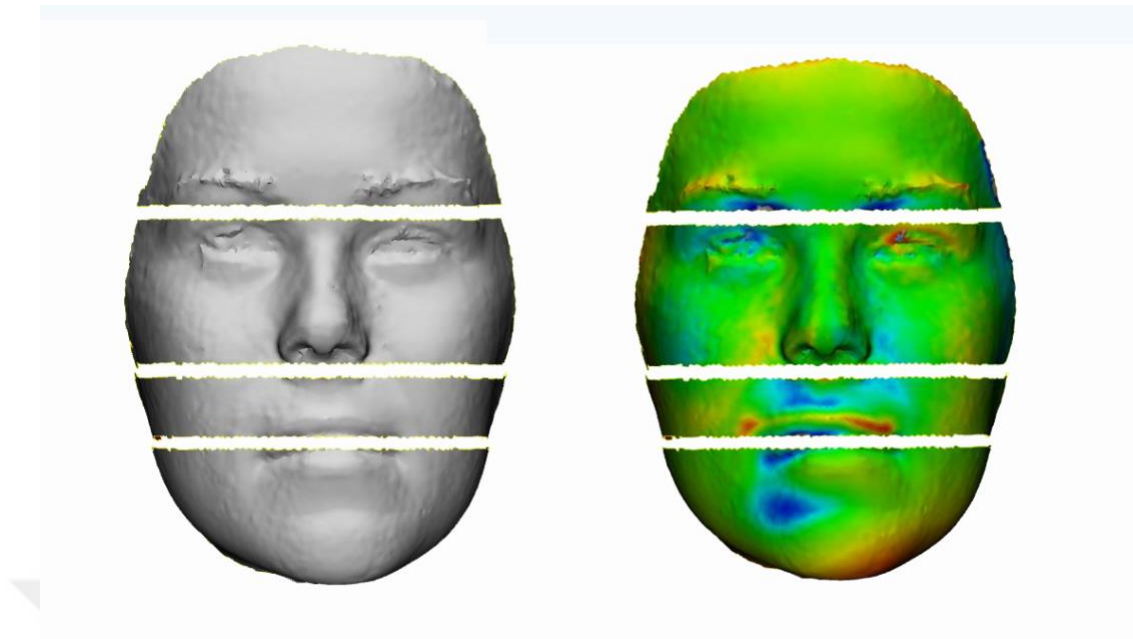


Figure 11: Color maps showing the asymmetry levels in each facial area after segmentation.

In addition to the calculation of the asymmetry with the use of the RMS value, a volumetric test was performed. For the volumetric test, an additional segmentation procedure was necessary. In order to assess the boundaries of the faces in the posterior-anterior direction, the orbitale point of the right hemiface was marked. A plane was created in a distance 25 mm posteriorly from the orbitale point (Figure 12). This plane was created perpendicular to the MSP and the Y-axis of the face. With the use of this plane, the posterior limit of the facial surface for the volumetric analysis was determined. Furthermore, the face was also divided into two hemifaces with the use of the MSP as reference. With this segmentation, the face was divided into a total of 8 parts, 4 in each hemiface (Figure 12).

The segmented stl files were consequently extracted to MIMICS software for the volumetric analysis. The volumetric differences were calculated between the same parts of each hemiface, calculating the difference between the whole volume of the two hemifaces and for each pair of segmentation parts separately between the two hemifaces.

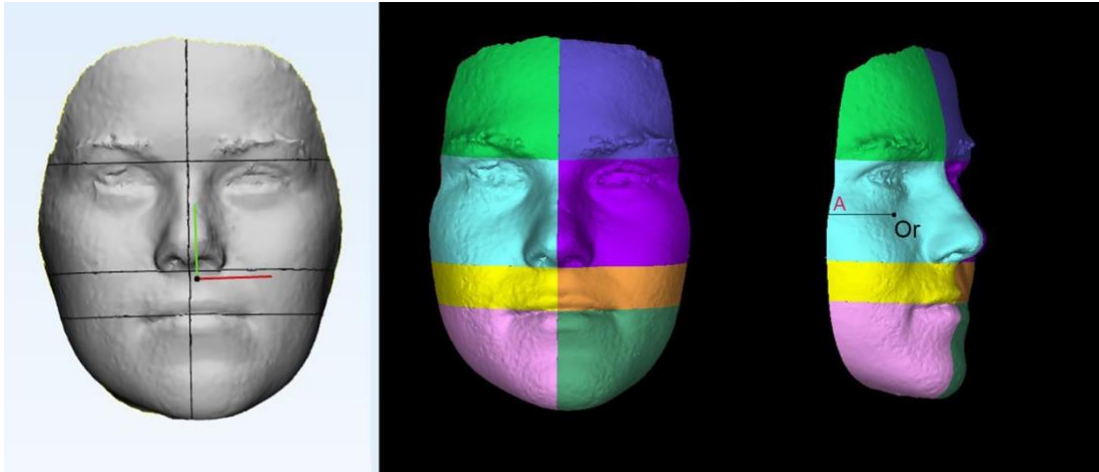


Figure 12: Volumetric analysis of the hemifaces and their parts. The A line represents the 25mm distance between the Or point and the posterior segmentation wall.

Finally, for the same areas, a comparison of the facial surfaces between the two hemifaces was also performed. The values of the facial surface area were automatically calculated by the software after the segmentation of the face. According to these values, the same comparisons as the volumetric analysis were performed.

All of the data in this study were measured, processed and analyzed by the author of the study. The gender and the age of every subject were recorded.

5.4 Statistical analysis

The statistical analysis of the data in this study was carried out by the IBM SPSS Statistics software for Windows, version 25.0 Armonk, NY: IBM Corp. Descriptive analyses were presented using means, standard deviations, and ranges for continuous data. The Intra-observer method error was investigated by measuring again the 40% of the total sample (16 subjects), after 4 weeks from the initial measuring. For the analysis of reliability regarding parameter measurements, intraclass correlation coefficient was calculated. Relationships between the variables were determined using Spearman's Correlation Coefficients. Wilcoxon signed rank test was used for comparisons between the two time intervals. A 5% type-I error level was used to infer a statistical significance. Statistical significance level was established at $P < 0,05$. G*Power 3.1.9.2 (Universität Düsseldorf, Düsseldorf, Germany) was used to calculate the post-hoc power of the results.

Three post-hoc analyses were performed. First, for the correlation of initial RMS values with the difference in RMS values after surgery a 99% post hoc power was achieved. Second and third, the post-hoc power of the Low RMS and High RMS groups when comparing the RMS values between T0 and T1 was found 81,4% and 99% for Low and High RMS groups, respectively. The minimum sample to achieve this correlation with power: 0,80 and α : 0,05, for these three effect sizes, was 19 patients. Furthermore, for the calculation of an ideal cut-off point in the sample, ROC curve analysis was performed.

6. Results

6.1 Reliability Test

Method error for the RMS, volume, surface and angle between mid-sagittal planes are shown in Table 3. Intraclass Correlation Coefficient was found to be close to 1 for all the measurements (Table 3). All the measurements were found to be reliable. The errors were non-fatal and did not affect the results of our measurements.

Table 3: Single observer's agreements between repeated measurements (0 = T0 time interval, 1 = T1 time interval, T = Total surface, U = Upper face, M= Midface, L = Lower face, Mx = Maxillary region, Md= Mandibular region, Vol = Volume, Sur = Surface, MSP= angle between mid-sagittal planes).

Time Region		Intraclass Correlation ^b	95% Confidence Interval	
			Lower Bound	Upper Bound
0 T RMS	Single Measures	,994 ^a	,992	,997
	Average Measures	,997 ^c	,995	,998
1 T RMS	Single Measures	,993 ^a	,992	,996
	Average Measures	,996 ^c	,994	,999
0 U RMS	Single Measures	,994 ^a	,993	,996
	Average Measures	,997 ^c	,995	,999
1 U RMS	Single Measures	,995 ^a	,994	,997
	Average Measures	,997 ^c	,995	,999
0 M RMS	Single Measures	,993 ^a	,990	,997
	Average Measures	,995 ^c	,994	,998
1 M RMS	Single Measures	,994 ^a	,992	,996
	Average Measures	,996 ^c	,994	,998
0 L RMS	Single Measures	,998 ^a	,997	,999
	Average Measures	,999 ^c	,998	1,000
1 L RMS	Single Measures	,997 ^a	,995	,999
	Average Measures	,999 ^c	,997	,999
0 Mx RMS	Single Measures	,993 ^a	,990	,994
	Average Measures	,995 ^c	,993	,997
1 Mx RMS	Single Measures	,994 ^a	,991	,995
	Average Measures	,996 ^c	,994	,998
0 Md RMS	Single Measures	,996 ^a	,996	,998
	Average Measures	,998 ^c	,997	,999

Table 3: Single observer's agreements between repeated measurements (0 = T0 time interval, 1 = T1 time interval, T = Total surface, U = Upper face, M= Midface, L = Lower face, Mx = Maxillary region, Md= Mandibular region, Vol = Volume, Sur = Surface, MSP= angle between mid-sagittal planes)

1 Md RMS	Single Measures	,997 _a	,996	,999
	Average Measures	,999 _c	,998	,999
MSP	Single Measures	,998 _a	,997	,999
	Average Measures	,999 _c	,998	1,000
0 T Vol	Single Measures	,993 _a	,992	,994
	Average Measures	,996 _c	,994	,997
1 T Vol	Single Measures	,992 _a	,990	,996
	Average Measures	,996 _c	,995	,998
0 M Vol	Single Measures	,990 _a	,989	,993
	Average Measures	,995 _c	,994	,996
1 M Vol	Single Measures	,991 _a	,988	,994
	Average Measures	,995 _c	,994	,998
0 L Vol	Single Measures	,995 _a	,994	,997
	Average Measures	,997 _c	,998	,999
1 L Vol	Single Measures	,995 _a	,994	,997
	Average Measures	,998 _c	,997	,999
0 Mx Vol	Single Measures	,991 _a	,987	,993
	Average Measures	,993 _c	,992	,995
1 Mx Vol	Single Measures	,989 _a	,987	,992
	Average Measures	,991 _c	,989	,994
0 Md Vol	Single Measures	,996 _a	,988	,999
	Average Measures	,998 _c	,994	1,000
1 Md Vol	Single Measures	,990 _a	,987	,998
	Average Measures	,995 _c	,990	,999
0 T Sur	Single Measures	,990 _a	,979	,993
	Average Measures	,993 _c	,985	,996
1 T Sur	Single Measures	,995 _a	,992	,999
	Average Measures	,998 _c	,997	,999
0 M Sur	Single Measures	,994 _a	,987	,999
	Average Measures	,997 _c	,992	,999
1 M Sur	Single Measures	,993 _a	,995	,999
	Average Measures	,997 _c	,996	,999
0 L Sur	Single Measures	,994 _a	,968	,999
	Average Measures	,997 _c	,984	,999
1 L Sur	Single Measures	,990 _a	,990	,998
	Average Measures	,992 _c	,992	,999

Table 3: Single observer's agreements between repeated measurements (0 = T0 time interval, 1 = T1 time interval, T = Total surface, U = Upper face, M= Midface, L = Lower face, Mx = Maxillary region, Md= Mandibular region, Vol = Volume, Sur = Surface, MSP= angle between mid-sagittal planes)

0 Mx Sur	Single Measures	,991 ^a	,989	,998
	Average Measures	,996 ^c	,990	,999
1 Mx Sur	Single Measures	,988 ^a	,982	,998
	Average Measures	,994 ^c	,990	,999
0 Md Sur	Single Measures	,993 ^a	,982	,997
	Average Measures	,991 ^c	,992	,998
1 Md Sur	Single Measures	,994 ^a	,969	,999
	Average Measures	,997 ^c	,984	,999

6.2 Demographics of the Study Group

The sample of this study is consisted of 40 patients who underwent double-jaw surgery between April 2012 and November 2018. 19 out of 40 patients were male and 21 female. The mean age in the group was 20,44 years (ranging from 17 to 27 years of age), measured on T0, 20,2 years old for women and 20,7 years old for men.

6.3 Comparison of the degree of asymmetry between time intervals

A mean RMS value of 1,21 (\pm 0,55 mm) was found for the T0 interval and a mean RMS value of 1,06 (\pm 0,30 mm) was found for the T1 time interval (Table 4, Figure 13). There was no statistically significant difference found in RMS values between T0 (pre-op) and T1 (post-op) for the 40 patients of the sample (Table 4).

Table 4: Comparison between RMS values before and after surgery.

	N	Mean	Std. Deviation	P value
RMS pre-op	40	1,2103	,55066	0,72
RMS post-op	40	1,0606	,30176	

Wilcoxon signed rank test

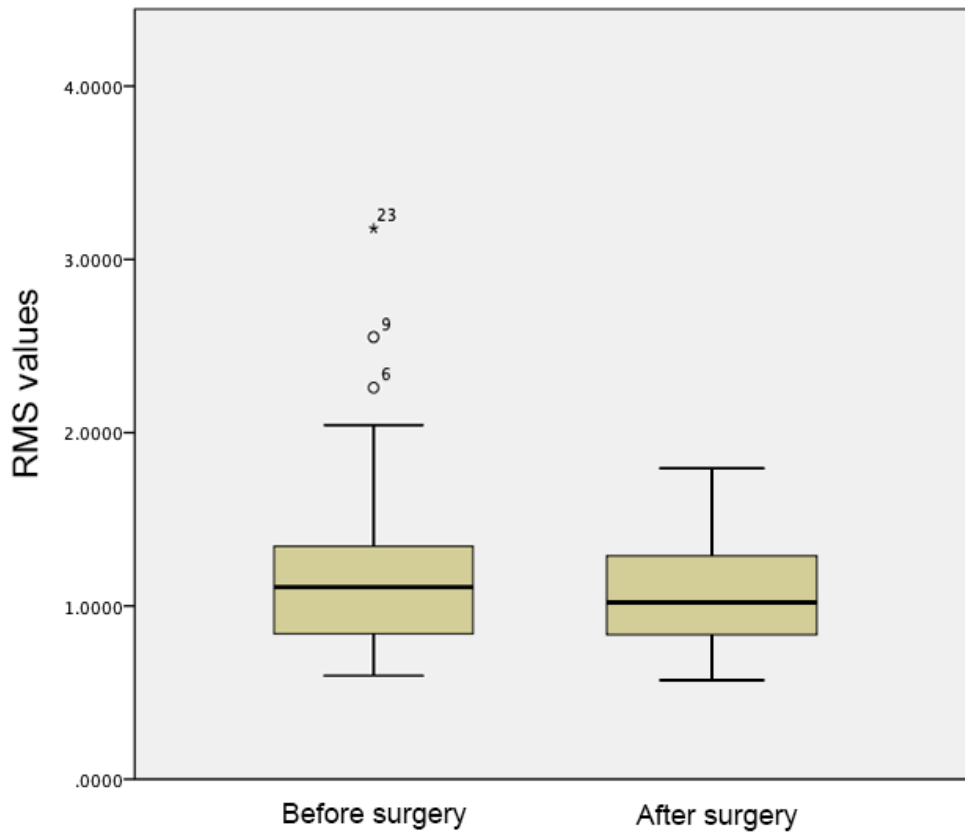


Figure 13: RMS values and SD before and after surgery. 6, 9, 23 numbers represent each a patient's number.

Upper, mid, lower, maxillary and mandibular parts of the face were compared in T0 with their equivalent part in T1. There was also no statistically significant difference observed for RMS values between all parts of the face and their equivalent parts between the two time intervals (Table 5).

Table 5: Difference between each segmentation part between T0 and T1 time intervals

RMS values	N	Mean	S D	Median	P value
Upper face T0	40	,835920	,3632372	,700550	0,270
Upper face T1	40	,798227	,3378579	,716250	
Midface T0	40	1,099808	,5314292	,948950	0,697
Midface T1	40	1,104990	,4550394	,975700	
Lower face T0	40	1,222275	,7645046	,983600	0,202
Lower face T1	40	1,058303	,3532630	1,040000	
maxilla T0	40	,901985	,4701284	,786700	0,294
maxilla T1	40	,907193	,3319471	,881950	
mandible T0	40	1,307665	,9360900	,995850	0,265
mandible T1	40	1,107785	,4422943	1,081000	

Wilcoxon signed rank test

To examine how the initial asymmetry levels of the facial surface connect with the results of orthognathic surgery on asymmetry, a correlation analysis was performed. A statistical significant positive correlation was found between the initial RMS values and the difference between RMS values in T0 and T1 ($P < 0,01$) (Table 6). This can be shown in detail in Figure 14, showing in detail when the change in RMS values is positive or negative.

The same correlation was found for each segmentation part (midface, lower face, maxillary, mandibular area) and the RMS difference in that area following the orthognathic surgery ($P < 0,01$) (Tables 7,8,9,10).

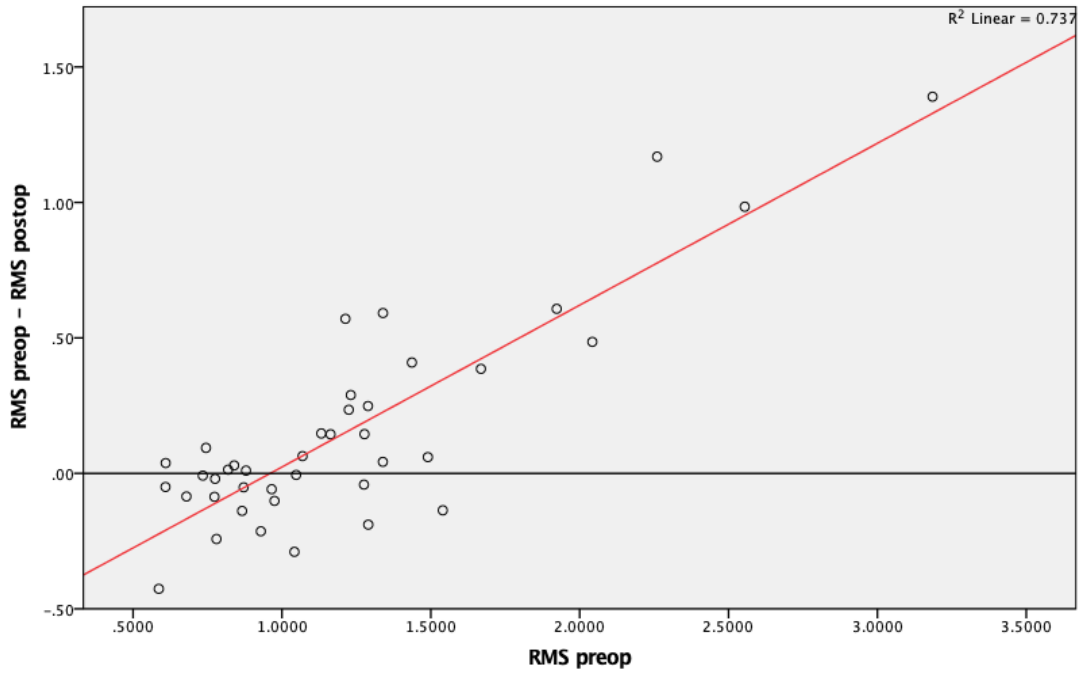


Figure 14: Linear correlation between RMS values before surgery and RMS difference after surgery.

Table 6: Correlation between RMS values before surgery and RMS difference after surgery.

		RMS preop	RMS preop – RMS postop
Spearman's rho	Correlation	1,000	,653**
	Coefficient		
	Sig. (2-tailed)	.	,000
	N	40	40
	Correlation	,653**	1,000
	Coefficient		
	Sig. (2-tailed)	,000	.
	N	40	40

** . Correlation is significant at the 0,01 level (2-tailed).

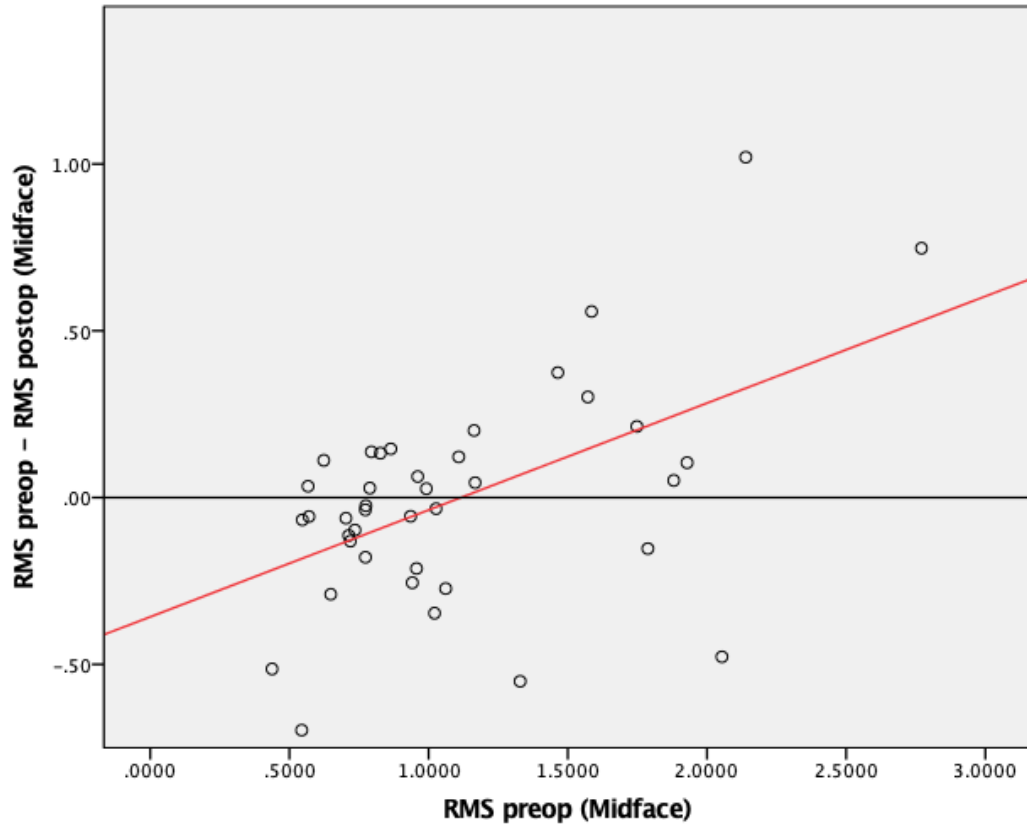


Figure 15: Linear correlation between RMS values before surgery and RMS difference after surgery for midface.

Table 7: Correlation between RMS values before surgery and RMS difference after surgery for midface.

Midface		RMS preop	RMS preop – RMS postop
Spearman's rho	Correlation	1,000	,431**
	Coefficient		
	Sig. (2-tailed)	.	,005
	N	40	40
RMS preop – RMS postop	Correlation	,431**	1,000
	Coefficient		
	Sig. (2-tailed)	,005	.
	N	40	40

** . Correlation is significant at the 0,01 level (2-tailed).

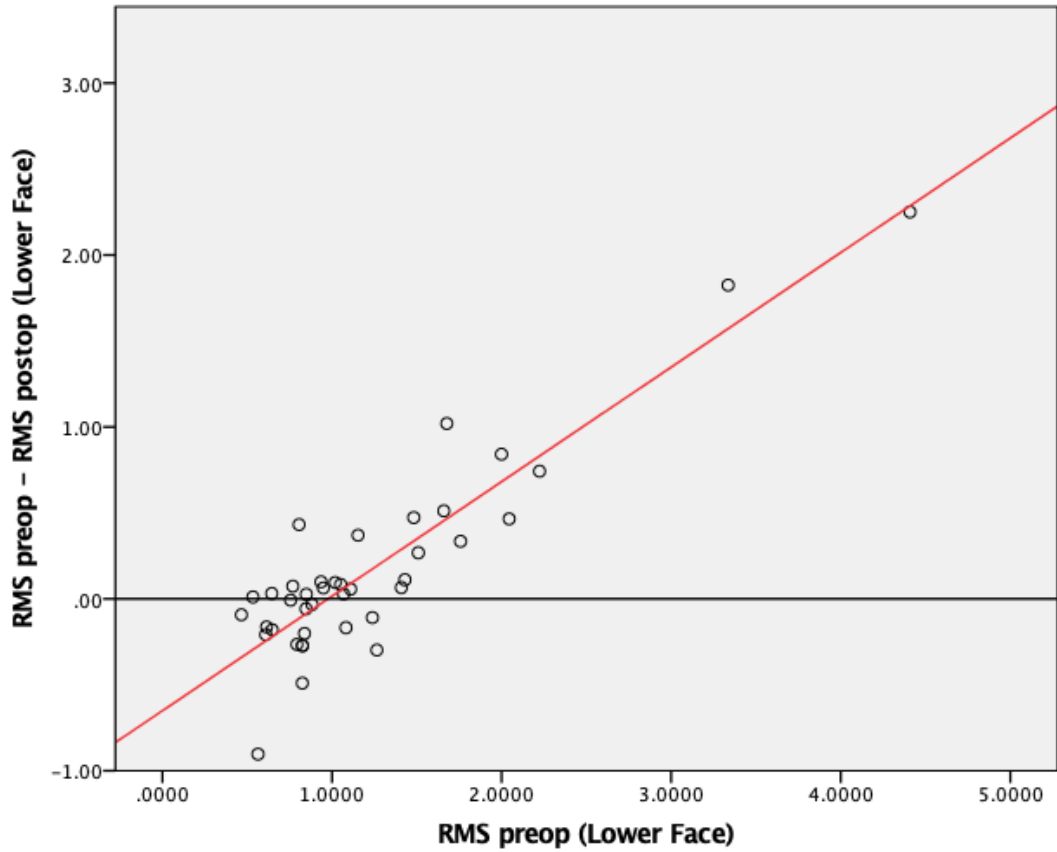


Figure 16: Linear correlation between RMS values before surgery and RMS difference after surgery for lower face.

Table 8: Correlation between RMS values before surgery and RMS difference after surgery for lower face.

Lower face		RMS preop	RMS preop – RMS postop
Spearman's rho	Correlation	1,000	,716**
	Coefficient		
	Sig. (2-tailed)	.	,000
	N	40	40
RMS preop – RMS postop	Correlation	,716**	1,000
	Coefficient		
	Sig. (2-tailed)	,000	.
	N	40	40

** . Correlation is significant at the 0,01 level (2-tailed).

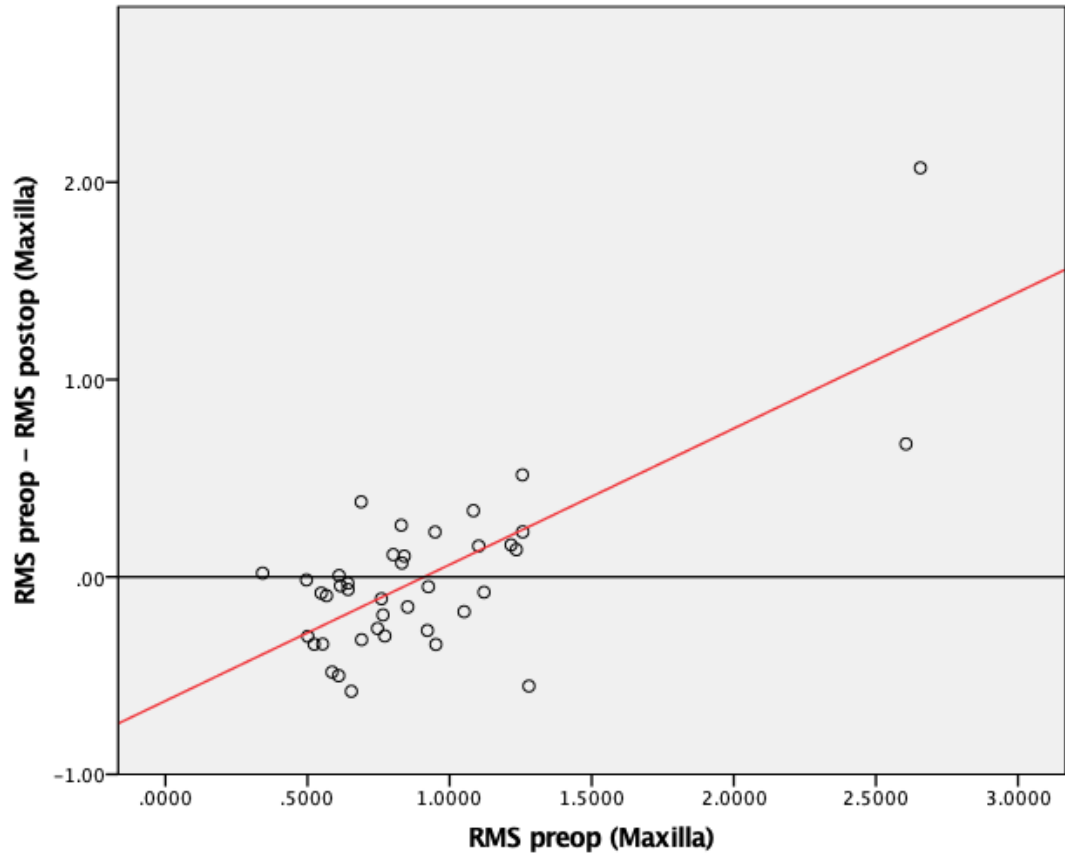


Figure 17: Linear correlation between RMS values before surgery and RMS difference after surgery for the maxillary area.

Table 9: Correlation between RMS values before surgery and RMS difference after surgery for the maxillary area.

Maxilla		RMS preop – RMS postop	RMS preop
Spearman's rho	Correlation	1,000	,445**
	RMS preop – RMS postop	Coefficient	,004
	Sig. (2-tailed)	.	,004
	N	40	40
RMS preop	Correlation	,445**	1,000
	Coefficient	,004	.
	Sig. (2-tailed)	,004	.
	N	40	40

** . Correlation is significant at the 0,01 level (2-tailed).

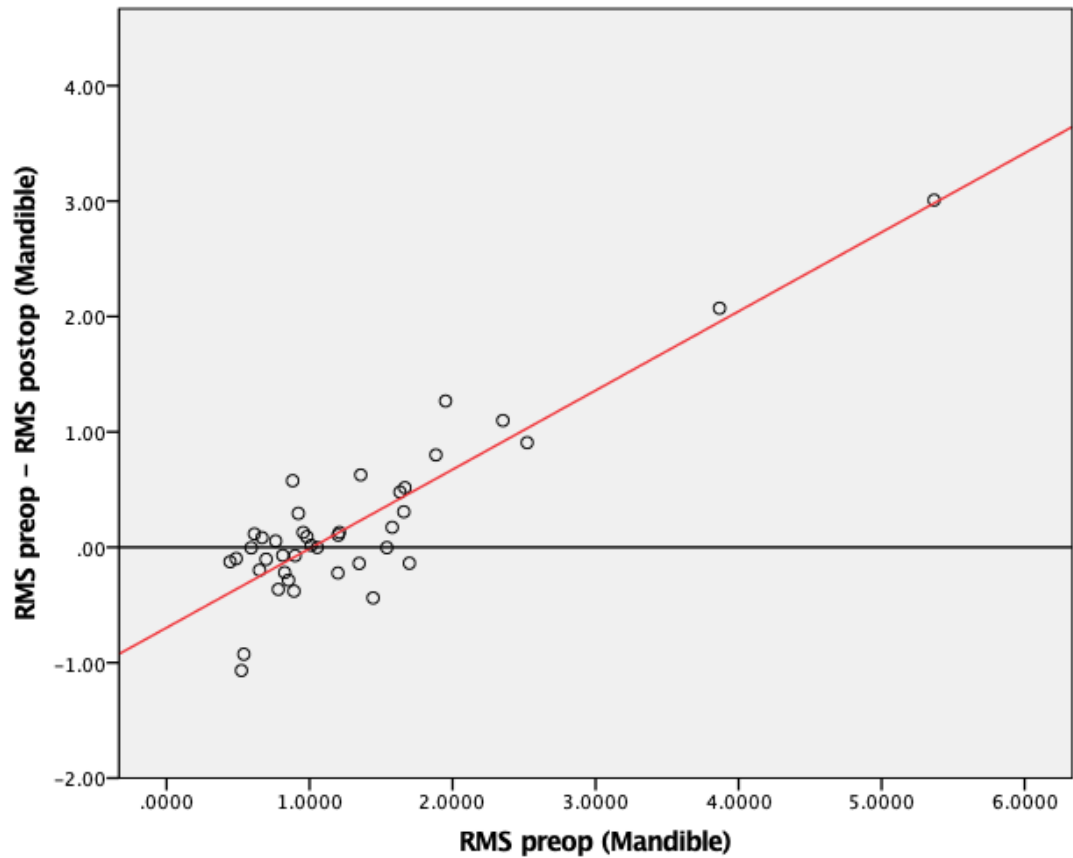


Figure 18: Linear correlation between RMS values before surgery and RMS difference after surgery for the mandibular area.

Table 10: Correlation between RMS values before surgery and RMS difference after surgery for the mandibular area.

Mandible		RMS preop	RMS preop – RMS postop
RMS preop	Correlation	1,000	,645**
	Coefficient		
	Sig. (2-tailed)	.	,000
	N	40	40
Spearman's rho	Correlation	,645**	1,000
	Coefficient		
	Sig. (2-tailed)	,000	.
	N	40	40

** . Correlation is significant at the 0,01 level (2-tailed).

6.4 Comparison of the degree of asymmetry between time intervals for subgroups

In addition, due to the positive correlation between the initial RMS values and the difference in RMS values after surgery, the sample was divided into 2 subgroups according to their pre-operative RMS value. For this purpose, a ROC curve analysis was performed in order to calculate the ideal cut-off point in the patients' sample. A Receiver Operating Characteristic (ROC) curve is a graphical plot that illustrates the diagnostic ability of a binary classifier system as its discrimination threshold is varied (Table 12). According to the Youden Index Association criteria, the best cut-off point on this study's data set according to the RMS pre-op value is $RMS > 1,0689$ (Table 11). Area Under the curve (AUC) for this cut-off point is 1 which is statistically significant with 95% CI 0,912 to 1, $P < 0,0001$ (Table 11). According to this, the total sample of the study can be divided into two subgroups of 20 patients, for a more in-depth analysis of the results. The subgroup with equal or lower RMS values than 1,0689 (Low RMS group) and the subgroup with RMS values higher than 1,0689 (High RMS group) (Table 13).

There is a significant increase in RMS values for the whole facial surface observed for the Low RMS group after orthognathic surgery ($P < 0,05$) (Table 14). For the High RMS group there is an opposite effect of the surgery in the RMS values, leading to a significant decrease in RMS values ($P < 0,001$) (Table 15).

Table 11: Youden Index Association criteria and Area under the ROC curve (AUC) for $RMS = 1,0689$.

Youden index J	1,0000
Associated criterion	$> 1,0689$
Sensitivity	100,00
Specificity	100,00
Area under the ROC curve (AUC)	1,000
Standard Error ^a	0,000
95% Confidence interval ^b	0,912 to 1,000
Significance level P (Area=0.5)	$< 0,0001$

^a DeLong et al., 1988

^b Binomial exact

Table 12: Criterion values and coordinates of the ROC curve.

Criterion	Sensitivity	95% CI	Specificity	95% CI	+LR	95% CI	-LR	95% CI
≥0,5863	100,00	83,2 - 100,0	0,00	0,0 - 16,8	1,00	1,0 - 1,0		
>0,5863	100,00	83,2 - 100,0	5,00	0,1 - 24,9	1,05	1,0 - 1,2	0,00	
>0,6088	100,00	83,2 - 100,0	10,00	1,2 - 31,7	1,11	1,0 - 1,3	0,00	
>0,6094	100,00	83,2 - 100,0	15,00	3,2 - 37,9	1,18	1,0 - 1,4	0,00	
>0,6792	100,00	83,2 - 100,0	20,00	5,7 - 43,7	1,25	1,0 - 1,6	0,00	
>0,7342	100,00	83,2 - 100,0	25,00	8,7 - 49,1	1,33	1,0 - 1,7	0,00	
>0,7447	100,00	83,2 - 100,0	30,00	11,9 - 54,3	1,43	1,1 - 1,9	0,00	
>0,7733	100,00	83,2 - 100,0	35,00	15,4 - 59,2	1,54	1,1 - 2,1	0,00	
>0,7753	100,00	83,2 - 100,0	40,00	19,1 - 63,9	1,67	1,2 - 2,4	0,00	
>0,7801	100,00	83,2 - 100,0	45,00	23,1 - 68,5	1,82	1,2 - 2,7	0,00	
>0,8192	100,00	83,2 - 100,0	50,00	27,2 - 72,8	2,00	1,3 - 3,1	0,00	
>0,8394	100,00	83,2 - 100,0	55,00	31,5 - 76,9	2,22	1,4 - 3,6	0,00	
>0,866	100,00	83,2 - 100,0	60,00	36,1 - 80,9	2,50	1,5 - 4,3	0,00	
>0,8713	100,00	83,2 - 100,0	65,00	40,8 - 84,6	2,86	1,6 - 5,2	0,00	
>0,8792	100,00	83,2 - 100,0	70,00	45,7 - 88,1	3,33	1,7 - 6,5	0,00	
>0,9289	100,00	83,2 - 100,0	75,00	50,9 - 91,3	4,00	1,9 - 8,5	0,00	
>0,9654	100,00	83,2 - 100,0	80,00	56,3 - 94,3	5,00	2,1 - 12,0	0,00	
>0,9748	100,00	83,2 - 100,0	85,00	62,1 - 96,8	6,67	2,3 - 18,9	0,00	
>1,0418	100,00	83,2 - 100,0	90,00	68,3 - 98,8	10,00	2,7 - 37,2	0,00	
>1,0477	100,00	83,2 - 100,0	95,00	75,1 - 99,9	20,00	3,0 - 135,1	0,00	
>1,0689	100,00	83,2 - 100,0	100,00	83,2 - 100,0			0,00	
>1,1321	95,00	75,1 - 99,9	100,00	83,2 - 100,0			0,050	0,007 - 0,3
>1,1633	90,00	68,3 - 98,8	100,00	83,2 - 100,0			0,100	0,03 - 0,4
>1,2132	85,00	62,1 - 96,8	100,00	83,2 - 100,0			0,15	0,05 - 0,4
>1,2246	80,00	56,3 - 94,3	100,00	83,2 - 100,0			0,20	0,08 - 0,5
>1,2312	75,00	50,9 - 91,3	100,00	83,2 - 100,0			0,25	0,1 - 0,5
>1,2753	70,00	45,7 - 88,1	100,00	83,2 - 100,0			0,30	0,2 - 0,6
>1,2771	65,00	40,8 - 84,6	100,00	83,2 - 100,0			0,35	0,2 - 0,6
>1,2889	60,00	36,1 - 80,9	100,00	83,2 - 100,0			0,40	0,2 - 0,7
>1,2898	55,00	31,5 - 76,9	100,00	83,2 - 100,0			0,45	0,3 - 0,7
>1,3389	50,00	27,2 - 72,8	100,00	83,2 - 100,0			0,50	0,3 - 0,8
>1,3393	45,00	23,1 - 68,5	100,00	83,2 - 100,0			0,55	0,4 - 0,8
>1,4363	40,00	19,1 - 63,9	100,00	83,2 - 100,0			0,60	0,4 - 0,9
>1,49	35,00	15,4 - 59,2	100,00	83,2 - 100,0			0,65	0,5 - 0,9
>1,5403	30,00	11,9 - 54,3	100,00	83,2 - 100,0			0,70	0,5 - 0,9
>1,6684	25,00	8,7 - 49,1	100,00	83,2 - 100,0			0,75	0,6 - 1,0
>1,9228	20,00	5,7 - 43,7	100,00	83,2 - 100,0			0,80	0,6 - 1,0
>2,0424	15,00	3,2 - 37,9	100,00	83,2 - 100,0			0,85	0,7 - 1,0
>2,2601	10,00	1,2 - 31,7	100,00	83,2 - 100,0			0,90	0,8 - 1,0
>2,5544	5,00	0,1 - 24,9	100,00	83,2 - 100,0			0,95	0,9 - 1,1
>3,1851	0,00	0,0 - 16,8	100,00	83,2 - 100,0			1,00	1,0 - 1,0

Table 13: Descriptive statistics for Low and High RMS groups before surgery.

RMS values	N	Minimum	Maximum	Mean	Std. Deviation
Low RMS group	20	,5863	1,0689	,829695	,1467019
High RMS group	20	1,1321	3,1851	1,593675	,5419478

Table 14: Comparison between RMS values before and after surgery for the Low RMS group.

Low RMS group	N	Mean	Std. Deviation	P value
RMS Pre-op	20	,829695	,1467019	0,025*
RMS Post-op	20	,906195	,1873105	

*. Difference is significant at the 0.05 level (2-tailed).

Wilcoxon signed rank test

Table 15: Comparison between RMS values before and after surgery for the high RMS group.

High RMS group	N	Mean	Std. Deviation	P value
RMS pre-op	20	1,593675	,5419478	0,001**
RMS post-op	20	1,216845	,3069725	

** . Correlation is significant at the 0,01 level (2-tailed).

Wilcoxon signed rank test

For the specific parts of the face, there was no statistically significant difference between pre-op and post-op RMS values between equivalent parts of the facial surfaces for the Low RMS group (Table 16). For the RMS values of the High RMS group, there is a statistically significant decrease of the RMS values after surgery in the lower third of the face ($P < 0.05$), specifically observed in the mandibular area ($P < 0.05$) (Table 17).

Table 16: Comparison between RMS values before and after surgery for each facial part separately for LOW RMS group.

Low RMS Group RMS values	N	Mean	Std. Deviation	P value
Upper face preop	20	,720605	,2072473	1,000
Upper face postop	20	,722985	,2197324	
Midface preop	20	,816390	,2236141	0,100
Midface postop	20	,935255	,3065587	
Lower face preop	20	,861615	,2388125	0,263
Lower face postop	20	,905225	,2761323	
Maxilla preop	20	,741230	,2444225	0,332
Maxilla postop	20	,792195	,2428730	
Mandible preop	20	,897985	,2936559	0,333
Mandible postop	20	,945870	,3542639	

Wilcoxon signed rank test

Table 17: Comparison between RMS values before and after surgery for each facial part separately for HIGH RMS group.

High RMS Group RMS values	N	Mean	Std. Deviation	P value
Upper face preop	20	,951235	,4470800	0,191
Upper face postop	20	,873470	,4172559	
Midface preop	20	1,383225	,6004903	0,279
Midface postop	20	1,274725	,5199893	
Lower face preop	20	1,582935	,9321057	0,023*
Lower face postop	20	1,211380	,3613537	
Maxilla preop	20	1,062740	,5826896	0,654
Maxilla postop	20	1,022190	,3732948	
Mandible preop	20	1,717345	1,1657923	0,033*
Mandible postop	20	1,269700	,4699459	

*. Difference is significant at the 0,05 level (2-tailed).
Wilcoxon signed rank test

6.4 Comparisons regarding the mid-sagittal plane (MSP)

Moreover, the angle between the MSP before surgery and the MSP after surgery was calculated for all patients. The mean value of this angle between the two MSPs is 0,62 degrees (\pm 0,33 degrees) (Table 18). There is a statistically significant negative correlation between the angle of the two mid-sagittal planes and the absolute difference of RMS values of the whole face before and after orthognathic surgery ($P < 0,05$) (Table 19). When we do the same comparison for specific parts of the face, no part showed statistical significant correlation with the angle between the mid-sagittal planes, except the mandibular part of the lower facial third ($P < 0,05$) (Table 20).

Table 18: Descriptive statistics for the angle between the MSPs before and after surgery

	N	Minimum	Maximum	Mean	Std. Deviation
Angle between MSPs	40	1,4753°	0,1499°	0,625248°	0,3326458°

Table 19: Correlation between the absolute difference in RMS values before and after surgery with the difference in the angulation of the mid-sagittal planes before and after surgery.

			RMS Preop- RMS Postop	Angle between Midlines
Spearman's rho	RMS Preop- RMS Postop	Correlation Coefficient	1,000	-0,392*
		Sig. (2-tailed)	.	,012*
		N	40	40
	Angle between Midlines	Correlation Coefficient	-0,392*	1,000
		Sig. (2-tailed)	,012*	.
		N	40	40
*. Correlation is significant at the 0,05 level (2-tailed).				

Table 20: Correlation between the absolute difference in RMS values for each facial part before and after surgery with the difference in the angulation of the mid-sagittal planes before and after surgery.

		Angle between Midline preop- Midline postop		
RMS preop – RMS postop		Correlation Coefficient	P value	N
Spearman's rho	Upper face	0,176	,276	40
	Midface	-0,125	,443	40
	Lower face	-0,278	,082	40
	Maxilla	-0,090	,581	40
	Mandible	-0,316*	,047*	40
	Angle between Midline preop- Midline postop	1,000	.	40
*. Correlation is significant at the 0,05 level (2-tailed).				

6.5 Volumetric and surface analyses

In addition, a volumetric analysis was performed and absolute volumetric differences were calculated for the whole face and for each individual part of the face. There was no statistically significant difference between the absolute volumetric difference between the two hemifaces before and after orthognathic surgery for the total subjects of the sample (Table 21). The same outcome was found for the same comparison between specific equivalent parts of the face, except the midface. For the midface, a statistically significant difference between pre-op and post-op values of the absolute volumetric difference ($P < 0,05$), with the pre-op difference to show higher values.

Table 21: Comparison of the absolute volumetric difference between hemifaces for T0 and T1 time intervals.

Absolute Volumetric difference	N	Mean	S D	P value
Total face T0	40	5617,5678	5039,00988	0,326
Total face T1	40	4248,0983	3267,59784	
Midface T0	40	3172,6030	2739,15665	0,042*
Midface T1	40	2517,7372	2941,63694	
Lower face T0	40	3326,4173	4593,07680	0,687
Lower face T1	40	2668,1190	3267,59784	

Table 21: Comparison of the absolute volumetric difference between hemifaces for T0 and T1 time intervals.

maxilla T0	40	802,8425	918,04868	0,242
maxilla T1	40	946,5792	734,60144	
mandible T0	40	2913,1263	4420,76048	0,904
mandible T1	40	2222,9588	1875,79035	

*. Difference is significant at the 0.05 level (2-tailed).

Wilcoxon signed rank test

Furthermore, the correlation between the RMS values and the absolute volumetric differences of the two hemifaces was examined. There was a statistically significant positive correlation ($P < 0,05$) between RMS values and the absolute volumetric difference between hemifaces and specific parts of the face (Table 22,23).

Table 22: Correlation between preop RMS and absolute volumetric difference value between hemifaces for each facial part.

Preop	RMS	Volume	Correlation Coefficient	P value	N
Spearman's rho	Total surface		,630**	,000**	40
	Mid face		,705**	,000**	40
	Lower face		,467**	,002**	40
	Maxillary region		,471**	,002**	40
	Mandibular region		,405**	,009**	40

** . Correlation is significant at the 0,01 level (2-tailed).

Table 23: Correlation between postop RMS and absolute volumetric difference value between hemifaces for each facial part.

Postop	RMS	Volume	Correlation Coefficient	Sig. (2-tailed)	N
Spearman's rho	Total surface		,270	,092	40
	Mid face		,434*	,030*	40
	Lower face		,224	,164	40
	Maxillary region		,366*	,020*	40
	Mandibular region		,465**	,003**	40

*. Correlation is significant at the 0,05 level (2-tailed).

**. Correlation is significant at the 0,01 level (2-tailed).

When doing the same comparison for volumetric changes on the Low RMS group, there was no statistically significant difference found among all separate facial parts, as well as for the whole facial volume between T0 and T1 time intervals (Table 24).

Table 24: Comparison of the absolute volumetric difference between hemifaces for T0 and T1 time intervals for the Low RMS group.

Absolute Volumetric difference	N	Mean	S D	P value
Total face T0	20	3024.6300	2302.06084	.232
Total face T1	20	3616.3480	3003.28864	
Midface T0	20	2191.6975	1937.93766	.502
Midface T1	20	1915.8590	2082.00112	
Lower face T0	20	1757.0275	1464.51083	.204
Lower face T1	20	2339.9400	2029.60585	

Table 24: Comparison of the absolute volumetric difference between hemifaces for T0 and T1 time intervals for the Low RMS group.

maxilla T0	20	661.8285	655.00694	.370
maxilla T1	20	810.1325	574.45752	
mandible T0	20	1439.7290	1356.18828	.478
mandible T1	20	1841.4055	1774.75508	

Wilcoxon signed rank test

For the High RMS group, a statistically significant difference was found between the whole facial volume before and after surgery, with the absolute difference between the 2 hemifaces decreasing after surgery ($P < 0,05$)(Table 25). For each segmentation part separately, no significant difference was observed between the two time intervals.

Table 25: Comparison of the absolute volumetric difference between hemifaces for T0 and T1 time intervals for the High RMS group.

Absolute Volumetric difference	N	Mean	S D	P value
Total face T0	20	8210,5055	5715,39912	,040*
Total face T1	20	4879,8485	3472,22956	
Midface T0	20	4153,5085	3101,55070	,052
Midface T1	20	3119,6155	3558,72349	
Lower face T0	20	4895,8070	5997,75137	,601
Lower face T1	20	2996,2980	2215,61715	

Table 25: Comparison of the absolute volumetric difference between hemifaces for T0 and T1 time intervals for the High RMS group.

maxilla T0	20	943,8565	1122,09099	,411
maxilla T1	20	1083,0260	859,35090	
mandible T0	20	4386,5235	5805,62405	,627
mandible T1	20	2604,5120	1940,64986	

*. Correlation is significant at the 0,05 level (2-tailed).

Wilcoxon signed rank test

Furthermore, when comparing the absolute volumetric difference between hemifaces with the angle between the mid-sagittal planes before and after surgery, there was also no significant correlation found (Table 26).

Table 26: Correlation between the absolute volumetric difference between hemifaces before and after surgery with the difference in the angulation of the mid-sagittal planes before and after surgery.

Correlations		Volume difference Preop-Postop	Angle between MSPs
Spearman's rho	Volume difference Preop-Postop	Correlation Coefficient	1,000
		Sig. (2-tailed)	.
		N	20
	Angle between MSPs	Correlation Coefficient	,120
		Sig. (2-tailed)	,613
		N	20

A surface analysis was also performed. There was an absolute correlation found between volume and surface values of the face before and after surgery. Correlation coefficient was found over 0,9 between all the values of the total and partial facial

surfaces before and after surgery (Tables 27, 28).

Table 27: Correlation between volumetric and surface values for each facial part before surgery.

Preop	Volume	Surface	Correlation Coefficient	Sig. (2-tailed)	N
Spearman's rho		Total surface	,932**	,000**	40
		Mid face	,915**	,000**	40
		Lower face	,942**	,000**	40
		Maxillary region	,923**	,000**	40
		Mandibular region	,951**	,000**	40

** . Correlation is significant at the 0.01 level (2-tailed).

Table 28: Correlation between volumetric and surface values for each facial part after surgery.

Postop	Volume	Surface	Correlation Coefficient	Sig. (2-tailed)	N
Spearman's rho		Total surface	,942**	,000**	40
		Mid face	,905**	,000**	40
		Lower face	,938**	,000**	40
		Maxillary region	,922**	,000**	40
		Mandibular region	,947**	,000**	40

** . Correlation is significant at the 0.01 level (2-tailed).

7. DISCUSSION

7.1. Discussion of the Aim

Symmetry is a crucial issue for facial aesthetics, making it a considerable factor while deciding on the outcomes of a surgical procedure. Although the main goal of orthognathic surgery procedure is to improve the function of jaws with the correction of their skeletal relationship, enhancement of facial aesthetics is always a welcome side effect, which is noticed and recognized by the patients. Furthermore, it is found that patients with dental malocclusions are more likely to exhibit higher levels of facial asymmetry (Sforza et al., 2007). Combining a possibly high preexisting asymmetry level with the possibility of the surgical procedure increasing inadvertently the asymmetry of the face, we can evaluate the importance of the control, and if possible prediction, of asymmetry levels through any intervention.

Facial asymmetry can be evaluated in terms of bony and soft tissues. Although for the evaluation of skeletal relations, techniques with radiation exposure to the patient are required, for soft tissue imaging, non-radiographic techniques have been developed. Stereophotogrammetry is the technique mainly used nowadays for three-dimensional image acquisition, providing a quick, noninvasive and practical tool for soft tissue analysis, without the exposure of the facial surface to any radiation. The resulting images are accurate, detailed and reproducible, giving us a strong tool in initial diagnosis. 3D stereophotogrammetry gives us the ability to follow Sir Harrold Gillies' advice of wisdom, "first diagnose, then treat", by enhancing our diagnostic capabilities. For our research, we used a method of calculating asymmetry that takes into consideration the whole facial surface, providing us with thorough results with the use of a computer algorithm. These surface-based methods for measurement of facial asymmetry are promising for extensive clinical use for the quantification of asymmetry values preoperatively and for evaluation of the outcomes of the medical procedures. In conclusion, our study has proved the validity of a landmark-independent method of calculating asymmetry of the facial surface and the outcomes of our analyses will hopefully contribute to further investigation of soft tissue response to double-jaw,

orthognathic surgery. The ability to predict this soft tissue response will benefit us with a more controlled approach to the management of the orthognathic surgical outcomes.

7.2. Discussion of Materials and Methods

One of the main principles in health sciences is the use of minimal invasive techniques when there is the possibility to do so. Stereophotogrammetry is a non-invasive technique, used as a diagnostic tool in the facial area. It's more advanced than conventional 2D capturing techniques by offering a three-dimensional template, without any radiation projected to the patient. The 3dMDface system (Atlanta, GA, USA) used in this study is considered a reliable and very widely used system for 3D surface imaging. By the use of active stereophotogrammetry, an unstructured pattern is projected on the subject's surface. For this reason, the procedure is not depending on ambient lighting for capturing (Lane and Harrell, 2008). The 3dMDface system also has a quick capturing speed of 1,5 milliseconds, eliminating this way undesirable products of facial movements, but also providing a complete, fully textured and accurate capture of the facial soft tissues (Lee, 2004; Honrado et al., 2006). No input from the operator is required for the image processing procedure (Metzler et al., 2013). These features make stereophotogrammetry a reliable tool for research, by providing a way to evaluate soft tissue changes with a patient-friendly procedure (Heike et al., 2010). Until today, numerous articles have proven the 3dMDface system reliable and accurate (Aldridge et al., 2005; Weinberg et al., 2006; Wong et al., 2008; Lubbers et al. 2010; Ort et al., 2012; Metzger et al., 2013; Eder et al., 2013; van der Meer et al., 2014; ; Nord et al., 2015). The use of laser scanners for image acquisition of facial surfaces has been also proved accurate. Nonetheless, the capturing time for the laser scanner is much longer, averaging at 7,5 seconds. In addition, the scan of the left and right sides are separately performed and, afterwards, a correction and merging process is required from the software, but also from the user manually, in order to acquire the final output (Kau et al., 2006).

Photogrammetry in three-dimensions has been used by many authors to assess the asymmetry levels on craniofacial patients and to examine the surgery's and molding's

effects on the facial surface (Maull et al., 1999; Sander et al., 2011; Kau, 2011; Ras et al., 1995). This technology gives us the possibility to exploit the facial surface by measuring the facial anatomy, by rotating it in the three planes of space and by calculating the symmetry of the surfaces (Taylor et al., 2014).

Historically, the asymmetry of the facial surfaces was calculated with the use of anthropometry or 2D photographs. The 2D analysis uses planar and linear differences between the two hemifaces to assess the asymmetry levels. Both of these techniques are susceptible to errors in measurements, plus, the use of 2D methods for calculating a three-dimensional concept is not ideal, as the measurements can be affected by even a slight tilt or rotation of the head during image capturing (de Moraes et al., 2011).

After the development of 3D stereophotogrammetry, the dominant method for calculating the facial asymmetry was the use of facial landmarks. This method has the disadvantage of taking into consideration only a small number of facial points in each hemiface in order to calculate the asymmetry in a whole facial surface. These landmarks are determined on both sides by the user, which puts a subjectivity aspect on the measurements and can lead to inexactness. The areas of landmark placement's also can lead to misconceptions about the overall asymmetry, if they are placed in highly asymmetric or symmetric area, or if there are areas of far between and few landmarks, the asymmetry might not be diagnosed (Blockhaus et al., 2014; Verhoeven et al., 2016; Alqattan et al., 2013). Therefore, an analysis that doesn't depend on landmarks was chosen for our study, based on the ICP algorithm and the mirroring and superimposition of the two halves of the facial surface. This analysis has proven to be highly effective, taking into consideration the whole facial surface of 10.000 to 16.000 correlated points for the asymmetry assessment, and reproducible (Blockhaus et al., 2014; Verhoeven et al., 2016; Meyer et al., 2011), as the only step of manual computation by the user is the facial area selection (Codari et al., 2016). When Kornreich et al. (2016) compared the ICP to the landmark method, they found the results comparable, but noted ICP as more accurate and reproducible method, showing a significantly lower rate of error than the landmark method.

The ICP forehead method was also used for the superimposition of the pre-operative and post-operative 3D models, for the calculation of the differences between the mid-sagittal planes in these two time intervals. According to Verhoeven et al. (2016), the

ICP forehead method of a 1-mm threshold, used in our study, was considered the optimal selection for clinical application, being consistently the nearest to the gold standard.

In our study, following the ICP method, the levels of asymmetry of the facial surface were objectively evaluated from a soft-tissue analysis by the 3matic software by Materialise (Materialise Europe, World Headquarters, Leuven, Belgium). This analysis provided us with the RMS value, which presents the asymmetry levels as explained before. The RMS value reaches its possible minimum when the most accurate superimposition is achieved between the original and the mirrored 3D image. This technique is similar to the Procrustes technique, used for analogous measurements (Goodall et al., 1991; Maull et al., 1999; Grayson et al., 1999; Sander et al., 2011) and is proven to be a powerful and reliable method for the facial asymmetry analysis (Codari et al., 2016; Ozsoy, 2016).

Additionally, the facial surface was separated in various ways for the optimal complete and partial analysis of asymmetry. Initially, the areas of the ears and the hair were cut out, areas that are pretty easily defined. In the contrary, the area of the neck is a wide area and exhibits a great amount of variation among individuals. Specifically in subjects with excessive submental fat or with a platysma banding, the neck can result to be remarkably asymmetric. As a result, the neck area can have a big influence on the procedure of surface registration and mislead the resulting values, therefore, it is preferable to be excluded (Verhoeven et al., 2016). Subsequently, the ICP registration of the native and reflected faces produces a MSP, separating the face into two hemifaces. This method was also proven to be highly valid and reproducible (Benz et al., 2002; Nkenke et al., 2006; Hartmann et al., 2007) as it was concluded that the lack of relevant random and systematic errors at the measurements, makes this technique applicable for clinical use (Nkenke et al., 2003, 2006).

When compared to the method of calculating the MSP with the use of the points alleged as “midline landmarks”, consisting of the nasion (Na), the subnasale (Sn), the labrale superius (Ls) and the labrale inferius (Li) landmarks, it was shown, in healthy children, that the resulting “landmark MSP” was not coinciding after superimposition to the mirrored images (Meyer et al., 2011). Lastly, the facial surface was separated with the use of horizontal planes to upper face, mid face and lower face, with the last

one to be subsequently separated into the maxillary and mandibular area. For this separation, only 3 landmarks were used, the nasion (Na), subnasale (Sn) and Helion (H) landmarks, as the horizontal planes were automatically generated vertical to the MSP and parallel to each other, showing great reproducibility. This separation was performed in order to have a more specific insight on the areas of asymmetry, as a single RMS number for valuing the facial symmetry can be useful in research, but not clinically practical (Kornreich et al., 2016; Verhoeven et al., 2016). Occasionally, a very symmetric part of the face can compensate the asymmetry in another part of the facial surface, resulting in a misleading of the findings if based on a single RMS value. This specificity of the areas of asymmetry is presented with our technique with the use of color maps for asymmetry that provide the most detailed information for the facial asymmetry. Due to the size of our sample though, it was optimal to subdivide the facial surface to our separation areas according to facial height, in order to be led to more systematic findings. Moreover, the division of the facial surface allows for more targeted treatment planning in the areas of interest of the orthodontic and oral and maxillofacial surgery fields, helping also the communication of the asymmetry levels to the patients, especially in cases that the asymmetry is located on areas above the level of the eyes, beyond the scope of the above mentioned fields (Alqattan et al., 2013; Codari et al., 2016)

All our patients underwent orthognathic surgery during the time of April 2012 to November of 2018. Ideally, it would be preferable that all the patients were operated by one single surgeon, yet they were operated by various surgeons in various medical facilities throughout Istanbul, Turkey.

Nevertheless, similar operating techniques and principles were used by the operating surgeons, with the goal being invariable, to obtain ideal skeletal harmony of the face. Likewise, due to the nature of this study being retrospective, different operators were involved in the three-dimensional image acquisition, yet all operators were acting in accordance with the ideal guidelines for the optimization of the image capturing. The 3D images that were found not to agree with these guidelines were excluded from our study.

7.3. Discussion of the Results

There was no statistically significant difference found between RMS values between T0 (pre-op) and T1 (post-op) for the whole sample of the 40 patients (Table 4). The same outcome was found when the RMS values of the different parts of face segmentation (upper, mid, lower face, maxillary and mandibular area) were compared in the T0 and T1 time intervals (Table 5). However, a statistically significant positive correlation was found between the initial RMS value and the difference in RMS values in T0 and T1 ($P < 0,001$) (Table 6). The same positive correlation was also found for every one of the 4 parts of our segmentation ($P < 0,01$ for the midface, $P < 0,001$ for the lower face, the maxillary and the mandibular area) (Tables 7-10). This shows us the positive relationship between the initial facial asymmetry and the effects of the orthognathic surgery. According to this correlation, we can conclude that the more asymmetric the facial surface before orthognathic surgery, the more improvement in symmetry of the soft tissues there will be, following the surgical procedure. The same also counts for the parts of the facial surface. The more asymmetric the soft tissues of the midface, the lower face, the maxillary and mandibular area respectively, the more improvement in the soft tissue symmetry will follow the orthognathic surgery. Nevertheless, according to this correlation, the opposite outcome appears for more symmetric patients. As we can observe in the correlation graph, negative values in the X-axis are also present, meaning that the patients with more symmetric facial soft tissues will have less improvement or even end up more asymmetric after surgery (Figure 14). The same counts also for the parts of the face that present lower asymmetry levels, as again the correlation points reach negative values in the X-axis (Figures 15-18). In an attempt to further analyze these results, our sample was separated into two subgroups of 20 subjects each, with the use of a ROC curve analysis (Tables 11,12). The two groups were divided according to the levels of asymmetry on the whole facial surface before they underwent orthognathic surgery (RMS preop) and the ideal cut-off point was found on an RMS value of 1,0689 ($P < 0,0001$). Our hypothesis, that more symmetric faces become more asymmetric after surgery, was confirmed with a significant increase in RMS values on the Low RMS group after orthognathic surgery ($P < 0,05$) (Table 14), as well that more asymmetric faces become

more symmetric after surgery, with a significant decrease in RMS values post-operatively ($P < 0,001$) (Table 15). To specify the areas of significant differences, we compared the RMS values on T0 and T1 for each part of the face for both groups. On the Low RMS group, there was no statistical significant increase in RMS values in any specific part of the face (Table 16), showing that there is no targeted area to blame for the increased asymmetry levels after surgery. On the other side, for the High RMS group, there was a statistically significant decrease in RMS values in the lower face ($P < 0,05$) and the mandibular area ($P < 0,05$) (Table 17). This shows us that in subjects with higher asymmetry levels, the area of bigger symmetry improvement is the lower face and specifically the mandibular area.

Furthermore, the correlation between the MSP changes and RMS changes after orthognathic surgery was investigated. There was a statistically significant negative correlation between the angle of the two mid-sagittal planes and the absolute difference of RMS values of the whole facial surface before and after orthognathic surgery ($P < 0,05$) (Table 19). This shows us that RMS values are highly correlated with the calculation of the MSP as any change in the RMS values can affect also the MSP of the face. This correlation was examined even further, by investigating the correlation of the MSP with the different parts of the face. It was found that the changes in MSP angles was highly correlated with changes in the mandibular area ($P < 0,05$) (Table 20). Subsequently, a volumetric analysis was performed for the two hemifaces and the individual parts of the face. There was a statistically significant positive correlation between RMS values and the absolute volumetric difference between hemifaces, before orthognathic surgery, for the whole facial surface and all specific segmentation parts ($P < 0,01$) (Table 22) and after surgery for the midface, maxillary ($P < 0,05$) and mandibular area ($P < 0,01$) (Table 23).

In a study from Wermker et al. (2014), a 3D method of calculating the facial asymmetry was used with the application of the ICP algorithm, like in our study. 48 patients who underwent double-jaw surgery were examined before and after surgery and an asymmetry index was calculated. They reported that the faces became more harmonic and symmetric after the orthognathic surgery procedure, but the symmetry improvement was not found statistically significant. Ferrario et al. (1999), in their study, used anthropometric digitized landmarks to calculate facial symmetry and

concluded in increased levels of asymmetry after the orthognathic surgery procedure, except from the lower third of the face which presented reduced levels of asymmetry following the orthognathic surgery. On 2012, Verze et al., with the use of lateral cephalometric x-rays and facial 3D scans on 15 patients who underwent orthognathic surgery, concluded from a landmark analysis that the double jaw surgery procedure can provide a major improvement on the facial symmetry levels. In another study, Lee et al. (2013) analyzed the facial asymmetry of 5 orthognathic surgery patients from 3D images with the use of facial landmarks and volumetric analysis and concluded that the facial soft tissues become more symmetric after surgery, especially in the mandibular area, confirmed also with the volumetric values of the face.

In a study with similar methodology with our study, Ostwald et al. (2015) analyzed 25 faces before and after orthognathic surgery. They used stereophotogrammetry and registered the original and mirror facial images with the ICP algorithm, in order to get a asymmetry value for each facial surface. They found a statistically non-significant decrease between pre-op and post-op asymmetry values, which agrees with our results for our whole sample. They also reported that 40% of their subjects showed increased asymmetry levels after the orthognathic surgery. The 4 of these 10 patients of increased asymmetry were the ones presenting the lowest asymmetry values before orthognathic surgery. Additionally, a statistically significant correlation between pre-surgical and post-surgical asymmetry values was reported ($r = 0,697$, $P < 0,001$) was found, showing that more asymmetric patients show a greater improvement in facial symmetry after orthognathic surgery, a finding that full confirms our study's findings ($r = 0,653$, $P < 0,001$).

When it comes to the interaction of hard and soft tissues, the literature has many contradictory findings (Burstone, 1998; Ferrario et al., 1994; Peck et al., 1991, Soncul et al., 2004). Although the source of facial asymmetry in the soft tissues is mainly skeletal, the soft tissues have the ability of even masking the asymmetries resulted from the skeletal asymmetric relationships (Burstone, 1998; Ferrario et al., 1994). Additionally, although the changes in the bony tissues generate changes also in soft tissues, the elasticity of the soft tissues makes the levels and the extent of the changes unpredictable (Soncul et al., 2004). Wermker et al. (2014) reported a moderate response of the soft tissues at the midface area following maxillary movements, even

when compared to similar movements of the mandible. They reasoned this to the surgical procedure during the reduction of the anterior part of the nasal spine for the harmonization of the skeletal relationships. As a result, there is an indirect reduction on the skeletal shift of the maxilla, ending up in an insignificant response on the soft tissues. Another explanation for this insignificant response can be the procedure of applied matching. As the area of the nose and eyes are being defined like constant regions, the 3D models before and after surgery are matched accordingly. Because of this, the soft tissue changes in the midfacial area might not be that obvious like in the mandibular area. The soft and hard tissues have a complex way of interacting, not completely understood yet, and orthognathic surgery results in changes in the reciprocal arrangements between them and their reciprocal arrangement (Ferrario et al., 1999). Consequently, it is mandatory that the asymmetry of the face is captured in a global way, providing a view to changes from orthognathic surgery. In this study, we tried to provide a pattern to help with the understanding of the facial soft tissue response to bony tissue movements, however our focus on the soft tissue asymmetries and movements and not on the skeletal reasoning of the asymmetry. This restriction can be overcome by the combination and superimposition of 3D soft tissue scans through stereophotogrammetry and 3D CT scans of the skeletal tissues (Hajeer et al., 2004).

For the evaluation of the facial asymmetry, the RMS values were calculated between the native and mirrored 3D surfaces, a method proven for its reliability in the literature (Taylor et al., 2014; Ostwald et al., 2015; Ozsoy, 2006). In other studies that used the RMS values for the same purpose, Taylor et al. (2014) used the data collected from 100 volunteers through 3D stereophotogrammetric scanning to calculate the RMS values of their facial surfaces and reach to values that represent the norms of asymmetry. They reported that the evaluation and rating of the asymmetry levels from independent observers proved to be highly unreliable due to low interobserver reliability values. Therefore, they focused on defining the asymmetry levels mathematically, by minimizing the RMS values between original and mirrored images through superimposition and registration. They found a mean RMS value of 0,80 (\pm 0,24 mm) for the subjects who were considered symmetric. These values come almost in agreement with our values for the Low RMS group (0,83 \pm 0,15mm) (Table 13).

Another study by Patel et al. (2015), created two groups of 28 and 27 subjects rated with symmetric and asymmetric faces respectively by three orthodontists and calculated their RMS values with a similar technique as in our study. They found a mean RMS value of 1,52 ($\pm 0,39$ mm) for the symmetric group and a value of 2,85 ($\pm 1,54$ mm) for the asymmetric group. They confirmed the statistically significant difference of these two values and attempted the creation of a template for the prediction of RMS values for subjects considered symmetric and asymmetric. Both of their mean values were considerably higher than our found mean RMS values for Low RMS and High RMS patients ($0,83 \pm 0,15$ mm and $1,59 \pm 0,54$ mm, respectively) (Table 13). In 2016, Kornreich et al., used a large sample of 339 adults to define the norms in RMS values. Their subjects were not categorized to symmetric and asymmetric faces and their mean RMS value was found 0.63 ($\pm 0,16$ mm), ranging from 0,27 mm to 1,23 mm, being considerably lower than our mean RMS value ($1,21 \pm 0,55$ mm) (Table 4). Finally, in another study by Ozsoy (2016), a mean RMS value for 51 healthy subjects was found 0,95 ($\pm 0,2$ mm). In comparison to these studies, we can observe the greater RMS values of our study when compared to mean RMS values from the general population. This can be explained by the higher level of asymmetries reported in Class III patients, who are about to undergo an orthognathic surgical treatment, when compared to the general population (Severt and Proffit, 1997; Willems et al, 2001; Haraguchi et al, 2002; Yoon et al, 2004; Chew, 2006).

Our study used the RMS value and a volumetric analysis to quantify facial asymmetry (Tables 4,21). However, these techniques of measuring facial asymmetry should be clearly divided from the measurement of facial attractiveness and human perception of facial asymmetry. The absolute symmetry in the face is an almost theoretical concept, with even the most attractive faces to exhibit a degree of asymmetry (Peck et al., 1991; Ferrario et al., 1995; Sforza et al., 2010). For example, the location of the asymmetry can play an important role on the perception for the whole facial surface. Amodeo (2017) reported that deviations on the area of the nose were more “eye-catching” than deviations in other facial areas. There is a variety of factors able to influence the perception of lay people for facial attractiveness (Bashour, 2006) and our study only covers an important, but small, part of those.

There are also limitations when measuring the soft tissues. Although it is proven that stereophotogrammetry is a reliable method for soft tissue analysis, providing a fast, detailed and radiation free solution to three-dimensional facial image acquisition (Choi et al., 2013; Stauber et al., 2008), it is not capable of providing a base on a technical level to acquire accurate morphologic predictions of the reaction of the soft tissues to the changes in skeletal relationships. Therefore, it shouldn't serve as a diagnostic tool, but as an addition to all the diagnostic tools available, helping with a more detailed visualization of the facial area.

When it comes to the volumetric and surface analyses, although a high correlation was found between RMS values and volume for the total facial surface and all parts of the face separately, except the total facial volume in T1, differences in the results from the RMS values were found for the rest of the comparisons (Tables 21,24,25,26). There was a statistically significant decrease in absolute volumetric values between hemifaces in the midface area between T0 and T1 (Table 21) and no correlation between angulation changes of the mid-sagittal planes (Table 26). Moreover, a significant decrease in absolute volumetric differences between hemifaces was observed for the High RMS group (Table 25), showing that the faces that show higher initial asymmetry values, have greater improvement in their volumetric differences in addition to the already significant improvement in symmetry values through the decrease in RMS values.

The surface analysis was performed as an additional measurement, in order to examine another way of measurement and its relation to the volumetric measurements. It was found that there is an absolute correlation between surface and volume (Tables 27,28), therefore no additional data can be obtained in comparison to the volumetric analysis. It is critical to mention at this point, that the volumetric differences between hemifaces is not a indicator of asymmetry and the volumetric analysis of the two sides of the face isn't a diagnostic tool for asymmetry. However, asymmetry can be related to bigger volumetric differences, without this being an absolute statement. This was found with the significant correlations between RMS and volumetric values among many parts of the facial surface.

8. Conclusion

Taking into consideration the limitations of the present study, the following conclusions can be made. Firstly, the value of three-dimensional stereophotogrammetry as an accurate, efficient and effective method for investigating the changes in the facial soft tissues without any radiation exposure to the patient.

Moreover, no significant changes were found in the asymmetry levels of the patients following the orthognathic surgery procedure, but there was a significant correlation between the initial facial symmetry levels and the symmetry improvement after surgery. Based on this, through additional analyses, it was concluded that faces who show bigger initial asymmetry levels, end up being more symmetric after surgery and patient who show bigger initial symmetry levels, end up being more asymmetric after surgery. The changes in asymmetry levels in the more symmetric patients were mostly observed in the midface region and in the more asymmetric patients mostly on the lower third of the face, specifically in the mandibular area.

Furthermore, it was found that the changes in asymmetry levels can affect the mid-sagittal plane's angulation, with these two factors being highly correlated with each other.

Finally, a significant correlation was found between facial symmetry and volumetric values of the face for most of our measurements, as well as between volumetric and surface values of the face.

9. REFERENCES

Abramson DI, Chu LS, Tuck S, Lee SW, Richardson G, Levin M. Effect of tissue temperature and blood flow on motor nerve conduction velocity (1996). *JAMA*. **198**: 1082-1088.

Aboul-Hosn Centenero S, Hernández-Alfaro F: 3D planning in orthognathic surgery: CAD/CAM surgical splints and prediction of the soft and hard tissues results, our experience in 16 cases (2012). *J Craniomaxillofac Surg* **40**: 162-168,

Achilleos S, Krogstad O, Lyberg T. Surgical mandibular setback and changes in uvuloglossopharyngeal morphology and head posture: a short and long-term cephalometric study in males (2000). *Eur J Orthod*. **22**: 383-394.

Aldridge K, Boyadjiev SA, Capone GT, DeLeon VB, Richtsmeier JT. Precision and error of three - dimensional phenotypic measures acquired from 3dMD photogrammetric images (2005). *Am J Med Genet A*. **138**: 247 – 253.

Al-Khateeb TH, Nusair Y. Effect of the proteolytic enzyme serrapeptase on swelling, pain and trismus after surgical extraction of mandibular third molars. *Int J Oral Maxillofac Surg* (2008). **37**: 264–268.

Alqattan, M., J. Djordjevic, A. I. Zhurov, and S. Richmond. "Comparison between landmark and surface-based three-dimensional analyses of facial asymmetry in adults(2013)." *The European Journal of Orthodontics* **37.1**: 1-12.

Amodeo, Chiara A. "The Central Role of the Nose in the Face and the Psyche: Review of the Nose and the Psyche (2007)." *Aesthetic Plastic Surgery* **31.4**: 406-410

Angle EH. Double Resection of the Lower Maxilla. *The Dental cosmos* (1898). **40(8)**; 635-638.

Aung SC, Ngim RC, Lee ST. Evaluation of the laser scanner as a surface measuring tool and its accuracy compared with direct facial anthropometric measurements. *Br J Plast Surg* (1995). **48**: 551 – 558.

Ayoub A, Garrahy A, Hood C, White J, Bock M, Siebert JP. Validation of a vision based, three - dimensional facial imaging system (2003). *Cleft Palate Craniofac J*. **40**: 523 –529.

Ayoub AF, Siebert P, Moos KF, Wray D, Urquhart C, Niblett TB. A vision-based three - dimensional capture system for maxillofacial assessment and surgical planning (1998). *Br J Oral Maxillofac Surg.* **36**: 353 –357.

Ayoub AF, Stirrups DR. The practicability of finite-element analysis for assessing changes in human cranio-facial morphology from cephalographs (1993). *Arch Oral Biol.* **38**: 679 –683.

Ayoub AF, Wray D, Moos KF, Jin J, Niblett TB, Urquhart C. A three-dimensional imaging system for archiving dental study casts: A preliminary report (1997). *Int J Adult Orthodon Orthognath Surg.* **12**: 79 – 84.

Ayoub AF, Wray D, Moos KF, Siebert P, Jin J, Niblett TB. Three-dimensional modeling for modern diagnosis and planning in maxillofacial surgery (1996). *Int J Adult Orthodon Orthognath Surg.* **11**: 225-233.

Baccetti T, Franchi L, McNamara JA, Jr. Cephalometric variables predicting the long-term success or failure of combined rapid maxillary expansion and facial mask therapy (2004). *Am J Orthod Dentofacial Orthop.* **126(1)**: 16-22.

Baccetti, Tiziano, Lorenzo Franchi, and James A. McNamara. "Growth in the Untreated Class III Subject (2007)." *Seminars in Orthodontics* **13.3**: 130-142.

Bamgbose BO, Akinwande JA, Adeyemo WL, Ladeinde AL, Arotiba GT, Ogunlewe MO. Effects of co-administered dexamethasone and diclofenac potassium on pain, swelling and trismus following third molar surgery (2005). *Head Face Med.* **7(1)**: 11.

Barnett A, Whitaker LA. Facial form analysis of the lower and middle face (1986). *Plast Reconstr Surg.* **78**: 158-165.

Bashour, Mounir. "History and Current Concepts in the Analysis of Facial Attractiveness (2006)." *Plastic and Reconstructive Surgery* **118.3**: 741-756.

Bauer RE, 3rd, Ochs MW. Maxillary orthognathic surgery (2014). *Oral Maxillofac Surg Clin North Am.* **26(4)**: 523-537.

Baysal A, Sahan AO, Ozturk MA, et al. Reproducibility and reliability of three-dimensional soft tissue landmark identification using three-dimensional stereophotogrammetry (2016). *Angle Orthod.* **86(6)**: 1004-1009.

Beard L, Burke PH. Evolution of a system of stereophotogrammetry for the study of facial morphology (1967). *Med Biol Illus.* **17**: 20-25.

Benetello V, Sakamoto FC, Giglio FP, Sakai VT, Calvo AM, Modena KC. The selective and non-selective cyclooxygenase inhibitors valdecoxib and piroxicam induce the same postoperative analgesia and control of trismus and swelling after lower third molar removal (2007). *Braz J Med Biol Res.* **40(8)**: 1133-1140.

Benz, M., Laboureaux, X., Maier, T., Nkenke, E., Seeger, S., Neukam, F., Häusler, G.: The symmetry of faces (2002). In: *Proceedings of Vision, Modeling and Visualization*, pp. **43–50**

Bergeron L, Tu CC, Chen YR. Single-split technique for correction of severe facial asymmetry: correlation between intraoperative maxillomandibular complex roll and restoration of mouth symmetry (2008). *Plast Reconstr Surg.* **122**: 1535

Berghagen M. Photogrammetric Principles Applied to Intra-Oral Radiodontia. A Method for Diagnosis and Therapy in Odontology (1951). Thesis, Royal School of Dentistry, Stockholm, Sweden.

Bjerin R. A comparison between the Frankfort horizontal and the sella turcica-nasion as reference planes in cephalometric analysis (1957). *Acta Odontol Scand.* **15**: 1-13.

Bjorn H, Lundqvist C, Hjelmstrom P. A photogrammetric method of measuring the volume of facial swellings (1953). *J Dent Res.* **33**: 295 – 308.

Blockhaus, M., et al. "Three-dimensional investigation of facial surface asymmetries in skeletal malocclusion patients before and after orthodontic treatment combined with orthognathic surgery (2014)." *Journal of Orofacial Orthopedics / Fortschritte der Kieferorthopädie*, vol. **75**, no. **2**: pp. 85-95.

Bourne CO, Kerr WJ, Ayoub AF. Development of a three-dimensional imaging system for analysis of facial change (2001). *Clin Orthod Res.* **4**: 105 – 111.

Braams JW, Stegenga B, Raghoobar GM, Roodenburg JL, van der Weele LT. Treatment with soft laser. The effect on complaints after the removal of wisdom teeth in the mandible (1994). *Ned Tijdschr Tandheelkd.* **101(3)**: 100-103.

Braun S, Lee KG, Legan HL. A reexamination of various extraoral appliances in light of recent research findings (1999). *Angle Orthod.* **69(1)**: 81-84.

Broca M. Sur les projections de la tete, et sur un nouveau procedé de cephalometrie (1862). *Bull Soc Anthropol Paris.* **3**: 514-544.

Burstone, Charles J. "Diagnosis and treatment planning of patients with asymmetries (1998)." *Seminars in Orthodontics* **4.3**: 153-164

Byrd KE. Masticatory movements and EMG activity following electrolytic lesions of the trigeminal motor nucleus in growing guinea pigs (1984). *Am J Orthod.* **81**: 292-298.

Cakirer B, Dean D, Palomo JM, Hans MG. Orthognathic surgery outcome analysis: 3-dimensional landmark geometric morphometrics (2002). *Int J Adult Orthodon Orthognath Surg.* **17(2)**: 116-132.

Caruso AJ, Stanhope SJ, McGuire DA. New technique for acquiring three - dimensional orofacial nonspeech movements (1989). *Dysphagia.* **4**: 127 – 32.

Chan GK. Class 3 malocclusion in Chinese (Cantonese): etiology and treatment (1974). *Am J Orthod.* **65(2)**: 152-157.

Chebib FS, Chamma AM. Indices of craniofacial asymmetry (1981). *Angle Orthod.* **51**: 214-226.

Cheong YW, Lo LJ. Facial asymmetry: etiology, evaluation and Management (2011). *Chang Gung Med J.* **34**: 341Y351

Chew MT. Spectrum and management of dentofacial deformities in a multiethnic Asian population (2006). *Angle Orthod.* **76**: 806-809.

Chiu CS, Clark RK. Reproducibility of Natural Head Position in Standing Subjects (1991). *J Dent.;* **19**: 130–131.

Choi BH, Min YS, Yi CK, Lee WY. A comparison of the stability of miniplate with bicortical screw fixation after sagittal split setback (2000). *Oral Surg Oral Med Oral Pathol Oral Radiol Endod.;* **90(4)**: 416-419.

Choi BH, Zhu SJ, Han SG, Huh JY, Kim BY, Jung JH. The need for intermaxillary fixation in sagittal split osteotomy setbacks with bicortical screw fixation (2005). *Oral Surg Oral Med Oral Pathol Oral Radiol Endod.* **100(3)**: 292-295.

Choi JW, Lee JY, Oh TS, Kwon SM, Yang SJ, Koh KS: Frontal soft tissue analysis using a 3 dimensional camera following two-jaw rotational orthognathic surgery in skeletal class III patients (2013). *J Craniomaxillofac Surg* 16. Jul **pp**: S1010-5182(13)00123-6

Codari, Marina, Valentina Pucciarelli, Fabiano Stangoni, Matteo Zago, Filippo Tarabbia, Federico Biglioli, and Chiarella Sforza. "Facial thirds–based evaluation of facial asymmetry using stereophotogrammetric devices: Application to facial palsy subjects (2017)." *Journal of Cranio-Maxillofacial Surgery* **45.1**: 76-81.

Cohen MM Jr. Perspectives of craniofacial asymmetry. Part III. Common and/or well known causes of asymmetry (1995). *Int J Oral Maxillofac Surg.* **24**: 127-133.

Cooke MS, Wei SH. The reproducibility of natural head position: a methodological study (1988). *Am J Orthod Dentofacial Orthop.* **93**: 280-288.

Copray JC, Dibbets JM, Kantomaa T. The role of condylar cartilage in the development of the temporomandibular joint (1988). *Angle Orthod* **58**: 369–80.

Da Silveira AC, Daw JL, Jr, Kusnoto B, Evans C, Cohen M. Craniofacial applications of three - dimensional laser surface scanning (2003). *J Craniofac Surg.* **14**: 449 – 456.

Darras BT, Jones HR, Ryan MM, De Vivo DC. *Neuromuscular disorders of infancy, childhood, and adolescence : a clinician's approach* (2015). 2nd edition. London: Elsevier

Day CJ, Robert T. Three-dimensional assessment of the facial soft tissue changes that occur postoperatively in orthognathic patients (2006). *World J Orthod.* **7(1)**: 15-26.

Dietrich UC. Morphological variability of skeletal Class 3 relationships as revealed by cephalometric analysis (1970). *Rep Congr Eur Orthod Soc.* **pp**: 131-143.

de Haan, IF Ciesielski R, Nitsche T, Koos B. Evaluation of relapse after orthodontic therapy combined with orthognathic surgery in the treatment of skeletal class III (2013). *Journal of Orofacial Orthopedics / Fortschritte der Kieferorthopädie.*; **74(5)**: 362-36.

de Moraes ME, Hollender LG, Chen CS, Moraes LC, Balducci I. Evaluating craniofacial asymmetry with digital cephalometric images and cone-beam computed tomography (2011). *Am J Orthod Dentofacial Orthop.***139**: e523–31.

Deli R, Galantucci LM, Laino A, D'Alessio R, Di Gioia E, Savastano C. Three-dimensional methodology for photogrammetric acquisition of the soft tissues of the face: a new clinical-instrumental protocol (2013). *Prog Orthod.* **14**: 32.

Deng Z, Neumann U, Lewis JP, Kim TY, Bulut M, Narayanan S. Expressive facial animation synthesis by learning speech coarticulation and expression spaces (2006). *IEEE Trans Vis Comput Graph.* **12**: 1523 – 1534.

Donatsky O, Bjørn-Jørgensen J, Hermund NU, Nielsen H, Holmqvist-Larsen M, Nerder PH: Accuracy of combined maxillary and mandibular repositioning and of soft tissue prediction in relation to maxillary antero-superior repositioning combined with mandibular set back A computerized cephalometric evaluation of the immediate postsurgical outcome using the TIOPS planning system (2009). *J Craniomaxillofac Surg* **37**: 279-284

Eder M, Brockmann G, Zimmermann A, Papadopoulos MA, Schwenzer-Zimmerer K, Zielhofer HF, Sader R, Papadopoulos NA, Kovacs L. Evaluation of precision and accuracy assessment of different 3-D surface imaging systems for biomedical purposes (2013). *Journal of Digital Imaging*. **26**: 163-172.

Eian J, Poppele R. A single camera method for three - dimensional video imaging (2002). *J Neurosci Methods*. **120**: 65-83.

Ellis E, 3rd, McNamara JA Jr. Components of adult Class III malocclusion (1984). *J Oral Maxillofac Surg*. **42(5)**: 295-305.

Enciso R, Memon A, Fidaleo DA, Neumann U, Mah J. The virtual craniofacial patient: 3D jaw modeling and animation (2003). *Stud Health Technol Inform*. **94**: 65 – 71.

Epker BN. Modifications in the sagittal osteotomy of the mandible (1977). *J Oral Surg*. **35(2)**: 157-159.

Farkas LG. *Anthropometry of the head and face*. New York: Raven Press. 1994.

Farrera, A., Villanueva, M., Quinto-Sánchez, M., & González-José, R. (2015). The relationship between facial shape asymmetry and attractiveness in Mexican students. *American Journal of Human Biology*, *27(3)*, 387–396.

Ferrario VF, Sforza C, Tartaglia GM, Sozzi D, Caru A. Three-dimensional lip morphometry in adults operated on for cleft lip and palate. *Plast Reconstr Surg*. 2003; **111**, 2149-2156.

Ferrario VF, Sforza C, Poggio CE et al (1994) Distance from symmetry: a three-dimensional evaluation of facial asymmetry. *J Oral Maxillofac Surg* **52**:1126– 1132

Ferrario VF, Sforza C, Miani A, Tartaglia G. Craniofacial morphometry by photographic evaluations. *Am J Orthod Dentofacial Orthop*. 1993;**103(4)**:327-337.

Ferrario VF, Sforza C, Miani A, Serrao G. A three dimensional evaluation of human facial asymmetry. *J Anat*. 1995;**186**:103-110.

Ferrario VF, Sforza C, Schmitz JH, Santoro F. Three-dimensional facial morphometric assessment of soft tissue changes after orthognathic surgery. *Oral Surg Oral Med Oral Pathol Oral Radiol Endod*. 1999;**88(5)**,549-556.

Foster TD, Day AJ. A survey of malocclusion and the need for orthodontic treatment in a Shropshire school population. *Br J Orthod*. 1974; **1(3)**, 73-78.

Gallego-Romero D, Llamas-Carrera JM, Torres-Lagares D, Paredes V, Espinar E, Guevara E, Gutiérrez-Pérez JL. Long-term stability of surgical-orthodontic correction of class III malocclusions with long-face syndrome. *Med Oral Patol Oral Cir Bucal*. 2012; 17(3), 435-441.

Gardner DE, Luschei ES, Joondeph DR. Alterations in the facial skeleton of the guinea pig following a lesion of the trigeminal motor nucleus. *Am J Orthod*. 1980;78: 66-80.

Gasparini G, Rodrigues de Siqueira IC, Rezende Costa L. Does low-level laser therapy decrease swelling and pain resulting from orthognathic surgery? *Int J Oral Maxillofac Surg*. 2014; 43(7), 868-873.

Gelgor IE, Karaman AI, Ercan E. Prevalence of malocclusion among adolescents in central anatolia. *Eur J Dent*. 2007; 1(3), 125-131.

Girod S, Keeve E, Girod B. Advances in interactive craniofacial surgery planning by 3D simulation and visualization. *Int J Oral Maxillofac Surg*. 1995; 24, 120 – 125.

Goodall C. Procrustes methods in the statistical analysis of shape. *J R Statist Soc B* 1991;53:285Y339

Gorlin RJ, Cohen MM, Levin LS. *Syndromes of the head and neck* (3rd edition). New York: Oxford University Press, 1990.

Grammer, K., & Thornhill, R. (1994). Human (*Homo sapiens*) facial attractiveness and sexual selection: The role of symmetry and averageness. *Journal of Comparative Psychology*, 108(3), 233.

Grayson BH, Santiago PE, Brecht LE, et al. Presurgical nasoalveolar molding in infants with cleft lip and palate. *Cleft Palate Craniofac J* 1999;36:486Y498

Gross MM, Trotman CA, Moffatt KS. A comparison of three - dimensional and two - dimensional analyses of facial motion. *Angle Orthod*. 1996; 66, 189 – 194.

Guest E, Berry E, Morris D. Novel methods for quantifying soft tissue changes after orthognathic surgery. *Int J Oral Maxillofac Surg*. 2001; 30, 484 –489.

Guyer EC, Ellis EE 3rd, McNamara JA Jr, Behrents RG. Components of Class III malocclusion in juveniles and adolescents. *Angle Orthod*. 1986; 56, 7-30.

Hagg U, Tse A, Bendeus M, Rabie AB. Long-term follow-up of early treatment with reverse headgear. *Eur J Orthod*. 2003; 25(1), 95-102.

Hajeer MY, Ayoub AF, Millett DT, Bock M, Siebert JP. Three-dimensional imaging in orthognathic surgery: The clinical application of a new method. *Int J Adult Orthodon Orthognath Surg*. 2002; 17, 318 – 330.

Hajeer MY, Millett DT, Ayoub AF, Siebert JP. Applications of 3D imaging in orthodontics . Part I. J Orthod. 2004; 31, 62–70.

Hajeer MY, Millett DT, Ayoub AF, Siebert JP. Applications of 3D imaging in orthodontics. Part II. J Orthod. 2004; 31, 154 – 62.

Halazonetis DJ. Cone-beam computed tomography is not the imaging technique of choice for comprehensive orthodontic assessment. Am J Orthod Dentofacial Orthop. 2012; 141(4), 403-407.

Hammond D, Williams RW, Juj K, O’Connell S, Isherwood G, Hammond N. Weight loss in orthognathic surgery: a clinical study. Journal of Orthodontics. 2015; 42(3), 220–228.

Hammond P, Hutton TJ, Allanson JE, Campbell LE, Hennekam RC, Holden S, Patton MA, Shaw A, Temple IK, Trotter M, Murphy KC, Winter RM. 3D analysis of facial morphology. Am J Med Genet A. 2004; 126, 339-348.

Haraguchi S, Takada K, Yasuda Y. Facial asymmetry in subjects with skeletal Class III deformity. Angle Orthod. 2002 ;72(1):28-35.

Hardy DK, Cubas YP, Orellana MF. Prevalence of Angle Class III malocclusion: a systematic review and meta-analysis. Open J Epidemiol. 2012; 2, 75-82.

Harrison JA, Nixon MA, Fright WR, Snape L. Use of hand held laser scanning in the assessment of facial swelling: A preliminary study. Br J Oral Maxillofac Surg. 2004; 42, 8 – 17.

Hartmann J, Meyer-Marcotty P, Benz M, et al. Reliability of a method for computing facial symmetry plane and degree of asymmetry based on 3D-data. J Orofac Orthop 2007;68:477–490

Haynes S. The prevalence of malocclusion in English children aged 11-12 years. Rep Congr Eur Orthod Soc. 1970, 89-98.

Hegtvedt AK. Diagnosis and management of facial asymmetry. In: Peterson LJ, Indressano AT, Marciani RD, Roser SM, eds. Oral and Maxillofacial Surgery. Vol 3. Philadelphia: Lippincott, 1993:1400-1414.

Heike CL, Cunningham ML, Hing AV, Stuhaug E, Starr JR. Picture perfect? Reliability of craniofacial anthropometry using 3D digital stereophotogrammetry. Plast Reconstr Surg. 2009; 124, 1261-1272.

Heike CL, Upson K, Stuhaug E, Weinberg SM. 3D digital stereophotogrammetry: a practical guide to facial image acquisition. *Head and Face Medicine*. 2010; 6, 18.

Hill DL, Berg DC, Raso VJ, Lou E, Durdle NG, Mahood JK. Evaluation of a laser scanner for surface topography. *Stud Health Technol Inform*. 2002; 88, 90 –94.

Hood C, Bock M, Hosey MT, Bowman A, Ayoub AF. Facial asymmetry-3D assessment of infants with cleft lip and palate. *Int J Pediatr Dent*. 2003; 13, 404 – 410.

Honrado CP, Lee S, Bloomquist DS, Larrabee WF, Jr. Quantitative assessment of nasal changes after maxillomandibular surgery using a 3-dimensional digital imaging system. *Arch Facial Plast Surg*. 2006; 8(1), 26-35.

Hume, D. K., & Montgomerie, R. (2001). Facial attractiveness signals different aspects of “quality” in women and men. *Evolution and Human Behavior*, 22(2), 93–112.

Hunsuck EE. A modified intraoral sagittal splitting technic for correction of mandibular prognathism. *J Oral Surg*. 1968; 26(4), 250-253.

Ishizaki K, Suzuki K, Mito T, et al. Morphologic, functional, and occlusal characterization of mandibular lateral displacement malocclusion. *Am J Orthod Dentofacial Orthop* 2010;137:454.e1Y454.e9

Ismail SF, Moss JP, Hennessy R. Three-dimensional assessment of the effects of extraction and nonextraction orthodontic treatment on the face. *Am J Orthod Dentofacial Orthop*. 2002; 121, 244 – 256.

Jacobson A, Evans WG, Preston CB, Sadowsky PL. Mandibular prognathism. *Am J Orthod*. 1974; 66(2), 140-171.

Ji Y, Zhang F, Schwartz J, Stile F, Lineaweaver WC. Assessment of facial tissue expansion with three - dimensional digitizer scanning. *J Craniofac Surg*. 2002; 13, 687 – 92.

Jones, B. C., Little, A. C., Penton-Voak, I. S., Tiddeman, B. P., Burt, D. M., & Perrett, D. I. (2001). Facial symmetry and judgements of apparent health: Support for a “good genes” explanation of the attractiveness–symmetry relationship. *Evolution and Human Behavior*, 22(6), 417–429.

Kaipainen, A. E., Sieber, K. R., Nada, R. M., Maal, T. J., Katsaros, C., & Fudalej, P. S. (2015). Regional facial asymmetries and attractiveness of the face. *The European Journal of Orthodontics*.

Kau CH, Cronin A, Durning P, Zhurov AI, Sandham A, Richmond S. A new method for the 3D measurement of postoperative swelling following orthognathic surgery. *Orthod Craniofac Res.* 2006; 9, 31-37.

Kau CH, Richmond S, Palomo JM, Hans MG. Three-dimensional cone beam computerized tomography in orthodontics . *J Orthod.* 2005; 32, 282–93.

Kau CH, Richmond S, Zhurov AI, Chestnutt I, Hartles FR, Knox J. Reliability of measuring facial morphology using a 3 - dimensional laser scanning system. *Am J Orthod Dentofacial Orthop.* 2005; 128, 424 – 430.

Kau CH, Zhurov AI, Knox J, Richmond S. The validity and reliability of a portable 3-dimensional laser scanner for field studies. In R. Giuliani and E. Galliani (Eds.), *Seventh European Craniofacial Congress, 2004.* Bologna, Italy: Monduzzi Editore, International Proceedings Division, 2004; 41–45.

Kau CH, Richmond S. *Three-Dimensional Imaging for Orthodontics and Maxillofacial Surgery.* 1st. ed. Singapore: Blackwell Publishing Ltd.; 2010, p:11-28.

Kau CH, Cronin AJ, Richmond S. A three-dimensional evaluation of postoperative swelling following orthognathic surgery at 6 months. *Plastic and Reconstructive Surgery.* 2007; 119(7), 2192–2199.

Kau CH, Richmond S. Three-dimensional analysis of facial morphology surface changes in untreated children from 12 to 14 years of age. *American Journal of Orthodontics and Dentofacial Orthopedics.* 2008; 134(6), 751-760.

Kazhdan, M., Chazelle, B., Dobkin, D., Funkhouser, T., Rusinkiewicz, S.: A reflective symmetry descriptor for 3D models (2003). *Algorithmica* 38(1), 201–225

Khambay B, Nebel JC, Bowman J, Walker F, Hadley DM, Ayoub A. 3D stereophotogrammetric image superimposition onto 3D CT scan images: The future of orthognathic surgery. A pilot study. *Int J Adult Orthodon Orthodon Orthognath Surg.* 2002; 17, 331 –341.

Kiliaridis S, Thilander B, Kjellberg H, Topouzelis N, Zafiriadis A. Effect of low masticatory function on condylar growth: a morphometric study in the rat. *Am J Orthod Dentofacial Orthop* 1999;116:121–5.

Kim DS, Huh KH, Lee SS, Heo MS, Choi SC, Hwang SJ, et al: The relationship between the changes in three-dimensional facial morphology and mandibular movement after orthognathic surgery (2013). *J Craniomaxillofac Surg Mar pp: S1010-5182*

Ko EW, Huang CS, Chen YR. Characteristics and corrective outcome

of face asymmetry by orthognathic surgery. *J Oral Maxillofac Surg* 2009;67:2201Y2209

Koff E, Borod JC, White B. Asymmetries for hemiface size and mobility. *Neuropsychologia*. 1981;19:825-830.

Koff E, Borod J, Strauss E. Development of hemiface size asymmetry. *Cortex*. 1985;21:153-156.

Kornreich, Davida, Adele A. Mitchell, Bryn D. Webb, Ingrid Cristian, and Ethylin W. Jabs. "Quantitative Assessment of Facial Asymmetry Using Three-Dimensional Surface Imaging in Adults: Validating the Precision and Repeatability of a Global Approach." *The Cleft Palate-Craniofacial Journal* 53.1 (2016): 126-131

Kusnoto B, Evans CA. Reliability of a 3D surface laser scanner for orthodontic applications. *Am J Orthod Dentofacial Orthop*. 2002; 122, 342 –348.

Kwon TG, Park HS, Ryoo HM, Lee SH. A comparison of craniofacial morphology in patients with and without facial asymmetry--a three-dimensional analysis with computed tomography. *Int J Oral Maxillofac Surg*. 2006;35(1):43-48.

Lane C, Harrell W, Jr. Completing the 3-dimensional picture. *Am J Orthod Dentofacial Orthop*. 2008; 133(4), 612-620.

Langlois, J. H., Roggman, L. A., & Musselman, L. (1994). What is average and what is not average about attractive faces? *Psychological Science*, 5(4), 214–220.

Laureano Filho JR, de Oliveira e Silva ED, Batista CI, Gouveia FM. The influence of cryotherapy on reduction of swelling, pain and trismus after third-molar extraction: a preliminary study. *J Am Dent Assoc*. 2005; 136, 774–778.

Lee, Jong-Hyeon, Dong-Soon Choi, Bong-Kuen Cha, Young-Wook Park, and Insan Jang. "Three-dimensional Assessment of Facial Soft Tissue after Orthognathic Surgery in Patients with Skeletal Class III and Asymmetry." *The Journal Of Korean Association of Maxillofacial Plastic and Reconstructive Surgeons* 35.6 (2013): 360-367.

Lee JW, Park KH, Kim SH, Park YG, Kim SJ. Correlation between skeletal changes by maxillary protraction and upper airway dimensions. *Angle Orthod*. 2011; 81(3), 426-432.

Lee S. Three-dimensional photography and its application to facial plastic surgery. *Arch Facial Plast Surg*. 2004; 6(6), 410-414.

Lew KK, Foong WC, Loh E. Malocclusion prevalence in an ethnic Chinese population. *Aust Dent J.* 1993;38, 442-449.

Lee TY, Kim KH, Yu HS, Kim KD, Jung YS, Baik HS. Correlation analysis of three-dimensional changes of hard and soft tissues in class III orthognathic surgery patients using cone-beam computed tomography. *J Craniofac Surg.* 2014; 25(4), 1530-1540.

Lewis, Michael B. "Fertility affects asymmetry detection not symmetry preference in assessments of 3D facial attractiveness." *Cognition* 166 (2017): 130-138.

Little, A. C., & Jones, B. C. (2006). Attraction independent of detection suggests special mechanisms for symmetry preferences in human face perception. *Proceedings of the Royal Society of London B: Biological Sciences*, 273(1605), 3093–3099.

Litton SF, Ackerman LV, Isaacson RJ, Shapiro B. A genetic study of Class III malocclusion. *Am J Orthod.* 1970;58:565-577.

Liu, Y., Schmidt, K., Cohn, J., Weaver, R.: Facial asymmetry quantification for expression invariant human identification (2003). *Comput. Vis. Image Understand.* 91(1–2), 138–159

Luebbers HT, Medinger L, Kruse A, Graetz KW, Matthews F. Precision and Accuracy of the 3dMD Photogrammetric system in craniomaxillofacial application. *The Journal of Craniofacial Surgery.* 2010; 21(3), 763–767.

Lundstrom A, Lundstrom F, Le Bret LM, Moorrees CF. Natural head position and natural head orientation: basic considerations in cephalometric analysis and research. *Eur J Orthod.* 1995; 17, 111-120.

Mah J, Bumann A. Technology to create the three - dimensional patient record. *Semin Orthod.* 2001; 7, 251 – 257.

Mah J, Hatcher D. Current status and future needs in craniofacial imaging. *Orthod Craniofac Res.* 2003; 6 (Suppl. 1), 10 – 16; discussion 179 – 182.

Mah J, Hatcher D. Three-dimensional craniofacial imaging. *American Journal of Orthodontics and Dentofacial Orthopedics.* 2004; 126(3), 308–309.

Mah J. 3D imaging in private practice. *Am J Orthod Dentofacial Orthop.* 2002; 121, 14.

Mah JK, Danforth RA, Bumann A, Hatcher D. Radiation absorbed in maxillofacial imaging with a new dental computed tomography device. *Oral Surg Oral Med Oral Pathol Oral Radiol Endod.* 2003; 96, 508 – 513.

Mauil DJ, Grayson BH, Cutting CB, et al. Long-term effects of nasoalveolar molding on three-dimensional nasal shape in unilateral clefts. *Cleft Palate Craniofac J* 1999;36:391Y397

McMaster WC, Liddle S. Cryotherapy influence on posttraumatic limb oedema. *Clin Orthop.* 1980; 150, 283-287.

Metzger TE, Kula KS, Eckert GJ, Ghoneima AA. Orthodontic soft-tissue parameters: A comparison of cone-beam computed tomography and the 3dMD imaging system. *American Journal of Orthodontics and Dentofacial Orthopedics.* 2013; 144(5), 672-681.

Meyer-Marcotty, P., A. Stellzig-Eisenhauer, U. Bareis, J. Hartmann, and J. Kochel. "Three-dimensional perception of facial asymmetry." *The European Journal of Orthodontics* 33.6 (2011): 647-653.

Meyer-Marcotty Philipp, and Angelika Stellzig-Eisenhauer. "Dentofacial Self-Perception and Social Perception of Adults with Unilateral Cleft Lip and Palate." *Journal of Orofacial Orthopedics / Fortschritte der Kieferorthopädie* 70.3 (2009): 224-236

Minolta. Polygon Editing Tool. 2001, Minolta, Osaka.

Moorrees CFA, Kean MR. Natural head position, a basic consideration in the interpretation of cephalometric radiographs. *Am J Phys Anthropol* 1958; 16, 213-234.

Moro A, Gasparini G, Marianetti TM, Boniello R, Cervelli D, Di Nardo F, Rinaldo F, Alimonti V, Pelo S. Hilotherm efficacy in controlling postoperative facial edema *Maxillofac Surg.* 2014; 43(7), 868-873.

Moss JP, Grindrod SR, Linney AD, Arridge SR, James D. A computer system for the interactive planning and prediction of maxillofacial surgery. *Am. J. Orthod. Dentofacial Orthop.* 1988; 94, 469.

Moss JP, Coombes AM, Linney AD, Campos J. Methods of three dimensional analysis of patients with asymmetry of the face. *Proc. Finn. Dent. Soc.* 1991; 87, 139.

Moss JP. Northcroft revisited. *Br J Orthod.* 1989; 16, 155 – 167.

Motoyoshi M, Namura S, Arai HY. A three-dimensional measuring system for the human face using three-directional photography. *Am J Orthod Dentofacial Orthop.* 1992; 101, 431 – 440.

Nagao M, Sohmura T, Kinuta S, Kojima T, Wakabayashi K, Nakamura T. Integration of 3 - D shapes of dentition and facial morphology using a high - speed laser scanner. *Int J Prosthodont.* 2001; 14, 497 – 503.

Neal CE, Kiyak HA. Patient perceptions of pain, paresthesia, and swelling after orthognathic surgery. *Int J Adult Orthodon Orthognath Surg.* 1991; 6(3), 169-81.

Nguyen C. 3 D Image Construction of the Craniofacial Complex. Master thesis, Temple University, 1999, Philadelphia.

Nkenke E, Langer A, Laboureaux X, Benz M, Maier T, Kramer M. Validation of in vivo assessment of facial soft - tissue volume changes and clinical application in midfacial distraction: A technical report. *Plast Reconstr Surg.* 2003; 112, 367 –380.

Nkenke, Emeka, Bernhard Lehner, Manuel Kramer, Gerd Haeusler, Stefanie Benz, Maria Schuster, Friedrich W. Neukam, Eleftherios G. Vairaktaris, and Jochen Wurm. "Determination of Facial Symmetry in Unilateral Cleft Lip and Palate Patients from Three-Dimensional Data: Technical Report and Assessment of Measurement Errors." *The Cleft Palate-Craniofacial Journal* 43.2 (2006): 129-137

Nkenke E, Benz M, Maier T, Wiltfang J, Holbach LM, Kramer M. Relative en-and exophthalmometry in zygomatic fractures comparing optical non-contact, non-ionizing 3D imaging to the Hertel instrument and computed tomography . *J Craniomaxillofac Surg.* 2003; 31, 362 – 368.

Nkenke E, Vairaktaris E, Kramer M, Schlegel A, Holst A, Hirschfelder U, Wiltfang J, Neukam FW, Stamminger M. Three-dimensional analysis of changes of the malar midfacial region after LeFort I osteotomy and maxillary advancement. *Oral Maxillofac Surg.* 2008; 12(1), 5-12.

Nooreyazdan M, Trotman CA, Faraway JJ. Modeling facial movement. Part II: A dynamic analysis of differences caused by orthognathic surgery. *J Oral Maxillofac Surg.* 2004; 62,1380 – 1386.

Nord F., Ferjencik R, Seifert B, Lanzer M, Gander T, Matthews F, Rücker M, Luebbers HT. The 3dMD photogrammetric photo system in cranio-maxillofacial surgery: Validation of interexaminer variations and perceptions. *Journal of Cranio-Maxillofacial Surgery.* 2015; 43(9), 1798-1803.

O'Mara, D., Owens, R.: Measuring bilateral symmetry in three dimensional magnetic

resonance images. In: Attikiouzel, Y. (ed.) 1996 IEEE Region Ten Conference: Digital Signal Processing Applications, IEEE Service Center, pp. 151–156

Obwegeser HL. The one time forward movement of the maxilla and backward movement of the mandible for the correction of extreme prognathism (in German). SSO Schweiz Monatsschr Zahnheilkd. 1970; 80, 547–556.

Obwegeser HL. Surgical correction of small or retrodisplaced maxillae. The "dishface" deformity. Plast Reconstr Surg. 1969; 43(4), 351-365.

Obwegeser HL, Makek MS. Hemimandibular hypertrophy, hemimandibular elongation. Journal of Maxillofacial Surgery 1986; 14: 183-208.

Oh AK, Wong J, Ohta E, Rogers GF, Deutsch CK, Mulliken JB. Facial asymmetry in unilateral coronal synostosis: long-term results after fronto-orbital advancement. Plast Reconstr Surg. 2008; 121, 545-562.

Ort R, Metzler P, Kruse AL, Matthews F, Zemann W, Gratz KW, Luebbers HT. The Reliability of a Three-Dimensional Photo System- (3dMDface-) Based Evaluation of the Face in Cleft Lip Infants. Plast Surg Int. 2012.

Ostwald, Julia, Philipp Berssenbrügge, Dieter Dirksen, Christoph Runte, Kai Wermker, Johannes Kleinheinz, and Susanne Jung. "Measured symmetry of facial 3D shape and perceived facial symmetry and attractiveness before and after orthognathic surgery." Journal of Cranio-Maxillofacial Surgery 43.4 (2015): 521-527

Ozsoy, Umut. "Comparison of Different Calculation Methods Used to Analyze Facial Soft Tissue Asymmetry: Global and Partial 3-Dimensional Quantitative Evaluation of Healthy Subjects." Journal of Oral and Maxillofacial Surgery 74.9 (2016): 1847.e1-1847.e9.

Ozsoy U, Demirel BM, Yildirim FB, Tosun O, Sarikcioglu L. Method selection in craniofacial measurements: advantages and disadvantages of 3D digitization method. J Craniomaxillofac Surg. 2009; 37, 285-290.

Park JY, Kim MJ, Hwang SJ: Soft tissue profile changes after setback genioplasty in orthognathic surgery patients. J Craniomaxillofac Surg 7. 2013 Feb pii: S1010-5182

Patel, Arti J., Syed M. Islam, Kevin Murray, and Mithran S. Goonewardene. "Facial asymmetry assessment in adults using three-dimensional surface imaging (2015)." Progress in Orthodontics 16.1

Peck BS, Peck L, Kataja M. Skeletal asymmetry in aesthetically pleasing faces. Angle Orthodontist. 1991;61: 43-48.

Peng L, Cooke MS. Fifteen-year reproducibility of natural head posture: a longitudinal study. *Am J Orthod Dentofacial Orthop.* 1999; 116, 82-85.

Perrett, D. I., Burt, D. M., Penton-Voak, I. S., Lee, K. J., Rowland, D. A., & Edwards, R. (1999). Symmetry and human facial attractiveness. *Evolution and Human Behavior*, 20(5), 295–307.

Phillips C, Blakey G, Jaskolka M. Recovery after orthognathic surgery: short-term health-related quality of life outcomes. *J Oral Maxillofac Surg.* 2008; 66, 2110–2115.

Pirttiniemi PM. Associations of mandibular and facial asymmetries-a review. *Am J Orthod Dentofacial Orthop* 1994;106: 191-200.

Posnick JC. *Orthognathic Surgery: Principles and Practice.* St. Louis: Saunders; 2013.

Rabey G. *Morphanalysis.* London: Hatch and Pinner; 1968.

Proffit WR, Fields HW, Jr., Moray LJ. Prevalence of malocclusion and orthodontic treatment need in the United States: estimates from the NHANES III survey. *Int J Adult Orthodon Orthognath Surg.* 1998; 13(2), 97-106.

Proffit WR, White RP. *Surgical-orthodontic treatment.* St. Louis: Mosby-Year Book. 1991.

Proffit W, White R, Sarver D. *Contemporary Treatment of Dentofacial Deformity.* St. Louis: Mosby. 2003.

Proffit WR, Fields HW, Sarver DM. *Contemporary orthodontics.* St. Louis, Mo.: Mosby Elsevier. 2007.

Quintero JC, Trosien A, Hatcher D, Kapila S. Craniofacial imaging in orthodontics: historical perspective, current status, and future developments. *Angle Orthod.* 1999; 69(6), 491-506.

Quist, M. C., Watkins, D. C., Smith, F. G., Little, A. C., DeBruine, L. M., & Jones, B. C. (2012). Sociosexuality predicts women's preferences for symmetry in men's faces. *Archives of Sexual Behaviour*, 4(6), 1415–1421.

Rana M, Gellrich NC, Joos U, Piffko J, Kater W. 3D evaluation of postoperative swelling using two different cooling methods following orthognathic surgery: a randomised observer blind prospective pilot study. *Int J Oral Maxillofac Surg.* 2011; 40 (7) 690-696.

Rana M, Gellrich NC, von See C, et al. 3D evaluation of postoperative swelling in treatment of bilateral mandibular fractures using 2 different cooling therapy methods: A randomized observer blind prospective study. *J Craniomaxillofac Surg.* 2013; 41,17

Ras F, Habets L, van Ginkel FC, Pahl-Andersen B. Quantification of facial morphology using stereophotogrammetry – demonstration of a new concept. *J Dent.* 1996; 24, 369 – 374.

Ras F, Habets LL, van Ginkel FC, Pahl-Andersen B. Longitudinal study on three - dimensional changes of facial asymmetry in children between 4 to 12 years of age with unilateral cleft lip and palate. *Cleft Palate Craniofac J.* 1995; 32, 463 – 468.

Ras F, Habets LL, van Ginkel FC, Pahl-Andersen B. Method for quantifying facial asymmetry in three dimensions using stereophotogrammetry. *Angle Orthod.* 1995; 65, 233 – 239.

Reisfeld, D., Wolfson, H., Yeshurun, Y.: Detection of interest points using symmetry (1990). In: *Proceedings of the International Conference on Computer Vision*, pp. 62–65

Reyneke JP. *Essentials of orthognathic surgery.* Hanover Park, IL: Quintessence Pub.; 2010.

Rhodes, G., Proffitt, F., Grady, J. M., & Sumich, A. (1998). Facial symmetry and the perception of beauty. *Psychonomic Bulletin & Review*, 5(4), 659–669.

Richmond S. *The Feasibility of Categorising Orthodontic Treatment Difficulty: The Use of Three-Dimensional Plotting.* MScD Dissertation, 1984, University of Wales, Cardiff.

Røynesdal AK, Bjørnland T, Barkvoll P, Haanaes HR. The effect of softlaser application on postoperative pain and swelling. A double-blind, crossover study. *Int J Oral Maxillofac Surg.* 1993; 22, 242–245.

Samman N , Tong AC, Cheung DL, Tideman H. Analysis of 300 dentofacial deformities in Hong Kong. *Int J Adult Orthodon Orthognath Surg.* 1992;7(3):181-185.

Sanborn R. Differences Between the Facial Skeletal Patterns Of Class III Malocclusion and Normal Occlusion. *The Angle Orthodontist.* 1955; 25(4), 208-222.

Sander M, Daskalogiannakis J, Tompson B, et al. Effect of alveolar bone grafting on nasal morphology, symmetry, and nostril shape of patients with unilateral cleft lip and palate. *Cleft Palate Craniofac J* 2011; 48:20Y27

Sawyer AR, See M, Nduka C. 3D stereophotogrammetry quantitative lip analysis. *Aesthetic Plast Surg.* 2009; 33, 497-504.

Sayin MO, Turkkahraman H. Malocclusion and crowding in an orthodontically referred Turkish population. *Angle Orthod.* 2004; 74(5), 635-639.

Schaberg SJ, Stuller CB, Edwards SM. Effect of methylprednisolone on swelling after orthognathic surgery. *J Oral Maxillofac Surg.* 1984; 42(6), 356-361.

Schaubel HJ: The local use of ice after orthopaedic procedures. *Am J Surg.* 1946; 72, 711-714.

Severt TR, Profitt WR. The prevalence of facial asymmetry in the dentofacial deformities population at the University of North Carolina. *Int J Adult Orthod Orthognath Surg* 1997;12:171Y176

Shah SM, Joshi MR. An assessment of asymmetry in the normal craniofacial complex. *Angle Orthod.* 1978;48:141-148.

Sforza C, Dellavia C, Colombo A, Serrao G, Ferrario VF. Nasal dimensions in normal subjects: conventional anthropometry versus computerized anthropometry. *Am J Med Genet A.* 2004; 130, 228-233.

Shetty V, Mohan A. A prospective, randomized, double-blind, placebo-controlled clinical trial comparing the efficacy of systemic enzyme therapy for edema control in orthognathic surgery using ultrasound scan to measure facial swelling. *Journal of Oral and Maxillofacial Surgery.* 2013; 71(7), 1261-1267.

Silva RG, Kang DS. Prevalence of malocclusion among Latino adolescents. *Am J Orthod Dentofacial Orthop.* 2001; 119(3), 313-315.

Simmons, L. W., Rhodes, G., Peters, M., & Koehler, N. (2004). Are human preferences for facial symmetry focused on signals of developmental instability? *Behavioral Ecology*, 15(5), 864–871.

Soncul M, Bamber MA. The optical surface scan as an alternative to the cephalograph for soft tissue analysis for orthognathic surgery. *Int J Adult Orthodon Orthognath Surg.* 1999; 14(4), 277-283.

Soncul M, Bamber MA. Evaluation of facial soft tissue changes with optical surface scan after surgical correction of Class III deformities. *Journal of Oral and Maxillofacial Surgery.* 2004; 62(11), 1331-1340.

Stauber I, Vairaktaris E, Holst A, et al. Three-dimensional analysis of facial symmetry in cleft lip and palate patients using optical surface

data. *J Orofac Orthop* 2008;69:268–282

Sukovic P. Cone beam computed tomography in craniofacial imaging. *Orthod Craniofac Res.* 2003; 6 (Suppl. 1), 31 – 6; discussion 179 – 182.

Swaddle, J. P., & Cuthill, I. C. (1995). Asymmetry and human facial attractiveness: Symmetry may not always be beautiful. *Proceedings of the Royal Society of London B: Biological Sciences*, 261(1360), 111–116.

Swanson AB, Livengood LC, Sattel AB. Local hypothermia to prolong safe tourniquet time. *Clin Orthop.* 1991; 264, 200-208.

Swennen GRJ, Schutyser F, Hausamen J-E. Three-dimensional cephalometry : a color atlas and manual. New York, NY: Springer; 2005.

Szolnoky G, Szendi-Horvath K, Seres L, Boda K, Kemeny L. Manual lymph drainage efficiently reduces postoperative facial swelling and discomfort after removal of impacted third molars. *Lymphology.* 2007; 40, 138–142.

Takasaki H. Moiré topography. *Appl Optics.* 1970; 9, 1457 – 1472.

Tasios T. Three-Dimensional evaluation of the soft-tissue changes due to Class III double-jaw orthognathic surgery: a retrospective study. M.U. İnstitute of Health Sciences, Master Thesis, 2015, İstanbul (Supervisor: Prof. Dr. B. Çakırer Bakkalbaşı).

Thornhill, Randy B., and Steven W. Gangestad. "Facial attractiveness." *Trends in Cognitive Sciences* 3.12 (1999): 452-460.

Taylor, Helena O., Clinton S. Morrison, Olivia Linden, Benjamin Phillips, Johnny Chang, Margaret E. Byrne, Stephen R. Sullivan, and Christopher R. Forrest. "Quantitative Facial Asymmetry." *Journal of Craniofacial Surgery* 25.1 (2014): 124-128.

Thornhill, R., & Møller, A. P. (1997). Developmental stability, disease and medicine. *Biological Reviews of the Cambridge Philosophical Society*, 72(04), 497–548.

Trotman CA, Faraway JJ. Modeling facial movement. Part I: A dynamic analysis of differences based on skeletal characteristics. *J Oral Maxillofac Surg.* 2004; 62, 1372 – 1379.

Trotman CA, Gross MM, Moffatt K. Reliability of a three - dimensional method for measuring facial animation: A case report. *Angle Orthod.* 1996; 66, 195 – 198.

Tuncay OC. Three - dimensional imaging and motion animation. *Semin Orthod.* 2001; 7, 244 – 250.

Tuzikov, A., Colliot, O., Bloch, I.: Brain symmetry plane computation in MR images using inertia axes and optimization. In: Proceedings of the International Conference on Pattern Recognition, pp. 516–519 (2002)

Tzou CH, Artner NM, Pona I, Hold A, Placheta E, Kropatsch WG, Frey M.. Comparison of three-dimensional surface-imaging systems. In *Journal of Plastic, Reconstructive and Aesthetic Surgery*. 2014; 67(4), 489-497.

Uslu O, Akcam MO, Evirgen S, Cebeci I. Prevalence of dental anomalies in various malocclusions. *Am J Orthod Dentofacial Orthop*. 2009; 135(3), 328-335.

van der Meer WJ, Dijkstra PU, Visser A, Vissink A, Ren Y. Reliability and validity of measurements of facial swelling with a stereophotogrammetry optical three-dimensional scanner. *Br J Oral Maxillofac Surg*. 2014; 52, 922.

van der Vlis M, Dentino KM, Vervloet B, Padwa BL. Postoperative swelling after orthognathic surgery: a prospective volumetric analysis. *J Oral Maxillofac Surg*. 2014; 72(11), 2241-2247.

Verzé, Laura, Francesca A. Bianchi, Eleonora Schellino, and Guglielmo Ramieri. "Soft Tissue Changes After Orthodontic Surgical Correction of Jaws Asymmetry Evaluated by Three-Dimensional Surface Laser Scanner." *Journal of Craniofacial Surgery* 23.5 (2012): 1448-1452

Verhoeven, Tim, Tong Xi, Ruud Schreurs, Stefaan Bergé, and Thomas Maal. "Quantification of facial asymmetry: A comparative study of landmark-based and surface-based registrations." *Journal of Cranio-Maxillofacial Surgery* 44.9 (2016): 1131-1136

Vig PS, Showfety KJ, Philips C. Experimental manipulation of head posture. *Am J Orthod*. 1980; 77, 258-268.

Vig PS, Hewitt AB. Asymmetry of the human facial skeleton. *Angle Orthod*. 1975;45:125-129.

Washburn SL. The effect of facial paralysis on the growth of the skull of the rat and rabbit. *The Anatomical Record*. 1946; 94(2):163-168.

Weber CR, Griffin JM. Evaluation of dexamethasone for reducing postoperative edema and inflammatory response after orthognathic surgery. *J Oral Maxillofac Surg*. 1994; 52(1), 35-39.

Weber DW, Fallis DW, Packer MD. Three-dimensional reproducibility of natural head position. *American Journal of Orthodontics and Dentofacial Orthopedics*. 2013; 143(5), 738-744.

Weeden JC, Trotman CA, Faraway JJ. Three-dimensional analysis of facial movement in normal adults: Influence of sex and facial shape. *Angle Orthod*. 2001; 71, 132 – 140.

Weinberg SM, Naidoo S, Govier DP, Martin RA, Kane AA, Marazita ML. Anthropometric precision and accuracy of digital three-dimensional photogrammetry: comparing the Genex and 3dMD imaging systems with one another and with direct anthropometry. *J Craniofac Surg*. 2006; 17(3), 477-483.

Wermker Kai, Johannes Kleinheinz, Susanne Jung, and Dieter Dirksen. "Soft tissue response and facial symmetry after orthognathic surgery." *Journal of Cranio-Maxillofacial Surgery* 42.6 (2014): e339-e345.

Willems G, De Bruyne I, Verdonck A, Fieuws S, Carels C. Prevalence of dentofacial characteristics in a belgian orthodontic population. *Clin Oral Investig*. 2001;5:220-226.

Williams S, Andersen CE. The morphology of the potential Class III skeletal pattern in the growing child. *Am J Orthod*. 1986; 89(4), 302-311.

Wolfe, Sara M., Eustaquio Araujo, Rolf G. Behrents, and Peter H. Buschang. "Craniofacial growth of Class III subjects six to sixteen years of age." *The Angle Orthodontist* 81.2 (2011): 211-216

Wong JY, Oh AK, Ohta E, Hunt AT, Rogers GF, Mulliken JB, Deutsch CK. Validity and reliability of craniofacial anthropometric measurement of 3D digital photogrammetric images. *Cleft Palate Craniofac J*. 2008; 45(3), 232-239.

Yamamoto S, Miyachi H, Fujii H, Ochiai S, Watanabe S, Shimozato K. Intuitive facial imaging method for evaluation of postoperative swelling: A combination of 3-dimensional computed tomography and laser surface scanning in orthognathic surgery. *J Oral Maxillofac Surg*. 2016; 74, 2506, 1-10.

Yáñez-Vico RM, Iglesias-Linares A, Torres-Lagares D, Gutiérrez-Pérez JL, Solano-Reina E: Three-dimensional evaluation of craniofacial asymmetry: an analysis using computed tomography. *Clin Oral Investig* 15: 729e736, 2011

Yoon KS, Jung YS, Kang GC, Park HS. Facial asymmetry with mandibular prognathism: a new trial of classification and interpretation. *J Korean Assoc Oral Maxillofac Surg*. 2004;30:108-120.

Xia J, Ip HH, Samman N, Wong HT, Gateno J, Wang D, Yeung RW, Kot CS, Tideman H. Three-dimensional virtual-reality surgical planning and soft-tissue prediction for orthognathic surgery. *IEEE Trans Inf Technol Biomed.* 2001; 5(2), 97- 107.

Xue, F., RWK Wong, and ABM Rabie. "Genes, genetics, and Class III malocclusion." *Orthodontics & Craniofacial Research* 13.2 (2010): 69-74





T.C.
MARMARA ÜNİVERSİTESİ
Diş Hekimliği Fakültesi
Klinik Araştırmalar Etik Kurulu

Projenin Adı: Three Dimensional Stereophotogrammetric Evaluation of Facial Soft Tissue Asymmetries Before and After Ortognathic Surgery in Skeletal Class III Patients

Proje yürütücüsü: Dr. Kadir BEYCAN

Projedeki Araştırmacılar: Dt.Georgios LOGOTHETİS

Onay tarihi ve sayısı:29.11.2018, 2018-226

Sayın Dr. Kadir BEYCAN

2018-235 Protokol nolu " Three Dimensional Stereophotogrammetric Evaluation of Facial Soft Tissue Asymmetries Before and After Ortognathic Surgery in Skeletal Class III Patients" isimli retrospektif çalışmanız Marmara Üniversitesi Klinik Araştırmalar Etik kurulu tarafından incelenmiş ve etik yönden uygunluğuna karar verilmiştir.

M.Ü.Diş Hekimliği Fakültesi

Klinik Araştırmalar Etik Kurulu Başkanı

Prof.Dr.Nimet Gençoğlu

Adı Soyadı

Prof. Dr. Nimet Gençoğlu

Prof. Dr. İlknur Tanboğa

Prof. Dr. Ali Recai Menteş

Prof. Dr. Yaşar Özkan

Prof. Dr. Ahu Acar

Prof. Dr. Zühre Hale Cimilli

Doç. Dr. Buket Evren

Prof. Dr. Şebnem Erçalık Yalçınkaya

Prof. Dr. Filiz Onat

Dr. Zerrin Kurşun

Prof. Dr. Afife Binnaz Hazar Yoruç

Dr.Öğr.Üyesi G. Hale Özcömert Coşkun

Dr.Öğr.Üyesi Gediz Kocabaş

Nuri Sertaç Sırma (sivil üye)



Marmara Üniversitesi
Nişantaşı Kampusu Diş
Hekimliği Fakültesi 34365
Nişantaşı /Şişli/İSTANBUL

0 (212) 246 52 47 (Faks)
0 (212) 231 91 20

dishekimligi@marmara.edu.tr
<http://dental.marmara.edu.tr>

Ayrıntılı bilgi için: İ.SOYADI Unvan

10. CURRICULUM VITAE

Name	Georgios	Surname	Logothetis
Place of Birth	Heraklion, Greece	Date of Birth	23/ 2/ 1990
Nationality	Greek	Tel	+90 5060257569
E-mail	Logothetis13@gmail.com		

Educational Level

	Name of the Institution where he/she was graduated	Graduation year
Undergraduate	Aristotle University of Thessaloniki, Greece	2015
High school	8 th high school of Heraklion, Greece	2007

Job Experience

	Duty	Institution	Duration (Year - Year)
1	General Dentist	Private dental clinic, Greece	04/2016 - 08/2016

Foreign Languages	Reading comprehension	Speaking*	Writing*
English	C1	C1	C1
German	A2	A2	A2

Foreign Language Examination Grade#								
YDS	ÜDS	IELTS	TOEFL IBT	TOEFL PBT	TOEFL CBT	FCE	CAE	CPE
		7,5						

Computer Knowledge

Program	Use proficiency
ECDL Core	Excellent